Design and synthesis of discontinuous protein binding site mimics of HIV gp120

Gwenn Mulder

Colophon

Printed by: Gildeprint Drukkerijen - The Netherlands

Cover design: Annouck Welhuis

Layout: Annouck Welhuis en Gwenn Mulder

ISBN number: 978-94-6108-467-5

Design and synthesis of discontinuous protein binding site mimics of HIV gp120

Ontwerp en synthese van mimetica van discontinue eiwit bindingsplaatsen van HIV gp120

(met een samenvatting in het Nederlands)

PROEFSCHRIFT

ter verkrijging van de graad van doctor aan de Universiteit Utrecht op gezag van de rector magnificus, prof.dr. G.J. van der Zwaan, ingevolge het besluit van het college voor promoties in het openbaar te verdedigen op maandag 24 juni 2013 des middags te 12.45 uur

door GWENN EVELINE MULDER
geboren op 3 september 1985 te Mook en Middelaar

Promotor: Prof.dr. R.M.J. Liskamp

Co-promotor: Dr.ir. J.A.W. Kruijtzer

Dit proefschrift werd mede mogelijk gemaakt met financiële steun van Bureau Interimair (www.interimair.info)

Table of contents

List of abbreviations

Ac_2O	acetic anhydride
AcOH	acetic acid
Alloc	allyl oxycarboyl
Ar	aromatic
Asc	ascorbate
Boc	tert-butyloxycarbonyl
BOP	(benzotriazol-1-yloxy)tris(dimethylamino) phosphonium hexafluorophosphate
Bzl	benzyl
Cbz	carboxybenzyl
CLIPS	chemical linkage of peptides onto scaffolds
CTV	cyclotriveratrylene
CuAAC	copper (I)-catalysed azide-alkyne cycloaddition
d	doublet
DBU	1,8-diazabicyclo[5.4.0]undec-7-ene
DCC	dicyclohexyl carbodiimide
DCM	dichloromethane
dd	double doublet
D*i*PEA	*N*,*N*-diisopropylethylamine
DMAP	4-dimethylaminopyridine
DMB	2,4-dimethoxybenzyl
DMF	*N*,*N*-dimethylformamide
DMSO	dimethyl sulfoxide
ELISA	enzyme-linked immunosorbent assay
ESI	electrospray ionization
ESI-MS	electrospray ionization mass spectrometry
Et_2O	diethyl ether
EtOAc	ethylacetate
EtOH	ethanol
Fmoc	9-fluorenylmethyloxycarbonyl

Fmoc-OSu	9-fluorenylmethyloxycarbonyl *N*-hydroxysuccinimide ester
HATU	*O*-(7-azabenzotriazol-1-yl)-*N*,*N*,*N*′,*N*′-tetramethyluronium hexafluorophosphate
HBTU	*O*-(benzotriazol-1-yl)- *N*,*N*,*N*′,*N*′-tetramethyluronium hexafluorophosphate
HIV	human immunodeficiency virus
HOAt	1-hydroxy-7-azabenzotriazole
HOBt	1-hydroxybenzotriazole
HPLC	high-performance liquid chromatography
HRP	horseradish peroxidase
IC_{50}	half maximal inhibitory concentration
iPrOH	isopropanol
m	multiplet
MALDI-ToF	matrix-assisted laser desorption/ionization- time of flight
mCPBA	meta-chloroperbenzoic acid
MeCN	acetonitrile
MeOH	methanol
MS	mass spectrometry
MTBE	methyl-tert-butyl ether
MTT	3-(4,5-dimethylthiazol-2-yl)- 2,5-diphenyltetrazolium bromide
NMP	*N*-methylpyrrolidone
NMR	nuclear magnetic resonance
o-NBS	ortho-nitrobenzyl sulfonyl
PBS	phosphate-buffered saline
Psoc	2-phenyl-2-trimethylsilyl ethoxycarbonyl
PTMSE	2-phenyl-2-trimethylsilyl ethyl
q	quartet
RCM	ring closing methathesis
s	singlet
SPPS	solid phase peptide synthesis
t	triplet
TAC	triazacyclophane
TBAB	tetra *n*-butylammonium bromide
TBAF	tetra *n*-butylammonium fluoride
TBTA	tris(benzyltriazolylmethyl)-amine

tBuOH	*tert*-butanol
TFA	trifluoroacetic acid
TFAc	trifluoroacetyl
TFE	2,2,2-trifluoroethanol
TIS	triisopropylsilane
TLC	thin layer chromatography
TMB	3,3',5,5'-tetramethylbenzidine
TMS	tetramethylsilane
Trt	triphenylmethyl (also trityl)
UV	ultra violet
δ	chemical shift

Amino acids

Ala	A	Alanine
Arg	R	Arginine
Asn	N	Asparagine
Asp	D	Aspartic acid
Cys	C	Cysteine
Gln	Q	Glutamine
Glu	E	Glutamic acid
Gly	G	Glycine
His	H	Histidine
Ile	I	Isoleucine
Leu	L	Leucine
Lys	K	Lysine
Met	M	Methionine
Phe	F	Phenylalanine
Pro	P	Proline
Ser	S	Serine
Thr	T	Threonine
Trp	W	Tryptophan
Tyr	Y	Tyrosine
Val	V	Valine

1

Introduction: Mimicry of protein binding sites

1.1 General introduction

1.1.1 – Protein-protein interactions

Essentially all cellular processes are mediated by protein-protein interactions and detailed knowledge about these interactions can aid in determining biological functions or provide opportunities for the treatment of human disease.[1,2] Extensive research has been performed on the development of modulators of protein-protein interactions, since these molecules could provide better understanding of the mechanisms of molecular recognition, lead to the identification of drug targets or provide access to novel therapeutics.[3,4] Peptide-based mimics of protein binding sites are promising candidates for this purpose. Despite the progress that has been made in the field of protein mimicry and the increasing understanding of protein-protein interactions, the development of molecules that can modulate these interactions remains a challenging task because of the complex nature of protein binding sites.

1.1.2 – The structural complexity of protein binding sites

Contact surfaces involved in protein-protein interactions are large (typically ≈1500 Å^2)[5], which poses a serious challenge for small molecules to act as a competitor in these types of interactions. In addition, protein binding sites usually have a complex architecture and key interacting residues are not easily identified.[3,4] The majority of protein binding sites is found to be discontinuous.[6] They consist of atoms from surface residues in the protein that are distant in the linear sequence, but are brought together by folding of the polypeptide chain, and their biological activity largely depends on the native conformation of the protein (Figure 1).

Since proteins tend to exert their biological activity through combinations of small regions of their folded surfaces, their function could in principle be modulated or reproduced by much smaller designer molecules that retain these bioactive surfaces.[7] The structural and functional mimicry of bioactive regions of proteins in smaller molecules presents one of the greatest challenges for medicinal chemists today.

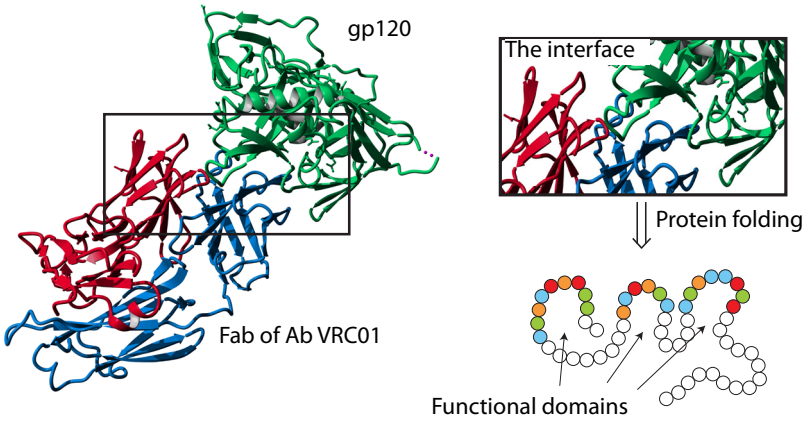

Figure 1 | The discontinuous character of protein binding sites. Functional domains are brought together by protein folding. PDB: 3NGB

1.1.3 – Identification of hot spots in protein binding sites

The identification of the specific amino acid residues that play essential roles in protein-protein interactions is an important step towards deciphering the functional mechanisms of proteins and designing protein mimics. Research in this field has been driven forwards over the past decade by the substantial growth in the 3D structural information of biological macromolecules and the complexes they form, which is mostly inferred from analysis of protein-protein complexes using X-ray crystallography, NMR spectroscopy or mass spectrometry.[8,9] These techniques have provided a considerable amount of information on important protein binding regions, however these studies mainly reveal *structural* information about the interaction.[10] Structural analysis alone cannot show whether all the contact residues are important for tight binding or if these residues are essential for *protein function*. The residues essential for protein function are known as hot spots; interface residues contributing the most to the binding free energy (more than 2 kcal/mol).[11,12] Hot spots can be located using mutagenesis strategies like alanine scanning[13], preferably in combination with binding assays that measure the effects of these mutations on protein function.[11,14] Extensive work has been done to underpin the concept of hot spots in protein-protein interactions, and over the last decade especially developments in bioinformatics have provided insight into the analysis of protein–protein interfaces and the detection of hot

spots.[15-17] Computational methods have been developed for the prediction of hot spots by combining experimental and structural data, modeling experiments and sequence homology studies.[18,19]

Perhaps most important is the realization that the hot spot clusters at protein interfaces have surface areas close to those of synthetic macrocyclic molecules and many natural products of 1–2 kDa.[1] Therefore, these types of molecules could be interesting starting points for the development of therapeutics targeting protein-protein interactions.

1.2 Cyclic peptides

1.2.1 – Cyclic peptides for mimicry of discontinuous protein binding sites

For accurate mimicry, not only detailed structural and functional understanding of the protein is a prerequisite, but also a state of the art chemical toolbox is demanded. Since discontinuous protein binding sites consist of peptide fragments, peptide-based compounds are likely to be suitable candidates for mimicry of these binding sites. However, linear peptides usually do not adopt the correct secondary and tertiary structure initially present in the corresponding residues of the correctly folded protein.[20] Given the critical role of conformation in molecular recognition and more specifically in peptide bioactivity, more advanced strategies are required to develop peptide-based constructs that correctly position the important functionalities in space. Nowadays a myriad of chemical methods is available for structural fixation of linear peptides and new strategies are still emerging.[21]

Structural fixation of linear peptides can be achieved in various ways, mostly involving chemical modifications of the peptide backbone or the sidechains.[22] Interacting peptide-fragments in protein binding sites often have loop-like conformations (Figure 2). Therefore, the most general and most frequently applied way for structural mimicry of these peptide-fragments is via peptide cyclization, either by macrolactamization or by the formation of a disulfide-bridge between two cysteine-residues. Cyclization of linear peptides is not only beneficial to their conformational stability, but also positively influences some important pharmacokinetic properties.[23-25] Cyclic peptides in general have an improved chemical and enzymatic stability as compared to their linear counterparts.

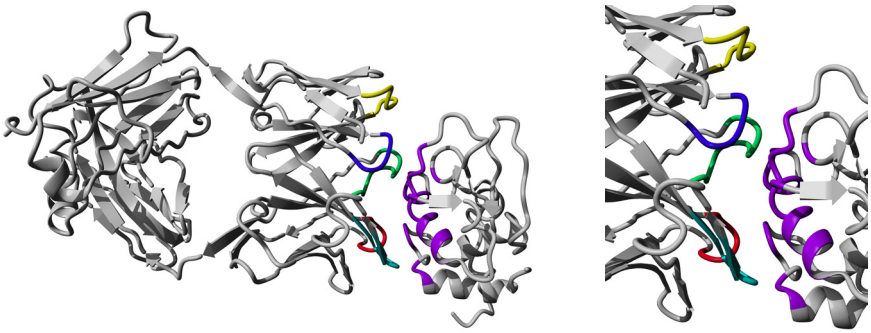

Figure 2 | The interaction between a discontinuous epitope on a lysozyme and Fab 9.13.7. PDB: 1FBI. The interacting protein fragments are indicated in color.

1.2.2 – Peptide cyclization strategies

Despite the large number of bioactive macrocyclic molecules and cyclic peptides and the value of this class of molecules for modern drug development, major challenges remain for the efficient synthesis of cyclic peptides. Many cyclic peptides are notoriously difficult to prepare and the success of the synthetic approach often largely depends on the amino acid constituents of the cyclic peptide, the specific site of ring-closure, the ring-closing strategy and the desired ring-size. These issues have stimulated the development of novel efficient methods for peptide cyclization. Macrocyclization can be achieved via classical reactions like amide-bond formation[26] or disulfide-formation.[27] Various strategies have been reported for peptide cyclization employing these classical methods, either by cyclization via the N- or C-terminus of the peptide or via its side-chains (Figure 3).

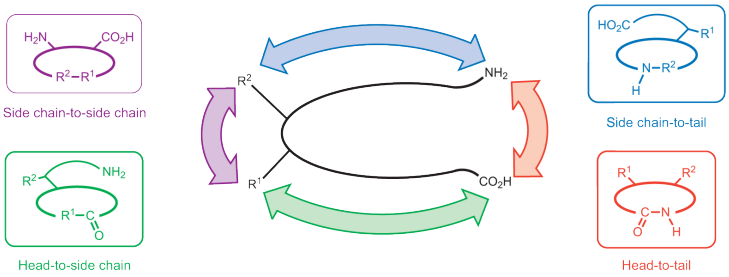

Figure 3 | Schematic representation of the four possible ways for peptide macrocyclization Reprinted by permission from Macmillan Publishers Ltd: Nature Chemistry, copyright 2011.[21]

In addition, alternative approaches have been developed that make use of orthogonal ligation methods. An important advantage of the use of orthogonal ligation methods over amide-bond formation for macrocyclization reactions is that cyclization can be performed on *sidechain-unprotected peptides*. This usually improves the solubility of these peptides and thereby increases the synthetic and analytical possibilities.[28]

The demand for a detailed understanding of complex biological processes has stimulated the development of highly advanced chemical tools, in order to improve the efficiency of peptide cyclization. Ideally, peptide cyclization should be sequence independent, the cyclization strategy should be applicable on both short and longer peptides and the strategy should only require easily accessible functionalities or chemical moieties. A variety of chemolesective ligation methods have been described for this purpose.

Existing chemoselective ligation methods, like the thiol-mediated intermolecular native chemical ligation (NCL) of peptide segments first reported by Kent and co-workers[29] have been heavily exploited for both existing and novel purposes. The feasibility of this method for peptide cyclization via intramolecular transthioesterification and ring contraction was first demonstrated by Tam and Zhang.[30] Later on, this method for the synthesis of head-to-tail cyclized peptides has also been extended to a solid-phase based approach.[31] An obvious limitation of NCL is the necessity of a cysteine residue at the site of cyclisation. In answer to that, several research efforts have focused on circumventing this requirement, resulting in a number of methods that has been reported for peptide cyclization mediated through removable sulfur-containing auxiliaries.[32,33]

Another powerful method for the introduction of ring-shaped constraints is ring-closing metathesis (RCM). The chemistry of RCM, relying on the action of Ruthenium-based catalysts, has been applied for the first time to rigidify amino acids and peptides by Grubbs and co-workers.[34]

The success of the copper catalysed azide-alkyne cycloaddition as developed by Sharpless and Meldal[35,36] has effectively been translated to the macrocyclization of peptides. In addition to the high efficiency and regioselectivity of this reaction, this triazole-forming reaction appeared to be of special value in the synthesis of the small cyclic peptides that are usually difficult to synthesize. The conformational restrictions imposed by the resulting triazole-ring can positively influence the formation of these

small macrocycles.[37,38]

Whereas above-mentioned methods for the synthesis of cyclic peptides make use of main chain- or (modified) sidechain functionalities of linear peptide precursors or involve removable auxiliaries, peptide cyclization can also be achieved using scaffold molecules. A successful example of the use of a synthetic scaffold for conformational fixation of peptides is CLIPS-technology (Chemical Linkage of Peptides onto Scaffolds).[39] A first example of this approach involves the immobilization of a dicysteine-containing linear peptide to an α,α' dibromoxylene-scaffold, resulting in a scaffolded cyclic peptide (Figure 4). After the introduction of CLIPS-technology for the generation of single peptide loops, the technology has been extended for the synthesis of multicyclic peptides towards the generation of mimics of more complex protein binding sites.[40]

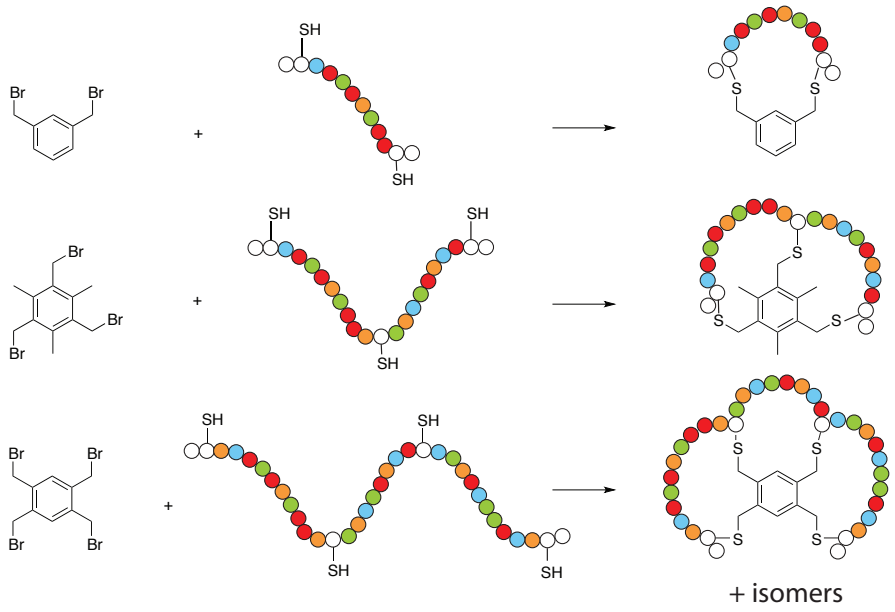

Figure 4 | Peptide cyclization using CLIPS technology

1.2.3 – Multicyclic peptides for mimicry of complex protein binding sites

The field of multicyclic peptide design for protein mimicry is rapidly developing, owing to the expected greater target affinity and selectivity of these compounds as compared to linear and monocyclic peptides. Recent studies on bicyclic peptides generated by CLIPS-technology have demonstrated the advantage of these compounds over their linear and monocyclic analogues, as large contact interfaces and improved binding properties were observed for the bicyclic peptides.[41] The importance of conformation in the field of protein mimicry was underscored in studies on ring-size of bicyclic peptides and experiments with different cyclization linkers.[42,43]

A fascinating class of naturally occurring multicyclic peptides is the family of cyclotides (Figure 5c). These plant-made defence proteins are characterized by a head-to-tail cyclic backbone combined with a conserved, six cystine knot.[44,45] This unique cyclic cystine knot motif engenders cyclotides with exceptional stability and this stability is a primary reason for interest in these peptides as pharmaceutical scaffolds. A limitation of cyclotides as a basis for drug design is caused by the sequence-specific folding of these multicyclic peptides. Consequently, only limited primary structural flexibility is tolerated for correct folding synthesis of the typical cyclic cysteine knot motif.[46] In answer to this, recently a method has been reported for orthogonal disulfide pairing and directed folding of multicyclic peptides.[47] In this work, a CXC (cysteine-any amino acid -cysteine) motif is incorporated in the peptides sequence. The CXC motif possesses unique dimerization features that can be exploited for both intermolecular and intramolecular cyclization, leading to dimeric, bicyclic and tricyclic peptides (Figure 5d). However, often CXC dimerization leads to the formation of multiple differently folded products and consequently the yields of desired products are low.

In recent years, multicyclic peptidic constructs have gained increasing attention because of the exceptional enzymatic and conformational stability of this class of compounds, and because of their potential for the generation of protein mimics. Despite this increasing attention, the synthetic possibilities for obtaining multicyclic peptides are still limited and novel approaches for this purpose are desired. In Figure 5 an overview of recent approaches towards multicyclic peptides is given.

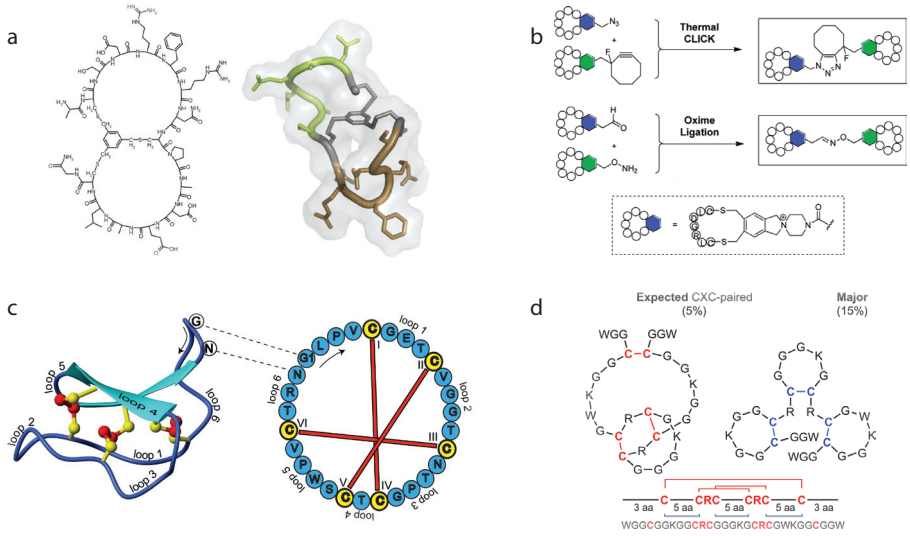

Figure 5 | Recent examples of multicyclic peptides: a) Structural formula and NMR-structure of a bicyclic peptide cyclized via CLIPS technology.[40] b) Modular method for combining two CLIPS-cyclized peptides. Reprinted with permission from Organic Letters[48], Copyright 2012, American Chemical Society. c) Structure and sequence of the cyclotide Kalata B1.[49] d) Multicyclic peptides via orthogonal disulfide pairing. Reprinted by permission from Macmillan Publishers Ltd: Nature Chemistry, copyright 2012. [47].

1.2.4 – Libraries of multicyclic peptides

Most recent examples of scaffolded bicyclic peptides include the earlier described studies based on CLIPS cyclization strategies, an extension of the CLIPS-technology on a novel water-soluble scaffold molecule[48] (Figure 5b) and a method by Ghosh and Hamilton for peptide-oligonucleotide click conjugation resulting in noncovalent self-assembling two-loop structures.[50] Heinis and Winter[40] describe a method for the generation of a library of random peptides containing three cysteine residues, displayed on filamentous phage and cyclized on a scaffold molecule prior to phage affinity selection.[40] After this first proof of concept experiment yielding a lead inhibitor (PK15; K_i = 1.5 nM) specific to human plasma kallikrein, the strategy was routinely applied in several other studies.[41-43,51] The synthetic strategy reported by Ghosh and Hamilton

for noncovalent template assembly of multiloop peptides is a proof of concept study and involves only two model peptides, but the authors also hint at potential use of their method as a route to combinatorial libraries by multicomponent self-assembly.[52]
In addition to the need for efficient synthetic strategies for the generation of multiloop systems, these recent approaches also emphasize the need for synthetic flexibility of the system in the search for biologically active compounds. While major efforts are being devoted to further refine the prediction of discontinuous protein binding site mimics, accurate prediction of the conformation of these compounds remains difficult.[2,10] Therefore, in addition to available strategies for structural analysis and computational (in silico) screening methods, methods for (combinatorial) peptide library preparation and microarray analysis might be of great value for finding potent protein mimics.

1.3 Molecular scaffolds

1.3.1 – Molecular scaffolds as templates for protein design

For mimicry of structurally complex protein binding sites using multicyclic peptides, efficient cyclization of the individual peptides is not the only requirement. In order to obtain decent activity, multicyclic peptides require adopting the proper secondary and tertiary structure of the native protein of interest. A commonly used method to achieve this is by assembly of (cyclic) peptide fragments on molecular scaffolds.[53]
Already in the late 80's, protein design was considered a promising field of research and the creation of new proteins with tailor-made structural and functional properties was the ultimate goal. Pioneering work in this field has been performed by Mutter[54] and DeGrado[55], who described the essential role of discontinuous peptide fragments in protein binding sites, and underlined the importance of cooperative assembly of these fragments into well-defined three-dimensional structures. Mutter and Vuilleumier described a first approach towards the assembly of peptide fragments in 1989, proposing a multifunctional carrier molecule for the construction of protein-like tertiary structures. A template molecule was designed and synthesized, which directs the attached peptide chains into protein-like arrangements. The resulting macromolecules were termed Template-Assembled Synthetic Proteins (TASP).[54] Since the introduction of TASP molecules as templates for protein design, a selection

of molecules has been developed as scaffolds for this purpose. In the field of protein mimicry, scaffolds allow chemists to replace the bulk of the protein and study the interaction of the binding site mimic with its target in great detail. Molecular scaffolds have been used either for the attachment of multiple peptide fragments, as structure-inducing devices, or a combination of both.

Whereas the TASP approach involves a cyclic peptide template, different classes of scaffold molecules have been described including porphyrins[56-58], carbohydrates[59], steroids[60], calixarenes[61] and small organic molecules (Figure 6). Most of these scaffolds have only been marginally explored with respect to their applicability in protein design, however some successful examples are known. The cyclotriveratrylene (CTV)[62] scaffold has successfully been used as structure-inducing device for collagen mimics[63], for the preparation of amino acid glycoconjugates[64] and for the synthesis of artificial receptors.[65,66] Similarly, calix[4]arene[67] scaffolds have been used for the preparation of synthetic receptors based on a design in which four peptide loops are arrayed around a central calilx[4]arene core.[68] Another scaffold molecule that has successfully been used for protein mimicry is Kemp's triacid (KTA).[69] This relatively rigid trivalent scaffold molecule was used to induce triple helix-formation in collagen peptides.[70] Even though several successful examples of scaffold-based protein mimics are known, it must be noted that these scaffolds mostly only allow the attachment of multiple *identical linear* peptides.

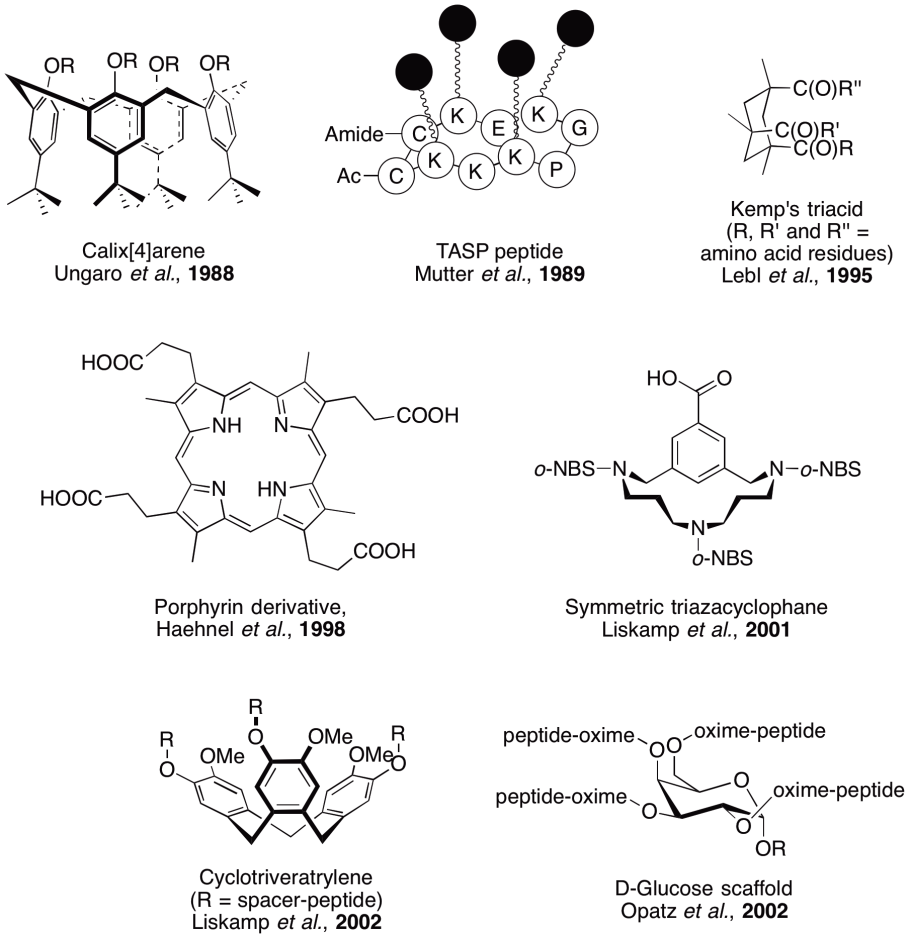

Figure 6 | Molecular scaffolds as templates for protein design

1.3.2 – Selectively addressable molecular scaffolds

While different types of molecular scaffolds were being developed and fields of application of these types of molecules were extended, Mutter and coworkers reported the synthesis of more elaborate TASP molecules as templates for protein mimicry. Several *selectively addressable sites* were incorporated in the cyclic peptide template, allowing the stepwise introduction of multiple *different* ligands (Figure 7). The resulting Regioselectively Addressable Functionalized Templates (RAFT)[71] were a first example of an important new development in scaffold design; orthogonally protected

templates for the assembly of a variety of different ligands. In addition, progress in the methodology of solid phase peptide synthesis encouraged the development of scaffold molecules that were compatible with Solid Phase Peptide Synthesis. In this context, Peluso and coworkers described the solid-phase assembly of a three loop TASP[72], a cholic acid analogue[73,74] was developed, Lönnberg and coworkers developed two orthogonally protected solid phase compatible scaffold molecules[75,76] and a pentaerythritol-based molecular scaffold[77] was synthesized as a platform for solid-phase combinatorial chemistry. Especially the TASP/RAFT approach has been of great value in the field of protein mimicry, since the template used here offers a myriad of synthetic possibilities. A possible downside of this template however is the large degree of flexibility in the cyclic peptide backbone. To achieve a higher degree of structural preorganization, we have developed a selectively addressable TriAzaCyclophane scaffold. This relatively small scaffold molecule can be synthesized on gram-scale, is compatible with solid phase peptide chemistry, and has been successfully applied in various studies involving synthetic receptors[78,79], papain inhibitors[80], the development of a whooping cough vaccine[81] and mimicry of protein discontinuous epitopes.[82]

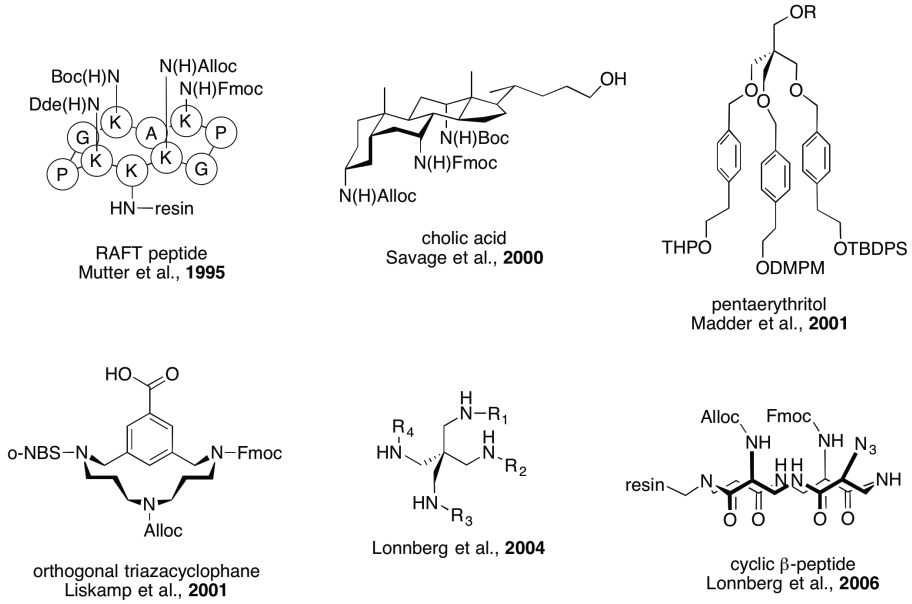

Figure 7 | Orthogonal molecular scaffolds for protein design

Current approaches in the development of scaffolds for protein mimicry all hint at the importance of multiple orthogonal conjugation possibilities and emphasize the need for efficient ligation techniques.[83] The advances in the field of chemoselective ligation have facilitated the development of heteromultifunctional scaffolds that harness 'click' reactions: "reactions that are modular, wide in scope, give very high yields, generate only inoffensive byproducts that can be removed by non-chromatographic methods and are stereospecific" as defined by Sharpless et al.[84] An additional advantage of the use of chemoselective ligation techniques for the assembly of peptides is that these techniques allow the use of unprotected peptides, which enhances the synthetic applicability in this field.

Although there are many scaffolds that contain a heterobifunctional linker and some examples of trifunctional crosslinkers are known[85-88], relatively few scaffolds combine the capacity of attaching multiple ligands with structural preorganization of the ligands. Most trifunctional scaffolds allow the attachment of a wide range of substrates, but approaches for accurate assembly and pre-organization of constrained peptides are limited. Scaffold-based approaches that do provide a certain degree of structural pre-organization and allow the attachment of sequence-independent cyclic peptides are limited to bicyclic systems.

1.4 Applications of discontinuous protein binding site mimics in drug design

Interactions on protein binding sites are critical in mediating a variety of biological processes, such as cell proliferation, growth and differentiation. Therefore, successful mimics of these binding sites could offer approaches to regulating and interfering in biological processes.

Toward this goal, small mimics have been devised for peptide structural elements like strands, sheets, helices, turns, and loops, but there are very few examples of medium-size mimics for discontinuous surfaces of proteins. A number of approaches to multi-loop mimicry have been described in recent years, as was summarized in the previous paragraph. Whereas the early approaches only describe the synthetic technology for the generation of multiloop constructs and hint at their possible future applications,

the more recent approaches use this technology for the development of biologically active compounds.

1.4.1 – Multiloop peptides as inhibitors of protein-protein interactions

Protein binding sites have proven to be complex targets for drug developers. The nature of these binding sites, including their large and shallow surfaces and discontinuous character, limits the success of typical (small molecule) HTS campaigns in discovering protein–protein interactions antagonists.[4,5]

The generation of multiloop peptides has resulted in some potent inhibitors of cellular processes. A number of recent studies using phage display libraries in combination with CLIPS-technology as described by Heinis and Winter[40], have led to the identification of potent and specific bicyclic peptide inhibitors of different serine proteases.

Other bicyclic peptide-based protein mimics have been developed, but these mostly involve single attempts that only lead to a proof of principle or a structural mimic of a single protein.[89,90]

1.4.2 – Protein mimics in structural vaccinology

Probably the most appealing application of multiloop peptides as protein mimics lies in the field of structural vaccinology and immunotherapy.[9] Advances in X-ray crystallography and NMR spectroscopy have increased the throughput of protein structure determination and have led to the identification of epitopes of antigens and other protein targets that are difficult to address by using standard immunotherapeutic approaches. The increasing amount of structural information in combination with the recent progress in chemical biology, brings scientists a step closer to developing vaccines against these targets, such as tuberculosis, malaria, HIV/AIDS or pandemic influenza.[91] For a long time it has been predicted that three dimensional structural information could be used to design novel and improved antigens, and currently first approaches of structure-based antigen design have become reality.[92-97]

Synthetic peptide-based constructs have multiple possible applications in antigen-design. Firstly, functional mimics of protein antigenic sites can be used to generate neutralizing antibodies against their cognate epitopes. Peptide mimics of linear protein epitopes have been successfully used for this purpose; however, immunogenic mimicry has proven to be difficult to achieve for discontinuous protein epitopes.[20,98] To date,

only a few peptides have been reported that act as immunogenic mimics of protein discontinuous epitopes, either selected from phage display peptide libraries[99,100] or based on rational design.[101] One of the reasons of this small number of successful candidates may relate to the inability of peptides to assume the desired conformation of the native epitopes. The structural preorganization that is offered by scaffolded- or multicyclic peptides could represent a significant improvement for this purpose. Indeed, some successful examples of constrained peptides have been developed in recent years. CLIPS-peptides mimics of the β3-loop of hFSH were able to generate antisera with high cross-reactivity to hFSH and neutralizing capacity[102], whereas attempts with the corresponding linear peptides failed.

A second application of peptide mimics of protein antigenic sites is in epitope mapping studies. The generation of overlapping sets of constrained peptides has revealed valuable information about the binding sites of antigens and therapeutic mAbs and had provided important insight into the mechanism of action of therapeutic antibodies.[103] The latest example of peptides[101,104,105] as mimics of complex antigenic sites provide a good perspective of what might be achievable for other protein targets, potentially even for the most challenging targets like GPCRs or even viruses like HIV.

1.4.3 – Mimicry of the discontinuous CD4-binding site of HIV-1 gp120

Despite the vast amount of research that is dedicated to the development of an HIV-1 vaccine, an effective vaccine against this chronic infection remains elusive.[106-111] A major obstacle for vaccine development is the genetic variability of the virus, which has given rise to multiple genetic subtypes of HIV-1 that exhibit a wide spectrum of antigenic diversity within and between subtypes.[112]

An effective vaccine against HIV-1 will need to induce antibodies that prevent initial infection of host cells or limit early events of viral dissemination. Therefore, such antibodies should target surface envelope glycoproteins of HIV-1. Efforts to develop an effective HIV-1 vaccine have emphasized the ability to elicit neutralizing antibodies (nAbs), however HIV-1 evades many nAbs by altering primary recognition sequences in surface loops and by shielding the more conserved epitopes with N-linked glycans. As a result, most anti-Env antibodies induced during HIV-infection or by vaccination with Env-based vaccines are non-neutralizing.

Various attempts have been undertaken to overcome these evasion strategies by

focusing on a more detailed understanding of these broadly neutralizing antibodies and their epitopes. Detailed atomic-level structural information of several regions of HIV-1 has provided important insight for HIV-1 vaccine design. Especially using epitope maps in conjunction with the X-ray crystal structure of a ternary complex that includes a gp120 core, CD4 and a neutralizing antibody, valuable knowledge was obtained on the Env-structure and neutralization epitopes on gp120.[113,114] Key binding residues on gp120 were revealed, and important conserved functional regions were detected on the surface glycoprotein. These conserved regions have served as important starting points for the design of novel vaccine immunogens.

Since the conserved CD4 binding site on gp120 involves discontinuous epitopes and is structurally complex, mimicry of this binding site might be achieved by a combination of constrained peptides. Several attempts towards this goal have been described, all involving combinations of linear peptides on relatively simple scaffold molecules.[115-117] These synthetic gp120 mimics were all based on the conserved regions C2, C3 and C4 and contained the five amino acids that are thought to be most important for binding to CD4; Thr^{257} (C2), Asp^{368} and Glu^{370} (C3) and Trp^{427} and Asp^{457} (C4). In addition to their highly conserved character, these residues fall within the epitope of a broadly reactive nAb.[118] The synthetic immunogens described in these studies were able to compete with gp120 for binding to CD4 with IC_{50} values in the micromolar range and some preliminary immunization experiments were performed. Although these results indicate the potential of peptide-based discontinuous epitope mimics as immunogens, further research is required towards functional mimics of the discontinuous CD4-binding site of HIV-1 gp120 as immunogen candidates. Taking a closer look at the X-ray crystal structure of the gp120 core, CD4 and a neutralizing antibody and focusing on the major binding residues of gp120, it is clearly visible that these residues are located in loop-like structures on the protein surface (Figure 8). Therefore, cyclic peptides might give closer mimics of the binding regions than their linear counterparts and a multicyclic peptide conjugate might be an accurate mimic of the discontinuous epitope of HIV-1 gp120.

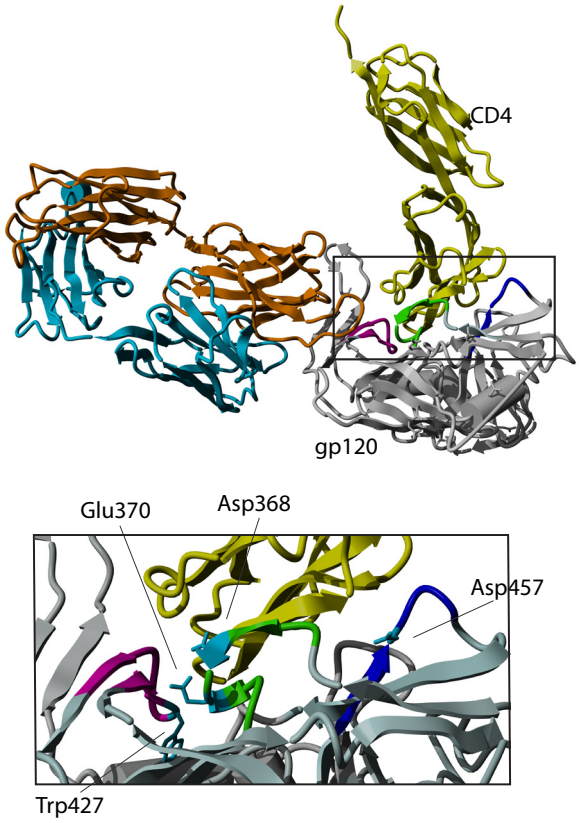

Figure 8 | Top: Crystal structure of the HIV-1 gp120 envelope glycoprotein in complex with the CD4 receptor and a neutralizing human antibody (cyan/orange). Bottom: The CD4 binding site of HIV-1 gp120. Conserved regions are indicated in blue, magenta and green. The key binding residues are indicated in cyan. PDB: 1GC1

Upon the start of the project that is described in this thesis, a first method for the synthesis of a discontinuous epitope mimic of HIV-1 had been developed.[82] This synthesis represents the first example of a multiloop compound carrying three different cyclic peptides corresponding to the conserved domains of the surface protein gp120. Although the desired compound has successfully been synthesized, the mimic was not capable of preventing viral infection in a cell-based assay. This result points at the potential problem of whether the ideal mimic has been synthesized. Considering the importance of 3D conformation in molecular recognition and the difficulty of predicting conformations of complex protein mimics, a more flexible and less time

consuming synthetic approach would be desired in search of effective discontinuous epitope mimics. Attempts towards this goal will be described in this thesis.

1.5 Aim and outline of this thesis

The research described in this thesis aims at the development of a method for the synthesis of mimics of discontinuous protein binding sites, as well as the study of the binding properties of the resulting molecules to their natural ligand. Of the many existing biologically relevant discontinuous protein binding sites, the HIV envelope protein gp120 was chosen as a target for mimicry in this thesis.

As was outlined in the previous paragraphs, multiple elements are required in order to obtain close structural and functional mimics of discontinuous protein binding sites. First of all, key binding regions should be identified and peptides representing these regions should be synthesized. Since these regions often have loop-like structures, adequate mimicry can be achieved using cyclic peptides. In addition, the assembly of multiple constrained peptides as well as the 3D-orientation of the ensemble of binding regions are crucial aspects in the development of discontinuous protein binding site mimics. A central element in this process is the use of molecular scaffolds which provide a proper arrangement, orientation and perhaps even pre-organization of the peptide segments that comprise the discontinuous protein binding site.

Essential components of the protein binding site mimics described in this thesis are cyclic peptides, representing the different peptide segments that constitute the discontinuous CD4 binding site of HIV gp120. The development of an efficient and reliable method for the synthesis of cyclic peptides is described in **chapter 2**. Once a reliable method for the synthesis of cyclic peptides is available, the second challenge in the construction of protein binding site mimics is the conjugation of multiple cyclic peptides in one molecule. Different strategies for the attachment of cyclic peptides to a scaffold molecule are described in **chapter 3**. The chemistry described in this chapter has provided important insights on working with cyclic peptides, the advantages and downsides of solid phase chemistry for these purposes and has underlined the importance of proper analysis of synthetic processes. The insights obtained in chapter 3 have resulted in a click chemistry based approach, which was applied for the first

time in **chapter 4** for the generation of a collection of mimics of the discontinuous epitope of HIV gp120. In addition, the thus-obtained mimics were tested for binding to their natural ligand using competitive ELISA.

The broad applicability of this approach is further demonstrated in **chapter 5**, where the approach is applied on different scaffold molecules. Furthermore, this chapter describes the incorporation of cyclic peptides with a different loop-size. The use of different scaffold molecules or cyclic peptides allowed the analysis of the effect of these different parameters on the binding of the resulting mimics to their target, and resulted in the synthesis of mimics with improved binding characteristics.

Based on the results of chapters 2-5, several suggestions for further research are proposed in **chapter 6.** This chapter will briefly summarize the most important results of this thesis, present some preliminary results of cell-based experiments and suggest some topics for future research based on the approach that was developed in this thesis.

Chapter 2: Approaches for the synthesis of cyclic peptides

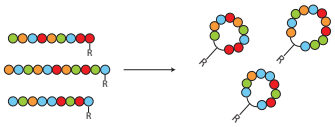

Chapter 3: Strategies for the attachment of cyclic peptides to the TAC-scaffold

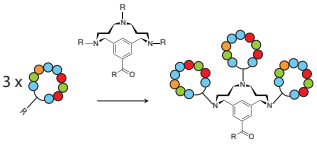

Chapter 4: A combinatorial approach toward libraries of mimics of the discontinuous epitope of HIV gp120

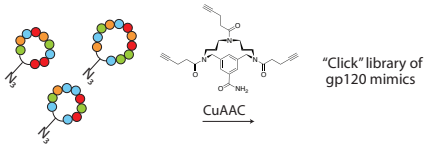

Chapter 5: Scaffold- and ring-size optimization in discontinuous epitope containing protein mimics

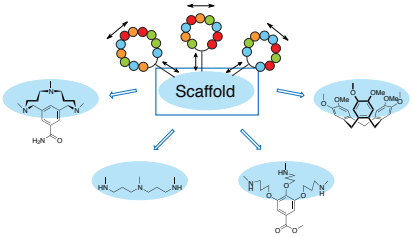

Chapter 6: Additional binding experiments and directions for future research

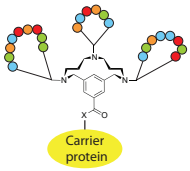

Figure 9 | Outline of this thesis

References:

(1) Robinson, J. A.; DeMarco, S.; Gombert, F.; Moehle, K.; Obrecht, D. *Drug Discov. Today* **2008**, *13*, 944–951.
(2) Kossiakoff, A. A.; Koide, S. *Curr. Opin. Struct. Biol.* **2008**, *18*, 499–506.
(3) Yin, H.; Hamilton, A. D. *Angew. Chem. Int. Ed.* **2005**, *44*, 4130–4163.
(4) Pellecchia, M. *J. Med. Chem.* **2013**, *56*, 13–14.
(5) Conte, L. L.; Chothia, C.; Janin, J. *J. Mol. Biol.* **1999**, *285*, 2177–2198.
(6) Wells, J. A.; McClendon, C. L. *Nature* **2007**, *450*, 1001–1009.
(7) Fairlie, D. P.; West, M. L.; Wong, A. K. *Curr. Med. Chem.* **1998**, *5*, 29–62.
(8) Rosen, O.; Anglister, J. Methods Mol. Biol., 2009; Vol. 524, pp. 37–57.
(9) Robinson, J. A. *J. Pept. Sci.* **2013**, *19*, 127–140.
(10) Sidhu, S. S.; Fairbrother, W. J.; Deshayes, K. *ChemBioChem* **2003**, *4*, 14–25.
(11) Clackson, T.; Wells, J. *Science* **1995**, *267*, 383–386.
(12) Bogan, A. A.; Thorn, K. S. *J. Mol. Biol.* **1998**, *280*, 1–9.
(13) DeLano, W. L. *Curr. Opin. Struct. Biol.* **2002**, *12*, 14–20.
(14) Wells, J. A. *Meth. Enzymol.* **1991**, *202*, 390–411.
(15) Ma, B.; Wolfson, H. J.; Nussinov, R. *Curr. Opin. Struct. Biol.* **2001**, *11*, 364–369.
(16) Ma, B.; Elkayam, T.; Wolfson, H.; Nussinov, R. *Proc. Natl. Acad. Sci.* **2003**, *100*, 5772–5777.
(17) Ezkurdia, I.; Bartoli, L.; Fariselli, P.; Casadio, R.; Valencia, A.; Tress, M. L. *Brief. Bioinform.* **2008**, *10*, 233–246.
(18) Mayrose, I.; Penn, O.; Erez, E.; Rubinstein, N. D.; Shlomi, T.; Freund, N. T.; Bublil, E. M.; Ruppin, E.; Sharan, R.; Gershoni, J. M.; Martz, E.; Pupko, T. *Bioinformatics* **2007**, *23*, 3244–3246.
(19) Liu, R.; Hu, J. *J. Proteomics Bioinform.* **2011**, *04*.
(20) Van Regenmortel, M. H. V. *Biologicals* **2001**, *29*, 209–213.
(21) White, C. J.; Yudin, A. K. *Nature Chem.* **2011**, *3*, 509–524.
(22) Rizo, J.; Gierasch, L. M. *Annu. Rev. Biochem.* **1992**, *61*, 387–416.
(23) Gilon, C.; Halle, D.; Chorev, M.; Selincer, Z.; Byk, G. *Biopolymers* **1991**, *31*, 745–750.
(24) Lambert, J. N.; Mitchell, J. P.; Roberts, K. D. *J. Chem. Soc., Perkin Trans. 1* **2001**, 471–484.
(25) Bock, J. E.; Gavenonis, J.; Kritzer, J. A. *ACS Chem. Biol.* **2013**, *8*, 488–499.
(26) Montalbetti, C. A. G. N.; Falque, V. *Tetrahedron* **2005**, *61*, 10827–10852.
(27) Albericio, F.; Hammer, R. P.; Garcia-Echeverria, C.; Molins, M. A.; Chang, J. L.; Munson, M. C.; Pons, M. Q.; Barany, G. *Int. J. Pept. Protein Res.* **2009**, *37*, 402–413.
(28) Camarero, J. A.; Muir, T. W. *Chem. Commun.* **1997**, *0*, 1369–1370.
(29) Kent, S.; Sohma, Y.; Liu, S.; Bang, D.; Pentelute, B.; Mandal, K. *J. Pept. Sci.* **2012**, *18*, 428–436.
(30) Zhang, L.; Tam, J. P. *J. Am. Chem. Soc.* **1997**, *119*, 2363–2370.
(31) Tulla-Puche, J.; Barany, G. *J. Org. Chem.* **2004**, *69*, 4101–4107.
(32) Shao, Y.; Lu, W.; Kent, S. B. *Tetrahedron Lett.* **1998**, *39*, 3911–3914.
(33) Kleineweischede, R.; Hackenberger, C. P. R. *Angew. Chem. Int. Ed.* **2008**, *47*, 5984–5988.
(34) Miller, S. J.; Blackwell, H. E.; Grubbs, R. H. *J. Am. Chem. Soc.* **1996**, *118*, 9606–9614.

(35) Rostovtsev, V. V.; Green, L. G.; Fokin, V. V.; Sharpless, K. B. *Angew. Chem. Int. Ed.* **2002**, 2596-2597.
(36) Tornøe, C. W.; Christensen, C.; Meldal, M. *J. Org. Chem.* **2002**, *67*, 3057–3064.
(37) Bock, V. D.; Perciaccante, R.; Jansen, T. P.; Hiemstra, H.; van Maarseveen, J. H. *Org. Lett.* **2006**, *8*, 919–922.
(38) Turner, R. A.; Oliver, A. G.; Lokey, R. S. *Org. Lett.* **2007**, *9*, 5011–5014.
(39) Timmerman, P.; Beld, J.; Puijk, W. C.; Meloen, R. H. *ChemBioChem* **2005**, *6*, 821–824.
(40) Heinis, C.; Rutherford, T.; Freund, S.; Winter, G. *Nature Chem. Biol.* **2009**, *5*, 502–507.
(41) Angelini, A.; Cendron, L.; Chen, S.; Touati, J.; Winter, G.; Zanotti, G.; Heinis, C. *ACS Chem. Biol.* **2012**, *7*, 817–821.
(42) Chen, S.; Morales-Sanfrutos, J.; Angelini, A.; Cutting, B.; Heinis, C. *ChemBioChem* **2012**, *13*, 1032–1038.
(43) Baeriswyl, V.; Rapley, H.; Pollaro, L.; Stace, C.; Teufel, D.; Walker, E.; Chen, S.; Winter, G.; Tite, J.; Heinis, C. *ChemMedChem* **2012**, *7*, 1173–1176.
(44) Craik, D. J.; Daly, N. L.; Bond, T.; Waine, C. *J. Mol. Biol.* **1999**, *294*, 1327–1336.
(45) Craik, D. J.; Swedberg, J. E.; Mylne, J. S.; Cemazar, M. *Expert Opin. Drug Discov.* **2012**, *7*, 179–194.
(46) Wong, C. T. T.; Rowlands, D. K.; Wong, C.-H.; Lo, T. W. C.; Nguyen, G. K. T.; Li, H.-Y.; Tam, J. P. *Angew. Chem. Int. Ed.* **2012**, *124*, 5718–5722.
(47) Wu, C.; Leroux, J.-C.; Gauthier, M. A. *Nature Chem.* **2012**, *4*, 1044–1049.
(48) Smeenk, L. E. J.; Dailly, N.; Hiemstra, H.; van Maarseveen, J. H.; Timmerman, P. *Org. Lett.* **2012**, *14*, 1194–1197.
(49) Craik, D. J. *Science* **2006**, *311*, 1563–1564.
(50) Ghosh, P. S.; Hamilton, A. D. *J. Am. Chem. Soc.* **2012**, *134*, 13208–13211.
(51) Rebollo, I. R.; Angelini, A.; Heinis, C. *Med. Chem. Commun.* **2013**, *4*, 145.
(52) Roy, L.; Case, M. A. *J. Am. Chem. Soc.* **2010**, *132*, 8894–8896.
(53) Singh, Y.; Dolphin, G. T.; Razkin, J.; Dumy, P. *ChemBioChem* **2006**, *7*, 1298–1314.
(54) Mutter, M.; Vuilleumier, S. *Angew. Chem. Int. Ed.* **1989**, *28*, 535–554.
(55) DeGrado, W. F.; Wasserman, Z. R.; Lear, J. D. *Science* **1989**, *243*, 622–628.
(56) Katz, E.; Heleg-Shabtai, V.; Willner, I.; Rau, H. K.; Haehnel, W. *Angew. Chem. Int. Ed.* **1998**, *37*, 3253–3256.
(57) Katz, E.; Heleg-Shabtai, V.; Bardea, A.; Willner, I.; Rau, H. K.; Haehnel, W. *Biosens. Bioelectron.* **1998**, *13*, 741–756.
(58) Willner, I.; Heleg-Shabtai, V.; Katz, E.; Rau, H. K.; Haehnel, W. *J. Am. Chem. Soc.* **1999**, *121*, 6455–6468.
(59) Opatz, T.; Kallus, C.; Wunberg, T.; Schmidt, W.; Henke, S.; Kunz, H. *Carbohydr. Res.* **2002**, *337*, 2089–2110.
(60) Davis, A. P.; Perry, J. J.; Williams, R. P. *J. Am. Chem. Soc.* **1997**, *119*, 1793–1794.
(61) Andreetti, G. D.; Ori, O.; Ugozzoli, F.; Alfieri, C.; Pochini, A.; Ungaro, R. *J. Inclusion Phenom.* **1988**, *6*, 523–536.
(62) Collet, A. *Tetrahedron* **1987**, *43*, 5725–5759.
(63) Rump, E. T.; Rijkers, D. T. S.; Hilbers, H. W.; de Groot, P. G.; Liskamp, R. M. J. *Chemistry* **2002**, *8*, 4613–4621.

(64) van Ameijde, J.; Liskamp, R. M. J. *Org. Biomol. Chem.* **2003**, *1*, 2661–2669.
(65) Chamorro, C.; Liskamp, R. M. J. *J. Comb. Chem.* **2003**, *5*, 794–801.
(66) Chamorro, C.; Liskamp, R. M. J. *Tetrahedron* **2004**, *60*, 11145–11157.
(67) Ikeda, A.; Shinkai, S. *Chem. Rev.* **1997**, *97*, 1713–1734.
(68) Park, H. S.; Lin, Q.; Hamilton, A. D. *J. Am. Chem. Soc.* **1999**, *121*, 8–13.
(69) Kemp, D. S.; Petrakis, K. S. *J. Org. Chem.* **1981**, *46*, 5140–5143.
(70) Goodman, M.; Feng, Y.; Melacini, G.; Taulane, J. P. *J. Am. Chem. Soc.* **1996**, *118*, 5156–5157.
(71) Dumy, P.; Eggleston, I. M.; Cervigni, S.; Sila, U.; Sun, X.; Mutter, M. *Tetrahedron Lett.* **1995**, *36*, 1255–1258.
(72) Peluso, S.; Dumy, P.; Eggleston, I. M.; Garrouste, P.; Mutter, M. *Tetrahedron* **1997**, *53*, 7231–7236.
(73) Barry, J. F.; Davis, A. P.; Nieves Pérez-Payan, M.; Elsegood, M. R. J.; Jackson, R. F. W.; Gennari, C.; Piarulli, U.; Gude, M. *Tetrahedron Lett.* **1999**, *40*, 2849–2852.
(74) Zhou, X. T.; Rehman, A.; Li, C.; Savage, P. B. *Org. Lett.* **2000**, *2*, 3015–3018.
(75) Katajisto, J.; Heinonen, P.; Lönnberg, H. *J. Org. Chem.* **2004**, *69*, 7609–7615.
(76) Virta, P.; Karskela, M.; Lönnberg, H. *J. Org. Chem.* **2006**, *71*, 1989–1999.
(77) Farcy, N.; De Muynck, H.; Madder, A.; Hosten, N.; De Clercq, P. J. *Org. Lett.* **2001**, *3*, 4299–4301.
(78) Chamorro, C.; Hofman, J.-W.; Liskamp, R. M. J. *Tetrahedron* **2004**, *60*, 8691–8697.
(79) Albada, H. B.; Liskamp, R. M. J. *J. Comb. Chem.* **2008**, *10*, 814–824.
(80) van Zoelen, D.-J.; Egmond, M. R.; Pieters, R. J.; Liskamp, R. M. J. *ChemBioChem* **2007**, *8*, 1950–1956.
(81) Hijnen, M.; van Zoelen, D. J.; Chamorro, C.; van Gageldonk, P.; Mooi, F. R.; Berbers, G.; Liskamp, R. M. J. *Vaccine* **2007**, *25*, 6807–6817.
(82) Chamorro, C.; Kruijtzer, J. A. W.; Farsaraki, M.; Balzarini, J.; Liskamp, R. M. J. *Chem. Commun.* **2009**, 821.
(83) Beal, D. M.; Jones, L. H. *Angew. Chem. Int. Ed.* **2012**, *51*, 6320–6326.
(84) Kolb, H. C.; Finn, M. G.; Sharpless, K. B. *Angew. Chem. Int. Ed.* **2001**, *40*, 2004–2021.
(85) Clavé, G.; Boutal, H.; Hoang, A.; Perraut, F.; Volland, H.; Renard, P.-Y.; Romieu, A. *Org. Biomol. Chem.* **2008**, *6*, 3065–3078.
(86) Clavé, G.; Volland, H.; Flaender, M.; Gasparutto, D.; Romieu, A.; Renard, P.-Y. *Org. Biomol. Chem.* **2010**, *8*, 4329–4345.
(87) Valverde, I. E.; Delmas, A. F.; Aucagne, V. *Tetrahedron* **2009**, *65*, 7597–7602.
(88) Beal, D. M.; Albrow, V. E.; Burslem, G.; Hitchen, L.; Fernandes, C.; Lapthorn, C.; Roberts, L. R.; Selby, M. D.; Jones, L. H. *Org. Biomol. Chem.* **2012**, *10*, 548–554.
(89) Franke, R.; Doll, C.; Wray, V.; Eichler, J. *Org. Biomol. Chem.* **2004**, *2*, 2847–2851.
(90) Singh, Y.; Stoermer, M. J.; Lucke, A. J.; Guthrie, T.; Fairlie, D. P. *J. Am. Chem. Soc.* **2005**, *127*, 6563–6572.
(91) Dormitzer, P. R.; Grandi, G.; Rappuoli, R. *Nature Rev. Microbiol.* **2012**, *10*, 807–813.
(92) Scarselli, M.; Arico, B.; Brunelli, B.; Savino, S.; Di Marcello, F.; Palumbo, E.; Veggi, D.; Ciucchi, L.; Cartocci, E.; Bottomley, M. J.; Malito, E.; Surdo, Lo, P.; Comanducci, M.; Giuliani, M. M.; Cantini, F.; Dragonetti, S.; Colaprico, A.; Doro, F.; Giannetti, P.; Pallaoro,

M.; Brogioni, B.; Tontini, M.; Hilleringmann, M.; Nardi-Dei, V.; Banci, L.; Pizza, M.; Rappuoli, R. *Sci. Transl. Med.* **2011**, *3*, 91ra62–91ra62.

(93) Nuccitelli, A.; Cozzi, R.; Gourlay, L. J.; Donnarumma, D.; Necchi, F.; Norais, N.; Telford, J. L.; Rappuoli, R.; Bolognesi, M.; Maione, D.; Grandi, G.; Rinaudo, C. D. *Proc. Natl. Acad. Sci.* **2011**, *108*, 10278–10283.

(94) Swanson, K. A.; Settembre, E. C.; Shaw, C. A.; Dey, A. K.; Rappuoli, R.; Mandl, C. W.; Dormitzer, P. R.; Carfi, A. *Proc. Natl. Acad. Sci.* **2011**, *108*, 9619–9624.

(95) McLellan, J. S.; Correia, B. E.; Chen, M.; Yang, Y.; Graham, B. S.; Schief, W. R.; Kwong, P. D. *J. Mol. Biol.* **2011**, *409*, 853–866.

(96) Steel, J.; Lowen, A. C.; Wang, T. T.; Yondola, M.; Gao, Q.; Haye, K.; García-Sastre, A.; Palese, P. *MBio* **2010**, *1*, 1–9.

(97) Johnson, S.; Tan, L.; van der Veen, S.; Caesar, J.; De Jorge, E. G.; Harding, R. J.; Bai, X.; Exley, R. M.; Ward, P. N.; Ruivo, N.; Trivedi, K.; Cumber, E.; Jones, R.; Newham, L.; Staunton, D.; Ufret-Vincenty, R.; Borrow, R.; Pickering, M. C.; Lea, S. M.; Tang, C. M. *PLoS Pathog.* **2012**, *8*, e1002981.

(98) Irving, M. B.; Craig, L.; Menendez, A.; Gangadhar, B. P.; Montero, M.; van Houten, N. E.; Scott, J. K. *Mol. Immunol.* **2010**, *47*, 1137–1148.

(99) Matthews, L. J.; Davis, R.; Smith, G. P. *J. Immunol.* **2002**, *169*, 837–846.

(100) Dorgham, K.; Dogan, I.; Bitton, N.; Parizot, C.; Cardona, V.; Debré, P.; Hartley, O.; Gorochov, G. *AIDS Res. Hum. Retroviruses* **2005**, *21*, 82–92.

(101) Villén, J.; Rodríguez-Mias, R. A.; Núñez, J. I.; Giralt, E.; Sobrino, F.; Andreu, D. *Chem. Biol.* **2006**, *13*, 815–823.

(102) Timmerman, P.; Puijk, W. C.; Meloen, R. H. *J. Mol. Recognit.* **2007**, *20*, 283–299.

(103) Timmerman, P.; Meloen, R. H.; Puijk, W. C.; Boshuizen, R. S.; van Dijken, P.; Slootstra, J. W.; Beurskens, F. J.; Parren, P. W. H. I.; Huber, A.; Bachmann, M. F. *Open Vaccine J.* **2009**, *2*, 56–67.

(104) Cao, Y.; Lu, Z.; Li, P.; Sun, P.; Fu, Y.; Bai, X.; Bao, H.; Chen, Y.; Li, D.; Liu, Z. *J. Virol. Methods* **2012**, *185*, 124–128.

(105) Peri, C.; Gagni, P.; Combi, F.; Gori, A.; Chiari, M.; Longhi, R.; Cretich, M.; Colombo, G. *ACS Chem. Biol.* **2013**, *8*, 397–404.

(106) Zhou, T.; Georgiev, I.; Wu, X.; Yang, Z.-Y.; Dai, K.; Finzi, A.; Kwon, Y. D.; Scheid, J. F.; Shi, W.; Xu, L.; Yang, Y.; Zhu, J.; Nussenzweig, M. C.; Sodroski, J.; Shapiro, L.; Nabel, G. J.; Mascola, J. R.; Kwong, P. D. *Science* **2010**, *329*, 811–817.

(107) Mascola, J. R.; Montefiori, D. C. *Annu. Rev. Immunol.* **2010**, *28*, 413–444.

(108) Walker, L. M.; Huber, M.; Doores, K. J.; Falkowska, E.; Pejchal, R.; Julien, J.-P.; Wang, S.-K.; Ramos, A.; Chan-Hui, P.-Y.; Moyle, M.; Mitcham, J. L.; Hammond, P. W.; Olsen, O. A.; Phung, P.; Fling, S.; Wong, C.-H.; Phogat, S.; Wrin, T.; Simek, M. D.; Protocol G Principal Investigators; Koff, W. C.; Wilson, I. A.; Burton, D. R.; Poignard, P. *Nature* **2011**, *477*, 466–470.

(109) Glidden, D. V. *Nature* **2012**, *490*, 350–351.

(110) Rolland, M.; Manocheewa, S.; Swain, J. V. *J. Virol.* **2013**.

(111) Shapiro, S. Z. *AIDS Res. Hum. Retroviruses* **2013**.

(112) Gilbert, P.; Wang, M.; Wrin, T.; Petropoulos, C.; Gurwith, M.; Sinangil, F.; D'Souza, P.;

Rodriguez Chavez, I. R.; DeCamp, A.; Giganti, M.; Berman, P. W.; Self, S. G.; Montefiori, D. C. *J. Infect. Dis.* **2010**, *202*, 595–605.

(113) Kwong, P. D.; Wyatt, R.; Robinson, J.; Sweet, R. W.; Hendrickson, W. A.; Sodroski, J. *Nature* **1998**, *393*, 648–659.

(114) Wyatt, R.; Kwong, P. D.; Desjardins, E. *Nature* **1998**.

(115) Howie, S. E.; Cotton, G. J.; Heslop, I.; Martin, N. J.; Harrison, D. J.; Ramage, R. *FASEB J.* **1998**, *12*, 991–998.

(116) Franke, R.; Hirsch, T.; Eichler, J. *J. Recept. Signal Transduct. Res.* **2006**, *26*, 453–460.

(117) Franke, R.; Hirsch, T.; Overwin, H.; Eichler, J. *Angew. Chem. Int. Ed.* **2007**, *46*, 1253–1255.

(118) Thali, M.; Moore, J. P.; Furman, C.; Charles, M.; Ho, D. D.; Robinson, J.; Sodroski, J. *J. Virol.* **1993**, *67*, 3978–3988.

2

Approaches for the synthesis of cyclic peptides containing conserved residues of the CD4-binding site of HIV-gp120

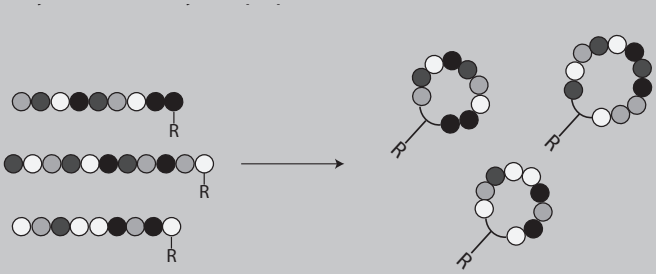

2.1 Introduction

Mimicry of discontinuous epitopes starts with the synthesis of molecules that could mimic the individual epitopes in a proper way. The epitopes of interest are usually short peptide sequences, often lying far apart in the linear protein sequence. Since interacting epitopes are most commonly present as loop-like structures, cyclic peptides are likely to be suitable candidates for mimicry of these protein fragments. In addition, cyclic peptides can bind with high affinity and specificity to disease targets and hence are an attractive molecule class for the development of therapeutics.[1] Moreover, cyclic peptides have some advantages over their linear counterparts in terms of chemical and enzymatic stability, and they may possess improved pharmacodynamic properties.[2-4] Another feature that contributes to the attractiveness of cyclic peptides as part of protein mimics, is their reduced conformational mobility and flexibility.[5]The structural pre-organization in cyclic peptides causes a decrease in loss of entropy upon binding to their targets and typically improves both their receptor affinity and -selectivity.[6-9]
As was described in the general introduction, we are interested in the CD4-binding

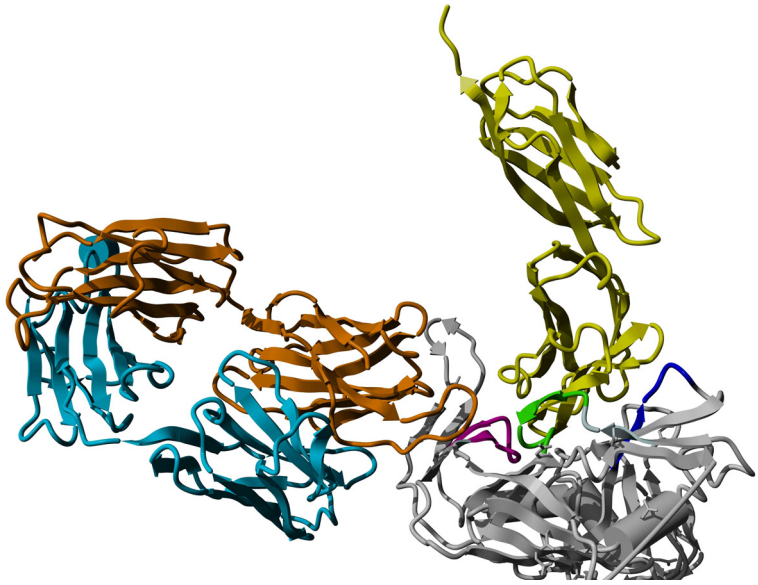

Figure 1 | Crystal structure of gp120 (grey) with a two-domain fragment of human CD4 (yellow) and an antigen-binding fragment of neutralizing antibody Fab 17b (light chain in light blue, heavy chain in orange). PDB: 1GC1

site on HIV gp120. This binding site has a discontinuous character, and detailed information on the residues important for CD4-binding could be obtained from the crystal structure of a gp120-CD4 complex[10,11] and previous studies on this interaction.[12] Primary contact residues in gp120 for its interaction with CD4 are D368, E370, W427, and D457, which are all conserved residues among primate immunodeficiency viruses. Thus, these residues, and the protein regions in which these contact residues are located, are important for inclusion in a discontinuous epitope mimic.

2.1.1 – Synthetic strategies for cyclic peptides

Crucial for the development of potent discontinuous epitope mimics, is the efficient synthesis of cyclic peptides representing the epitopes. Although widely used in every conceivable branch of chemistry and biology, synthesis and purification of cyclic peptides irrespective of their size and amino acid composition remains a great challenge.[13] Many cyclic peptides are notoriously difficult to prepare, and the success of the synthetic approach is often heavily influenced by the amino acid constituents of the cyclic peptide, the ring-closing strategy and the desired ring-size. Numerous approaches for the synthesis of cyclic peptides have been described, and all of them have both advantages and limitations.[13-27]

Depending on its functional groups, on the application of the cyclic peptides and/or on the desired technique for conjugation to other molecules, a peptide can be cyclized in four different ways: head-to-tail (C-terminus to N-terminus), head-to-side chain, side chain-to-tail or side chain-to-side chain[3] (Figure 2). Cyclization can take place via classical amide-bond formation reactions[28], disulfide-formation[29], or via the use of orthogonal ligation methods[13,20,30-34]. Peptide macrocyclization reactions can be performed in solution or on the solid support and especially the field of solid-supported macrocyclizations has been actively explored in recent years. The main advantage of solid-supported macrocyclizations is that the standard washing and filtration procedures used in solid phase peptide synthesis are often enough for purification. Macrocyclizations in solution are usually best performed in very dilute conditions to minimize unwanted intermolecular reactions. Although these conditions increase the selectivity of the reaction, they generally slow down the reaction speed, thereby increasing reaction times and the risk on side product-formation. In addition, macrocyclization in solution is usually performed on partially protected peptides, and the solubility of these peptides is unpredictable and often poor.

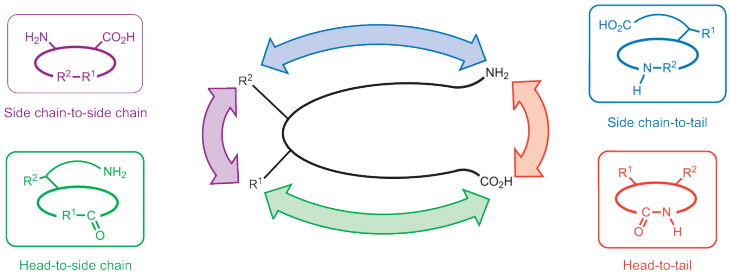

Figure 2 | The four possible ways for macrocyclization of peptides. Reprinted by permission from Macmillan Publishers Ltd: Nature Chemistry, copyright 2011.[3]

In addition to these synthetic considerations, also functional and conformational properties need to be taken into account when synthesizing cyclic peptides for mimicry of protein binding sites. The interactions between protein binding sites often do not involve backbone-interactions between large peptide- or protein-fragments, but mostly heavily rely on certain contact residues that are present in the epitopes. When cyclic peptides are used for mimicry of these epitopes, proper positioning of the main contact residues is of great importance, and peptide conformation is a crucial feature with respect to its biological activity. Therefore, the site and method for macrocyclization must be carefully selected, since these factors can strongly influence the peptide conformation.

This chapter describes the development of a high-yielding method for the synthesis of cyclic peptides, representing conserved regions in the CD4-binding site of HIV gp120. Both solid-supported and solution-phase methods for peptide macrocyclization were explored, and special attention was paid to the purification of the resulting cyclic peptides.

2.2 Results and discussion

2.2.1 – The non-stop solid phase synthesis of a discontinuous epitope mimic

The first synthesis of a discontinuous epitope mimic of the CD4-binding site of HIV gp120 carrying multiple different cyclic peptides, was a non-stop solid phase approach (Scheme 2). In this approach, linear peptides are built up followed by a solid-

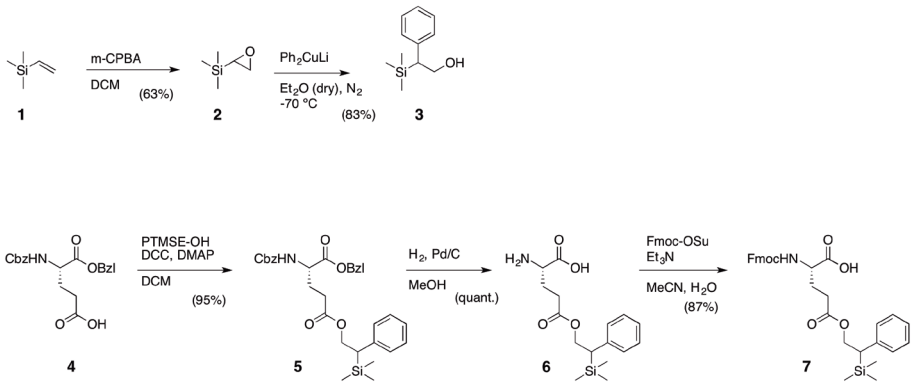

Scheme 1 | Synthesis of Fmoc-Glu(OPTMSE)-OH (**7**) used for solid-supported macrocyclizations.

supported macrocyclization reaction. An important prerequisite for solid supported macrocyclizations is the availability of an orthogonal protecting-group strategy. This was provided by the introduction of Fmoc-Glu(OPTMSE)-OH. The PTMSE-group used for protection of the sidechain carboxylic acid can be removed selectively after cleavage of the N-terminal Fmoc-group[35], facilitating a cyclization reaction between the glutamic acid sidechain and the peptide's N-terminus. Synthesis of the PTMSE-group was started with epoxidation of trimethylvinylsilane **1** using *m*-chloroperbenzoic acid (mCPBA) to give 2-(trimethylsilyl)oxirane **2**. Subsequent reaction with lithium diphenylcuprate, prepared from phenyllithium and copper(I)iodide, yielded (2-phenyl-2-trimethylsilyl)ethanol **3** (Scheme 1) . Coupling of this alcohol to the carboxylic acid of Cbz-Glu-OBzl **4** was achieved using DCC in the presence of DMAP. Subsequently, the Cbz and Bzl protecting groups were simultaneously removed by hydrogenolysis. Lastly, the thus liberated amine was protected with an Fmoc-group to facilitate solid phase peptide synthesis.

For the non-stop solid phase synthesis of discontinuous epitope mimics, the TriAzaCyclophane scaffold that was developed in our group was chosen as a platform for conjugation of the cyclic peptides.[36] Prior to attachment of this scaffold molecule to the solid support, an alkyne functionalized serine building block was coupled to Tentagel S RAM resin. In a next step, the orthogonally protected TAC-scaffold was attached, followed by synthesis of a linear peptide sequence on the Fmoc-protected secondary amine of the TAC-scaffold via Fmoc/^{t}Bu chemistry protocols (Scheme 2).[37] Synthesis of this linear peptide sequence was started with two glycines, followed by the incorporation of Fmoc-Glu(OPTMSE)-OH. After Fmoc-deprotection of the N-terminal amino acid, the PTMSE side chain protecting group was removed by

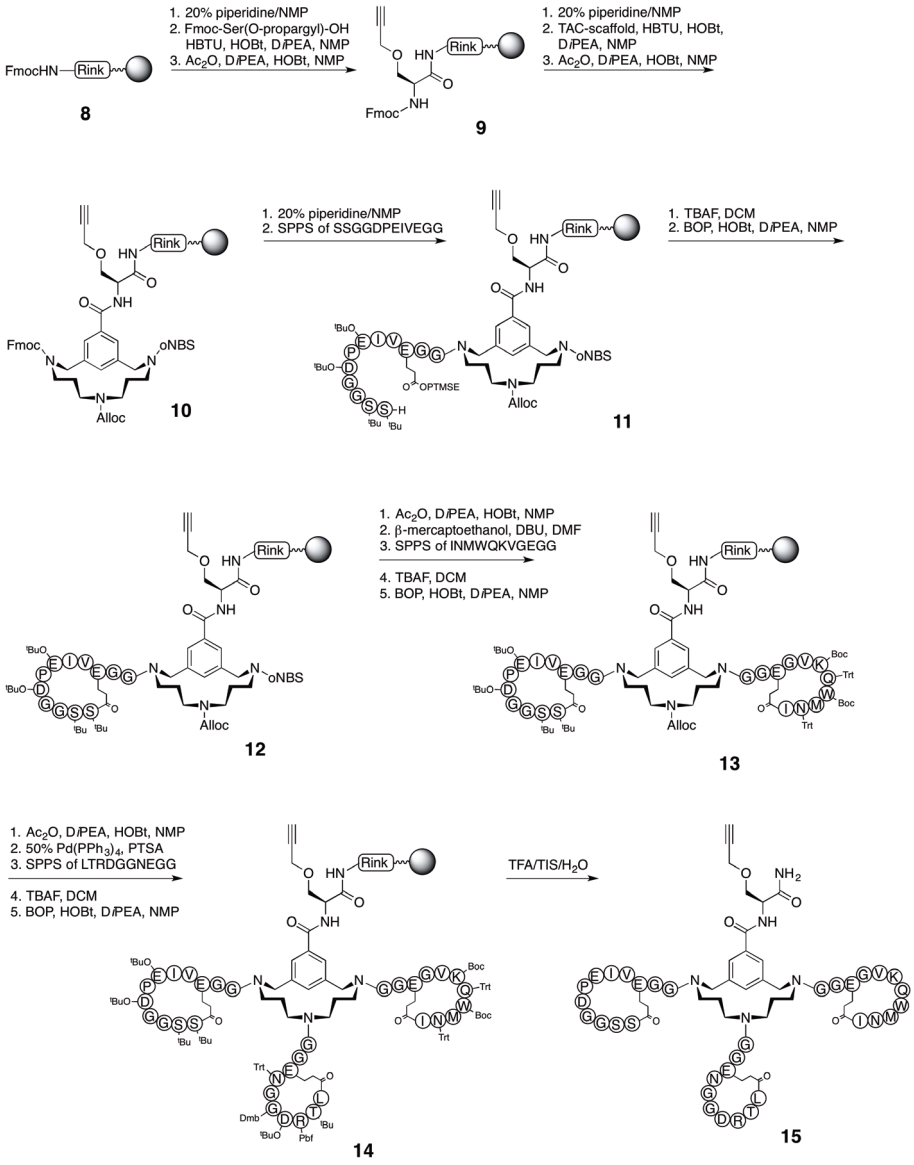

Scheme 2 | Non-stop solid phase synthesis of a discontinuous epitope mimic of HIV gp120

treatment with TBAF in dichloromethane. BOP-mediated macrocyclization between the N-terminus and glutamic acid sidechain was now performed affording intermediate **12.**

Following the same strategy for peptide synthesis and –cyclization, cyclic peptides

were synthesized on the two remaining secondary amine positions of the TAC-scaffold, yielding discontinuous epitope mimic **14**. This compound was cleaved from the resin and lyophilized. Unfortunately, only a very small amount (38 mg) of compound **15** was obtained, and the purity of the resulting crude discontinuous epitope mimic was very low. Tedious purification with preparative HPLC yielded a very modest amount (1.5 mg) of pure compound **15**. Although the desired compound was obtained via this non-stop solid phase synthesis as depicted in Scheme 2, a faster, more flexible and more efficient synthetic approach was desired for the synthesis of discontinuous epitope mimics. It would be highly advantageous to develop a modular approach that allows the introduction of individual cyclic peptides. In this way, synthesis and cyclization of the peptides could be performed in a more controllable fashion, providing more insight in the synthesis and more possibilities for optimization of the approach.

2.2.2 – A modular approach: synthesis of protected cyclic peptides

In a first attempt to a modular synthesis of the TAC-scaffolded discontinuous epitope mimic shown in Scheme 2, a method was designed for the synthesis of protected cyclic peptides using sidechain-to-tail cyclization between the side chain of an orthogonally protected glutamic acid residue. The approach allows the cyclization reaction to be performed on a solid support, which has some advantages over solution-phase cyclization reactions. An excess of coupling reagents can be used, simple washing and filtration are often enough for purification and it has been stated that separation of reactive functional groups bound to the same polymer can be maintained when a peptide is attached to the solid support (also known as the pseudo-dilution effect).[16,38] Three different protected cyclic peptides were synthesized, representing the conserved epitopes that are present in the earlier described HIV gp120 discontinuous epitope mimic (Scheme 2). Synthesis of the linear peptides **18** was initiated by coupling of Fmoc-glycine to a 2-chlorotrityl chloride resin (Scheme 3). This resin was chosen because it allows cleavage of the peptide from the resin without affecting the sidechain protecting groups, yielding a peptide with a C-terminal carboxylic acid, which can be used for conjugation to the TAC scaffold. After coupling of Fmoc-Gly-OH and subsequent removal of the Fmoc-group, Fmoc-Glu(OPTMSE)-OH **7** was coupled as the second amino acid. Subsequently the desired linear peptide sequences could

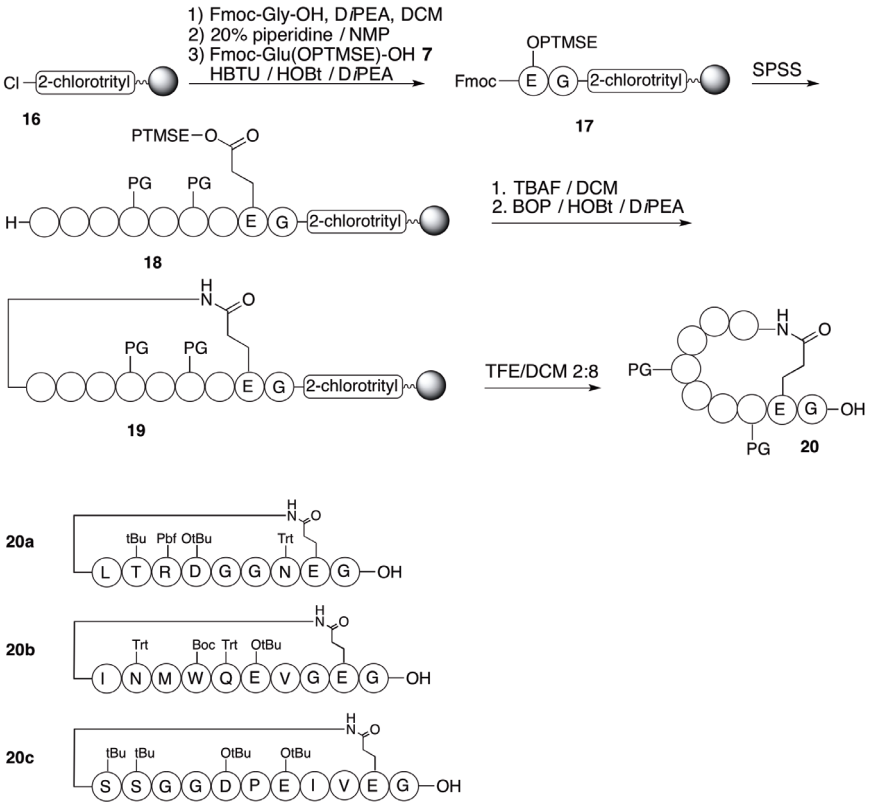

Scheme 3 | Synthesis of protected cyclic peptides

be assembled by Fmoc solid phase peptide synthesis.[37] Removal of the N-terminal Fmoc-group was followed by treatment with TBAF in dichloromethane to remove the PTMSE sidechain protecting group. Tail-to-sidechain cyclization was now performed using BOP as coupling reagent and its completion was confirmed by a Kaiser test.[39] The protected cyclic peptide **19** was cleaved from the resin by treatment with a solution of trifluoroethanol in dichloromethane (Scheme 3).

The crude cyclic peptides were obtained in decent crude yields (**20a**: 192 mg, 51%, **20b**: 529 mg, quantitative, **20c**: 191 mg, 61%), however problems occurred when attempts were made to purify these protected cyclic peptides. The solubility of all three peptides turned out to be poor in almost any solvent. The crude protected cyclic peptides were analysed with analytical HPLC, which showed that a standard buffer system (acetonitrile and water) and C18 reverse phase columns could be used to elute

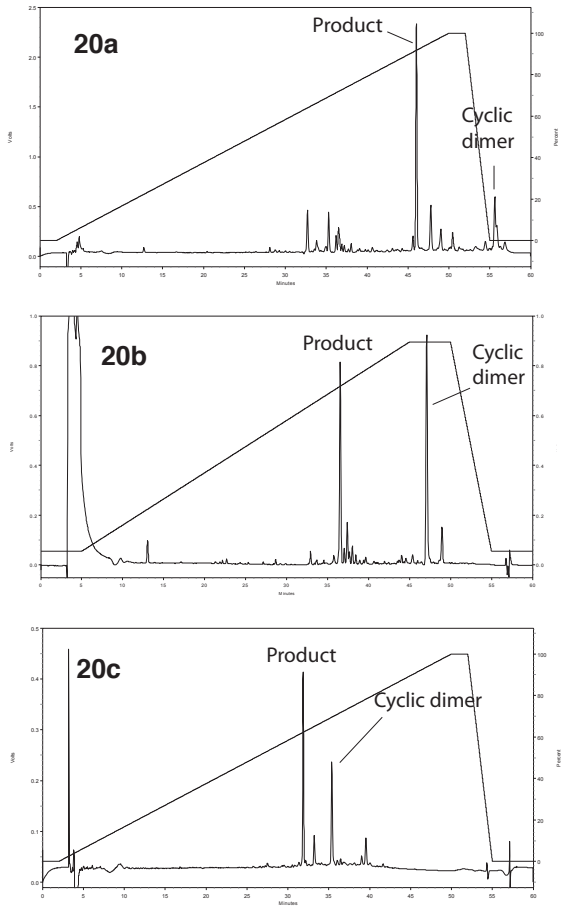

Figure 3 | HPLC chromatograms of protected cyclic peptides LTRDGGN (**20a**), INMWQEVG (**20b**) and SSGGDPEIV (**20c**)

these compounds (Figure 3). Samples were prepared for preparative HPLC, but the only solvent in which the peptides were sufficiently soluble was DMSO. All preparative reverse phase attempts resulted in very low to no yields at all. Therefore, a more hydrophobic buffer system was attempted in which buffer A contained 20% acetonitrile in water and buffer B consisted of water, isopropanol and acetonitrile in a 20/45/50 ratio.[40] These more hydrophobic buffers clearly caused the peptides to elute more in the middle of the gradient. However, yields of the purified protected cyclic peptides did not exceed 10% and analytical HPLC of the fractions after purification showed that the purity of the products was still not-satisfactory.

An additional drawback of the approach described above is that some of the peptide syntheses led to the formation of significant amounts of side products. The formation of side products is partially due to the presence of the acid labile DP-sequence and the DG-sequence, which is prone to base-catalysed aspartimide formation. Repeating the synthesis showed that the degree of side product-formation was unpredictable, but the same type of side product was produced in every synthesis. Careful LC-MS analysis revealed that the most abundant side product usually was a dimer of the desired cyclic peptide. These results add to the growing number of examples showing that the so-called pseudo-dilution effect[16,38,41], which is supposed to favour an intramolecular reaction over an intermolecular reaction, is untrue.[42,43] The formation of dimers was a recurring problem in the synthesis described here.

2.2.3 – Synthesis of unprotected cyclic azidopeptides

Because the synthesis and especially the purification of protected cyclic peptides has proven to be very complicated, a different approach for the construction of discontinuous epitope mimics was developed. A crucial feature of this approach is the use of unprotected cyclic peptides. Since the cyclic peptides need to be conjugated to the TAC scaffold after their synthesis, the use of unprotected peptides requires an orthogonal method for this. We chose to use "click" chemistry[44,45] for conjugation of the peptides to the scaffold molecule, and therefore the cyclic peptides were equipped with an azide functionality. The azide was incorporated via a modified lysine building block that was synthesized from the commercially available Fmoc-Lys(Boc)-OH in two steps using imidazole-1-sulfonyl azide hydrochloride. This crystalline diazotransfer reagent **21** was synthesized in a three step one-pot procedure from sulfuryl chloride, imidazole and sodium azide (Scheme 4).[46]

Fmoc-Lys(Boc)-OH was treated with a saturated solution of hydrogen chloride in diethylether to deprotect the ε-amino group. The resulting hydrochloric acid salt was treated with a solution of imidazole-1-sulfonyl azide in the presence of base and a catalytic amount of $CuSO_4$ to yield Fmoc- ε-azidolysine **23**.

Synthesis of cyclic azidopeptides was performed on TentaGel S RAM resin, following standard Fmoc/^{t}Bu protocols. Since the loading of this resin is generally lower than the loading of the 2-chlorotrityl chloride polystyrene resin that was used in the procedure described in section 2.2.2, the formation of peptide dimers during solid-supported

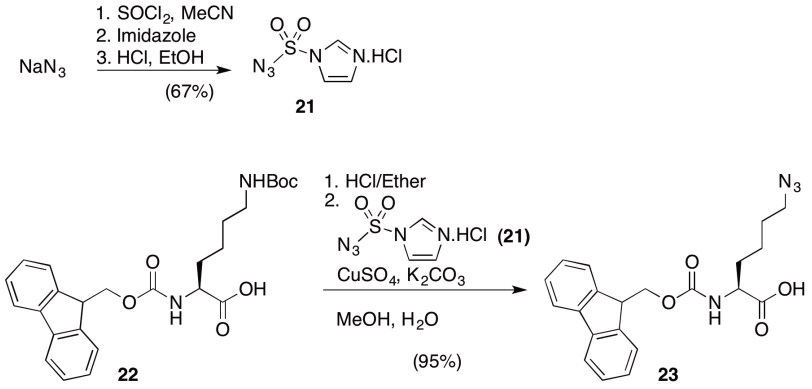

Scheme 4 | Synthesis and use of diazotransfer reagent imidazole-1-sulfonyl azide hydrochloride

macrocyclization was not expected to occur here.

Synthesis of every desired peptide sequence was initiated by coupling of Fmoc-Glu(OPTMSE)-OH C-terminal amino acid, followed by the incorporation of Fmoc-ε-azidolysine. After deprotection of the N-terminal Fmoc-group and subsequent removal of the PTMSE-group using TBAF in dichloromethane, a solid supported tail-to-sidechain cyclization was performed using BOP as coupling reagent. Unprotected cyclic azidopeptide **27** was obtained after acidolytic cleavage from the resin and simultaneous removal of the remaining sidechain protecting groups (Scheme 5).

Crude cyclic azidopeptides **27** were obtained in yields varying from 20% up to 72% depending on the peptide sequence. Purification by preparative HPLC however largely reduced the yields for two out of three peptides, and the quantities obtained after

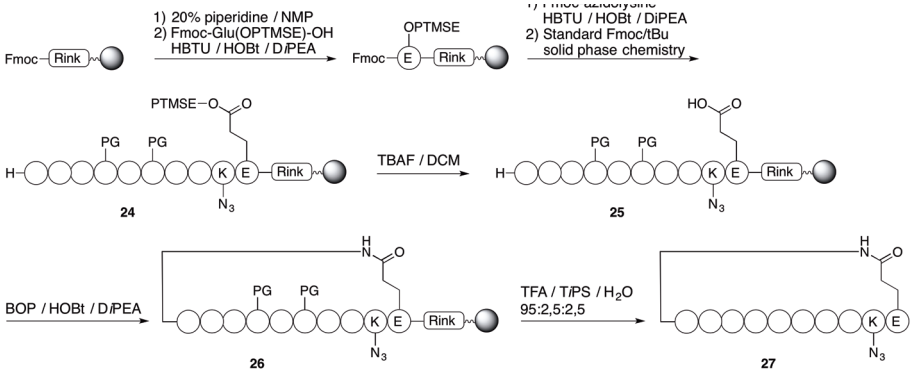

Scheme 5 | Synthesis of tail-to-sidechain cyclized azidopeptides

purification were too small for use as intermediates in the synthesis of larger constructs. Since the purification appeared to be the bottleneck in the procedure described above, and especially sample preparation prior to preparative HPLC was troublesome, a new strategy for cyclization was proposed which provides the cyclic peptide with an extra charged residue. This would suggest an improved solubility in the acidic aqueous environment that is used for preparative HPLC. The new procedure largely follows the synthesis depicted in Scheme 5, but at the N-terminus an extra orthogonally protected lysine was coupled that facilitates sidechain-to-sidechain cyclization of the resin-bound linear peptide, and provides the resulting cyclic peptide with an extra charged residue (Scheme 6). The α-amine of this lysine building block was protected with a Boc-group, since this allows it to be removed under standard conditions for cleavage from the resin and simultaneous deprotection. For the ε-amine the (2-phenyl-2-trimethylsilyl)ethoxycarbonyl (Psoc) protecting group was chosen[47], a silicon containing protecting group very similar to the earlier described PTMSE group. The Psoc-group can be cleaved under the same conditions as the PTMSE-group, thereby facilitating sidechain-to-sidechain cyclization between lysine and glutamic acid.

Synthesis of the linear peptide was initiated by coupling of Fmoc-Glu(OPTMSE)-OH followed by coupling of Fmoc-azidolysine. After this, the desired peptide sequences were assembled by standard Fmoc-^{t}Bu SPPS and Boc-Lys(Psoc)-OH was coupled as the N-terminal amino acid. The lysine ε-amine group and glutamic acid γ-carboxyl moiety were liberated by treating the resin with a solution of tetra n-butylammonium fluoride (TBAF) in dichloromethane, followed by sidechain-to-sidechain cyclization of the peptide using BOP as a coupling reagent. Cleavage of the peptide from the resin and sidechain-deprotection yielded cyclic azidopeptide **31**.

Unexpectedly, the solubility of the peptides in HPLC buffers was not improved compared to that of the sidechain-to-tail cyclized peptides **27** (Scheme 5). In addition, the purity of the crude cyclic peptide was poor and dimer formation was observed in almost 1:1 ratio with the monocyclic product.

So far none of the above described approaches were able to deliver cyclic peptides in large quantities, irrespective of their size and amino acid composition. Therefore, it was decided to switch to an approach that allows peptide cyclization in solution. Some limitations of the reaction of this approach have been mentioned in paragraph 2.1, including the need for highly diluted reaction conditions resulting in longer reaction

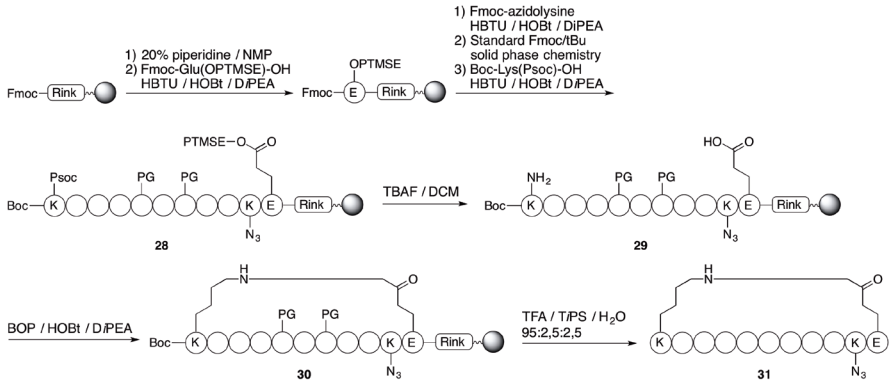

Scheme 6 | Synthesis of sidechain-to-sidechain cyclized azidopeptides

times. However, this approach also has two important advantages over the solid-supported cyclization method: i) the progress of the solution-phase reaction can easily be monitored and ii) purification of the *protected* cyclic peptide can be performed using normal phase column chromatography. Another advantage for is that since the N- and C-terminus are not required for further conjugation purposes now, the use of a three dimensional protecting-group strategy is not necessary when the right type of resin is chosen. Here, synthesis was performed on 2-chlorotrityl chloride resin. This resin allows cleavage of the peptide from the resin, without affecting the sidechain protecting groups. Cleavage of the peptide from the resin provides a protected peptide with a C-terminal carboxylic acid, which can now be used for head-to-tail cyclization.

Syntheses of the head-to-tail cyclized azidopeptides started by loading of 2-chlorotrityl chloride resin with Fmoc-Gly-OH. Glycine was chosen as the C-terminal amino acid for every synthesis, since in this way any racemization during the cyclization reaction was avoided. Synthesis of the linear peptides was performed following standard Fmoc/^{t}Bu protocols and an azide-functionality was introduced via Fmoc-azidolysine **23**. After deprotection of the N-terminal Fmoc-group, the peptides **32a-c** were cleaved from the resin under very mild acidic conditions that did not affect the sidechain protecting groups. The protected linear peptides **33a-c** were cyclized in solution using BOP as a coupling reagent and dichloromethane or dimethylformamide as solvent, depending on the solubility of the protected peptide. Cyclization reactions were performed under high dilution and were monitored by analytical HPLC.

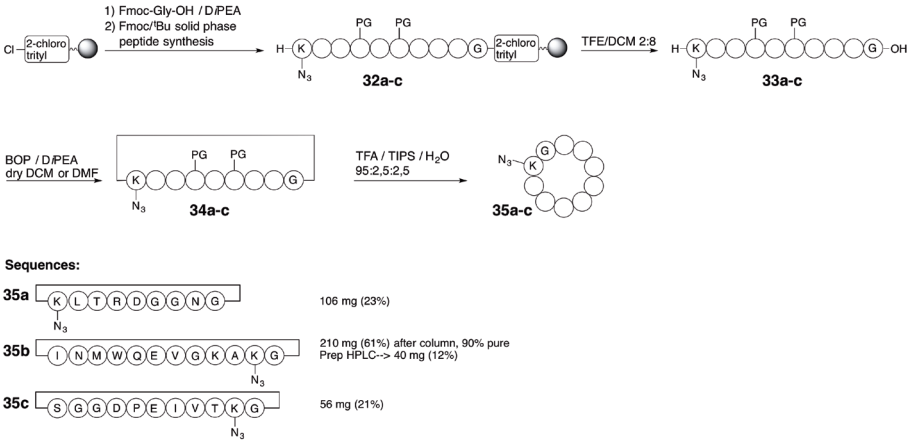

Scheme 7 | Synthesis of head to tail cyclized azidopeptides

After aqueous workup, the protected cyclic peptides **34a-c** could be purified using normal silica column chromatography. This was highly advantageous as compared to purification by preparative reverse phase HPLC, since yields were much higher (up to 23% overall yield) and larger quantities could be purified in a single run. The purity of the cyclic peptides was assessed after removal of the sidechain protecting groups, and was satisfactory for two out of three peptides. Although one of the deprotected peptides still had to be purified by preparative reverse phase HPLC, the synthetic procedure described here is a large improvement compared to earlier used methods (Scheme 7). This is illustrated in Figure 4, by comparing the HPLC chromatograms of purified cyclic peptides **35a-c** with the chromatogram of *protected* cyclic peptide **20b,** which was synthesized according to the method shown in Scheme 3.

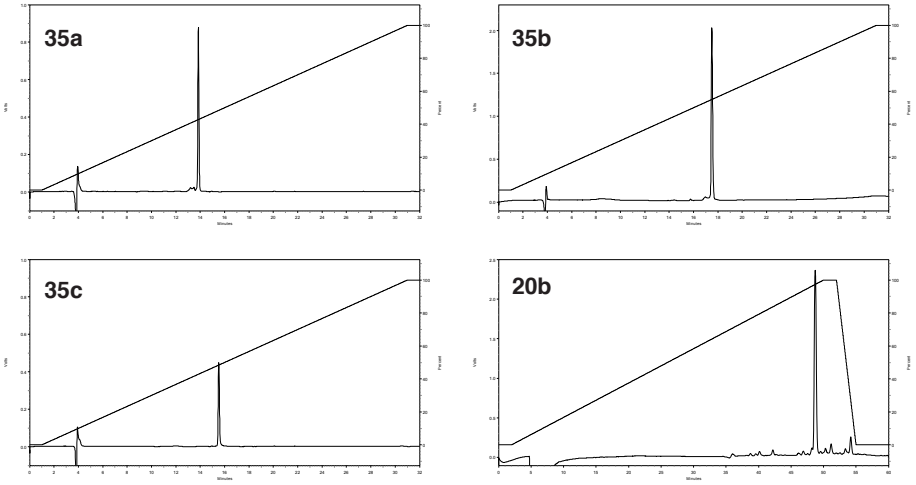

Figure 4 | HPLC chromatograms of cyclic peptides **35a-c**, in comparison with protected cyclic peptide **20b** after HPLC-purification.

2.3 Conclusions

The work described in this chapter demonstrated again that although widely used in every conceivable branch of chemistry and biology, synthesis and purification of cyclic peptides irrespective of their size and amino acid composition is not at all a straightforward. Major factors that determine the efficiency of the synthetic procedure are i) is the final product a sidechain-protected or unprotected peptide? ii) does the cyclization reaction take place in solution or on the solid support? and iii) does the resulting cyclic peptide have to be purified by preparative HPLC or can other methods be employed for its purification?

In our hands, the most successful method for synthesis of cyclic azidopeptides involved head-to-tail cyclization of partially protected peptides in solution. In this way, dimerization can be avoided by carrying out the reactions under diluted conditions (1mM). Moreover, the progress of the reaction could easily be monitored by analytical HPLC. We were able to obtain cyclic peptides **35a-c** in high purity, in overall yields of 12 up to 23% which was an adequate quantity considering the ultimate synthetic goal of combining multiple cyclic peptides on a scaffold molecule. The results described here provide a firm starting point for further research towards this goal.

2.4 Experimental procedures

Reagents, materials and analysis methods

Unless stated otherwise, chemicals were obtained from commercial sources and used without further purification. Peptide grade DiPEA, CH_2Cl_2, NMP, TFA and HPLC grade solvents were purchased from Biosolve B.V. (Valkenswaard, The Netherlands). Fmoc-protected amino acids were purchased from GL Biochem Ltd. (Shanghai, China). Sidechain protecting groups for amino acids were as follows: Ser(tBu), Asp(OtBu), Glu(OtBu), Thr(tBu), Asn(Trt), Trp(Boc), Gln(Trt), Lys(Boc), Arg(Pbf). Boc-Lys(Psoc)-OH was earlier synthesized in our group. TentaGel S RAM resin functionalized with a Rink linker (particle size 90 μm, capacity 0.20-0.27 mmol/g) was purchased from Rapp Polymere GmbH (Tübingen, Germany). 2-Chlorotrityl chloride resin (100-200 mesh, 1% DVB, 1.0-1.6 mmol/g) was purchased from Iris Biotech GmbH and was used for synthesis of the cyclic peptides. Solid phase peptide synthesis was carried out in plastic syringes with a polyethylene frit (20 μm) obtained from Screening Devices B.V. The resin loading was determined by measuring the UV absorbance of the piperidine-dibenzofulvene adduct (λ_{max} 300 nm).[37] Reactions were performed at room temperature. Solution phase reactions were monitored by TLC analysis and Rf-values were determined on Merck pre-coated silica gel 60 F-254 (0.25 mm) plates. Spots were visualized with UV-light, and by heating plates dipped in ninhydrine, Cl_2/N,N,N,N'-tetramethyl-4,4'-diaminodiphenylmethane (TDM)[48] or a KMnO4 solution. Column chromatography was performed using Silica-P Flash silica gel (60 Å, particle size 40-63 μm; Silicycle). ^{1}H NMR experiments were conducted on a 300 MHz Varian G-300 spectrometer, and chemical shifts are given in ppm (δ) relative to TMS (0.00 ppm). ^{13}C NMR spectra were recorded at 75 MHz at a Varian G-300 spectrometer and chemical shifts are given in ppm (δ) relative to $CDCl_3$ (77 ppm). Analytical HPLC was accomplished on a Shimadzu-10Avp (Class VP) system using UV-detector operating at 214 and 254 nm. The mobile phase was 0.1% TFA in CH_3CN/H_2O 5:95 (buffer A) and 0.1% TFA in CH_3CN/H_2O 95:5 (buffer B). For analysis of protected (cyclic) peptides the mobile phase was 0.1% TFA in CH_3CN/H_2O 20:80 (buffer A) and 0.1% TFA in CH_3CN/iPrOH/H_2O 50:45:5 (buffer B). A Phenomenex Gemini C18 column (110 Å, 5 μm, 250×4.6 mm) was used at a flow rate of 1 mL min^{-1} using a standard protocol: 100% buffer A for 1 min, then a linear gradient of buffer B (0-100% in 30 min). Purification of the peptide-containing compounds was performed on a Prep LCMS-QP8000α HPLC system (Shimadzu) using a Phenomenex Gemini C18 column (10 μm, 110 Å, 250×21.2 mm) at a flow rate of 12.5 mL min^{-1} using a standard protocol: 100% buffer A for 5 min followed by a linear gradient of buffer B (0-55% in 100 min) using the same buffers as described for analytical HPLC. Electrospray ionization mass spectrometry (ESI-MS) was performed on a Shimadzu LCMS-QP8000 single quadrupole bench-top mass spectrometer operating in a positive ionization mode or a Thermo-Finnigan LCQ Deca XP Max ion trap mass spectrometer. Analytical LC-MS

was preformed on Thermo-Finnigan LCQ Deca XP Max. MALDI-TOF-MS spectra were recorded on a Kratos Analytical (Shimadzu) AXIMA CFR mass spectrometer using α-cyano-4-hydroxycinnamic acid (CHCA) or sinapic acid as a matrix and human ACTH (18-39) or bovine insulin oxidized B chain as references. High resolution electrospray ionization (ESI) mass spectra were measured on a Micromass LCT mass spectrometer calibrated with CsI. All reported mass values are monoisotopic.

2-(trimethylsilyl)oxirane 2

To a cooled (ice/water, 0ºC) solution of *m*-CPBA (196.0 g (70-75%), 795.2 mmol) in 1L CH_2Cl_2, a solution of vinyltrimethylsilane (68.48 g, 662.7 mmol) in 250 mL CH_2Cl_2 was added dropwise in 1.5 h. The mixture was stirred during 30 minutes at 0° C and after that it was stirred at room temperature overnight. A white precipitate was now formed. Next, the mixture was cooled down to 0° C during 1 h and filtered to remove the precipitate. The residue was washed with CH_2Cl_2 and the filtrate was washed with 1M $NaHCO_3$, 1M $NaHSO_4$ (2 ×), H_2O, 1M $NaHCO_3$ and brine. After drying (Na_2SO_4) the crude product was concentrated at room temperature to a volume of 200 mL. The product was purified with vacuum distillation (300-350 mbar, bp 70-76°C). 2-(trimethylsilyl)oxirane was obtained as a colourless liquid (48.74 g, 63%). ^{1}H-NMR (300 MHz, $CDCl_3$, TMS): δ 0.00 (s, 9H, TMS-C*H*$_3$), 2.11-2.12 (dd, 1H, O-C*H*$_2$), 2.47-2.51 (dd, 1H, C*H*$_2$), 2.82-2.86 (t, 1H, TMS-C*H*). ^{13}C-NMR (75 MHz, $CDCl_3$): δ -3.9, 44.0, 44.5

(2-phenyl-2-trimethylsilyl) ethanol 3

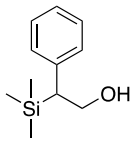

To remove any traces of moisture, dried (vacuum exsiccator, P_2O_5) CuI (17.0 g, 89.3 mmol) was flame-dried in a roundbottom flask (1L) under N_2 atmosphere. Subsequently, the dry CuI was suspended in 350 mL dry Et_2O (freshly distilled over $LiAlH_4$), which was added to the flask via a cannula. The suspension was cooled to -6ºC with and ice-salt bath, and the phenyllithium (1.8 M solution in dibutylether, 100 mL, 180 mmol) was added dropwise via a cannula. The reaction mixture was stirred at -6ºC during 1.5 h and after that it was cooled down to -70ºC (solid CO_2 in EtOH). 2-(trimethylsilyl)oxirane (6 g, 51.6 mmol) was added dropwise to the reaction mixture and the suspension was stirred at -70ºC during 3 h followed by stirring at -20ºC overnight. The reaction mixture was quenched with a saturated solution of NH_4Cl (125 mL), followed by addition of a 25% NH_4OH solution. The resulting mixture was filtered and the two layers were separated. The organic layer was washed with a saturated solution of NH_4Cl, a 25% NH_4OH solution to dissolve the remaining copper-salts and the combined aqueous layers were extracted with Et_2O. The combined organic layers were washed with a saturated solution of NH_4Cl and brine and dried (Na_2SO_4). After evaporating the solvent, crude product was purified by crystallization. Product was dissolved in 500 mL hexanes and stored overnight at -20ºC. After that, the white suspension was gently shaken and

filtered. After drying *in vacuo* (2-phenyl-2-trimethylsilyl) ethanol was obtained as a white colourless crystalline compound (7.80 g, 78%). ^{1}H-NMR (300 MHz, $CDCl_3$, TMS): δ 0.00 (s, 9H, TMS-C*H*$_3$), 1.39 (br. s, 1H, O*H*), 2.46-2.51 (dd, 1H, TMS-C*H*), 3.98-4.03 (dd, 1H, C*H*$_2$OH), 4.14-4.22 (t, 1H, C*H*$_2$OH), 7.11-7.20 (m, 3H, *o/p*-^{AR}C*H*), 7.28-7.34 (t, 2H, *m*-^{AR}C*H*). ^{13}C-NMR (75 MHz, $CDCl_3$): δ -2.7, 41.9, 63.0, 124.7-128.2, 140.2

Synthesis of Cbz-Glu-(OPTMSE)-OBzl 5

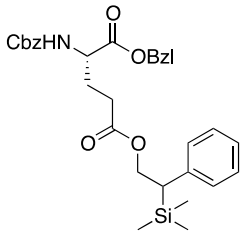

To a cooled solution (ice/water, 0ºC) of the commercially available Cbz-Glu-OBzl (5.56 g, 15 mmol) and (2-phenyl-2-trimethyl-silyl) ethanol (3.20 g, 16.5 mmol) in DCM (90 mL), a solution of DCC (3.09 g, 15 mmol) in DCM (5 mL) was added dropwise. After stirring for 10 min at 0ºC, a catalytic amount of DMAP (0.18 g, 1.5 mmol) was added and the suspension was stirred at room temperature overnight. The reaction mixture was filtered, the filtrate was concentrated and redissolved in EtOAc (100 mL). The mixture was washed with 1M $KHSO_4$ (2 × 75 mL), H_2O (75 mL), and brine (75 mL). After drying (Na_2SO_4) and evaporation of the solvent, the crude product was purified by column chromatography using hexanes/Et_2O, (7:3, v/v) to afford **5** (7.51 g, 91%) as a colourless oil. Rf = 0.51 (Et_2O/hexanes, 1:1 v/v). ^{1}H NMR ($CDCl_3$, 300 MHz) δ: 7.26 (m, 10H, C*H*^{Ar}-Cbz, Bzl), 7.19 (t, 3H, C*H*^{Ar}-PTMSE, J= 7.7 Hz), 7.06, 7.00 (2d, 2H, C*H*^{Ar}-PTMSE), 5.59 (bt, 1H, NH, J= 10.5 Hz), 5.06, 5.02 (ds, 4H, C*H*$_2$Ph), 4.56 (t, 1H, C*H*$_2$a-PTMSE, Ja,b = 11.2 Hz), 4.46-4.39 (m, 1H, C*H*$_2$b- PTMSE), 4.32-4.30 (m, 1H, C*H*-α), 2.52, 2.48 (dd, 1H, C*H*-PTMSE, JCH,CH$_2$a= 4.7 Hz, JCH,CH$_2$b= 4.4 Hz), 2.18-2.16 (m, 2H, C*H*$_2$-γ), 2.10-2.00 (m, 1H, C*H*$_2$a-β), 1.84-1.79 (m, 1H, C*H*$_2$b-β), -0.04 (s, 9H, TMS-C*H*$_3$). ^{13}C NMR ($CDCl_3$, 75 MHz) δ: 172.6, 171.4, 155.7, 140.2, 136.0, 135.0, 128.3, 128.2, 128.0., 127.9, 127.8, 127.1, 124.8, 66.8, 66.6, 65.3, 53.1, 36.9, 29.8, 26.9, 2.9.

H-Glu-(OPTMSE)-OH 6

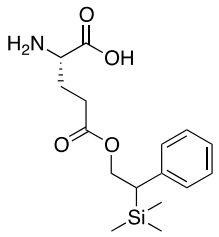

To a cooled solution (ice/water, 0ºC) of **5** (7.39 g, 13.5 mmol) in methanol (200 mL), 10% Pd/C (0.74 g, 10% w/w) was added and the suspension was stirred under a H_2 atmosphere from a balloon at room temperature overnight. The reaction was filtrered through Hyflo and the filtrate was concentrated *in vacuo*. The crude was purified by column chromatography using a gradient of CH_2Cl_2/MeOH (85:15, v/v) to CH_2Cl_2/MeOH (70:30, v/v) to give **6** (4.23 g, 97%) as white foam. Rf = 0.22 ($CHCl_3$/MeOH/25% NH_4OH, 8:3:0.5 (v/v/v)) ^{1}H NMR (CD_3OD, 300 MHz) δ: 7.24 (t, 2H, C*H*^{Ar}-PTMSE, J= 7.3 Hz), 7.13-7.07 (m, 3H, C*H*^{Ar} -PTMSE), 4.65 (bt, 1H, C*H*$_2$a-PTMSE, Ja,b= 11.3 Hz), 4.55-4.48 (m, 1H, C*H*$_2$b-PTMSE), 3.52-3.48 (m, 1H, C*H*-α), 2.62, 2.58 (dd, 1H,

C*H*-PTMSE, JCH,CH_2a= JCH,CH_2b= 4.4 Hz), 2.45-2.37 (m, 2H, CH_2-γ), 2.04-1.99 (m, 1H, CH_2-β), 0.00 (s, 9H, CH_3). ^{13}C NMR (CD_3OD, 75 MHz) δ: 175.4, 174.8, 142.2, 129.5, 128.9, 126.4, 67.0, 55.5, 38.7, 31.3, 27.5, - 2.4.

Fmoc-Glu-(OPTMSE)-OH 7

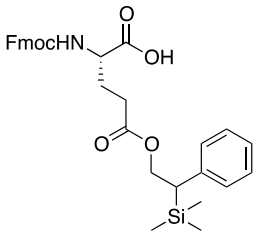

Compound **6** (4.16 g, 12.87 mmol) was dissolved in water (30 mL) and the pH adjusted to 9.0-9.5 with Et_3N. To this mixture, a solution of Fmoc-OSu (4.34 g, 12.87 mmol) in CH_3CN (45 mL) was added in one portion. The mixture was stirred at room temperature for 1.5 h and the pH maintained at 8.5-9.0 by addition of Et_3N. The reaction mixture was concentrated *in vacuo* to remove CH_3CN and the pH was adjusted to pH~2 with $KHSO_4$ (1M). The aqueous layer was extracted with EtOAc (3 × 100 mL) and the combined organic layers were washed with $KHSO_4$ (1M) (100 mL), H_2O (100 mL), and brine (100 mL). After drying (Na_2SO_4) and evaporating the solvent, the crude product was purified by column chromatography using a gradient of CH_2Cl_2 to CH_2Cl_2/MeOH (80:20, v/v) to give a colourless oil. Co-evaporation with Et_2O led to **7** as a white foam (1.45 g, 89 %). Rf = 0.36 (CH_2Cl_2: MeOH : AcOH, 90:10:0.5, v:v:v). 1H NMR ($CDCl_3$, 300 MHz) δ: 8.71-8.51 (bs, 1H, COOH), 7.63, 7.46 (dd, 4H, CH^{Ar}-Fmoc, J= 6.0 Hz), 7.27, 7.20 (2t, 4H, CH^{Ar}-Fmoc), 7.13, 7.00 (2t, 3H, CH^{Ar}-PTMSE, J= 7.4 Hz), 6.94 (d, 2H, CH^{Ar} -PTMSE), 5.49, 5.44 (dd, 1H, N*H*, J= 8.2 Hz, J= 7.7 Hz), 4.58-4.44 (m, 1H, CH_2a-PTMSE), 4.39-4.34 (m, 1H, CH_2b-PTMSE), 4.28 (d, 2H, OCH_2-Fmoc, J= 6.8 Hz), 4.21, 3.93 (2m, 1H, C*H*-α), 4.09 (t, 2H, C*H*-Fmoc), 2.47, 2.43 (2d, 1H, C*H*-PTMSE, JCH, CH_2a= 3.6 Hz, JCH,CH_2b= 3.07 Hz), 2.20, 2.10 (2m, 2H, CH_2-γ), 2.06-1.96 (m, 1H, CH_2a-β), 1.95-1.78 (m, 1H, CH_2b-β), -0.08 (s, 9H, TMS-CH_3). ^{13}C NMR ($CDCl_3$, 75 MHz) δ: 175.5, 173.3, 156.1, 143.7, 143.5, 141.2, 140.3, 128.2, 127.6, 127.3, 127.0, 125.0, 119.9, 67.0, 65.7, 53.1, 47.0, 37.1, 30.2, 26.9, -2.8. MS (ESI) *m/z* (monoisotopic mass) [M+H]+ calcd for $C_{31}H_{36}NO_6Si$: 546.2, found: 546.9. HPLC (Adsorbosphere C8, TFA buffers): Rt= 24.04 min, purity >99%.

Imidazole-1-sulfonyl azide hydrochloride[46] 21

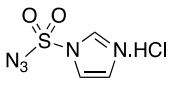

Sulfuryl chloride (16.1 mL, 200 mol) was added drop-wise to a cooled (0°C) suspension of NaN_3 (13.0 g, 200 mmol) in MeCN (200 mL) and the mixture was stirred overnight at room temperature. Subsequently, the reaction mixture was cooled again (ice/water, 0°C) and imidazole (25.9 g, 380 mmol) was added to the mixture portion-wise. The resulting suspension was stirred for 3 h at room temperature. The mixture was diluted with EtOAc (400 mL) and washed with H_2O (2 × 400 mL), a saturated aqueous $NaHCO_3$ (2 × 400 mL) and dried over $MgSO_4$ and filtered. A solution of HCl in EtOH was prepared by the drop-wise addition of AcCl (21.3 mL, 300 mmol) to ice-cooled absolute ethanol (75 mL). This

solution was added drop-wise to the ice-cooled filtrate under stirring to form imidazole-1-sulfonylazide hydrochloride, which precipitated as a solid. The mixture was filtered and the filter cake was washed with EtOAc (3 × 100 mL) to give imidazole-1-sulfonyl azide hydrochloride as colorless needles (23.7 g, 56%). ^{1}H NMR (300 MHz, D_2O) δ = 7.68 (dd, 1 H, H-4), 8.09 (dd, 1 H, 2.2 Hz, H-5), 9.53 (dd, 1 H, H-2); 13C NMR (75 MHz, D_2O) δ = 120.8, 123.4, 138.3.

Fmoc-L-ε-azidolysine 23

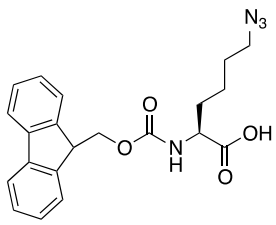

Fmoc-Lys(Boc)-OH **22** (10 g, 21.32 mmol) was dissolved in 100 mL CH_2Cl_2. To this solution, a saturated solution of HCl in Et_2O was added. The resulting solution was stirred during 1 hour after which a white suspension was obtained. The solvents were evaporated and the residue was dissolved in 100 mL water and 200 mL MeOH. $CuSO_4$ (53.2 mg, 0.21 mmol) was added and the pH of the solution was brought to 8.5 with K_2CO_3. Imidazole sulfonyl azide HCl salt (5.36 g, 25.59 mmol) was added and the pH of the reaction mixture was maintained at 8.5 by addition of K_2CO_3. The clear blue solution was stirred overnight, after which MeOH was evaporated and the aqueous solution was acidified to pH 2 by addition of 2N HCl. The aqueous phase was extracted four times with 100 mL CH_2Cl_2 and the combined CH_2Cl_2 fractions were dried over Na_2SO_4 and concentrated *in vacuo*. The resulting yellow oil was purified by column chromatography, using a gradient of MeOH/acetone/AcOH 95:5:1 to CH_2Cl_2/acetone/AcOH 90:10:1. Pure product was obtained as a colourless oil that crystallized into a white solid. Yield: 7.91 g (94%). R_f: 0.35 (CH_2Cl_2/acetone/AcOH 90:10:1). ^{1}H-NMR (300 MHz, $CDCl_3$, TMS): δ 1.26-1.32 (m, 2H, Lys-$^{\delta}$CH_2), 1.46-1.49 (m, 1H, Lys-$^{\gamma}$CH_2), 1.58-1.65 (m, 1H, Lys-$^{\gamma}$CH_2), 1.65-1.80 (m, 1H, Lys-$^{\beta}$CH_2), 1.85-2.01 (m, 1H, Lys-$^{\beta}$CH_2), 3.26-3.30 (t, 2H, Lys-$^{\varepsilon}$CH_2), 4.20-4.24 (t, 1H, Lys-$^{\alpha}$C*H*), 4.42-4.44 (d, 2H, Fmoc-CH_2), 4.55 (br.s, 1H, Fmoc-C*H*), 5.26-5.29 (d, 1H, N*H*), 7.23-7.43 (m, 4H, Fmoc-^{AR}C*H*), 7.57-7.60 (d, 2H, Fmoc-^{AR}C*H*), 7.75-7.77 (d, 2H, Fmoc-^{AR}C*H*). ^{13}C-NMR (75 MHz, $CDCl_3$): δ 176.7, 156.1, 143.6, 141.3, 127.7, 127.1, 125.0, 120.0, 67.1, 53.5, 51.0, 47.1, 31.8, 28.3, 22.4

Peptide synthesis

2-Chlorotrityl chloride resin (100-200 mesh, 1% DVB, 1.0-1.6 mmol/g, Iris Biotech GMBH) was used for synthesis of the cyclic peptides. Peptides were synthesized using conventional Fmoc/tBu chemistry.[37] Solvents used for synthesis were dried on molsieves (4Å), 10 mL solvent per gram of resin was used.

Immobilization of the first monomer: Resin (1 g, 1.0-1.6 mmol) was swelled in CH_2Cl_2 (3 × 2 min × 10 mL). To the resin, a solution of 2 mmol Fmoc-amino acid and 5

mmol DiPEA dissolved in 10 mL CH_2Cl_2 was added and the mixture was shaken during 1 hour at room temperature. After that, the reaction vessel was drained and the resin was washed with DMF (2 × 2 min × 10 mL), followed by treatment (2 × 10 min) with 10 mL of a mixture of CH_2Cl_2/MeOH/DiPEA (80:15:5 (v/v/v)) to quench any remaining 2-chlorotrityl chloride. The resin was washed again with DMF (3 × 2 min, 10 mL) and CH_2Cl_2 (3 × 2 min, 10 mL) and dried *in vacuo*. The loading efficiency was determined by spectrophotometric quantification of the absorbance of the dibenzofulvene-piperidine adduct at 300 nm obtained after piperidine removal of the Fmoc-group from an aliquot of the resin.

Linear peptide synthesis: The resin was washed with NMP (3 × 10 mL per gram of resin, 2 min). The *N*-terminal Fmoc protecting group was removed using 20% piperidine in NMP (3 × 10 mL per gram of resin, 8 min) followed by washing steps with NMP (3 × 10 mL, 2 min), CH_2Cl_2 (3 × 10 mL, 2 min) and NMP (3 × 10 mL, 2 min). The amino acid coupling mixtures were prepared by dissolving 4 equivalents of amino acid, 4 equivalents of HOBt and HBTU and 8 equivalents of DiPEA in NMP and coupled during 60 min. Fmoc-azidolysine was coupled overnight using 2 equivalents of amino acid, 2 equivalents of the coupling reagents HBTU and HOBt and 4 equivalents of DiPEA. The resin was washed with NMP (3 × 10 mL, 2 min) and CH_2Cl_2 (3×10mL, 2 min) after every coupling step. The coupling steps and deprotection steps were monitored using the Kaiser test[39] or bromophenol blue test in case of secondary amines.[49]

After coupling of the final Fmoc-amino acid, capping (i.e acetylation) was carried out to protect amino acid residues which had not reacted and prevent them from participation in the cyclization reaction. The resin was treated with 10 mL capping solution containing Ac_2O (4.72 mL, 42.7 mmol), DiPEA (2.18 mL, 22.8 mmol) and HOBt (0.23 g, 1.7 mmol) in NMP (100 mL) for 2 × 15 min, followed by washing steps with NMP (3 × 10 mL, 2 min), CH_2Cl_2 (3 × 10 mL, 2 min) and NMP (3 × 10 mL, 2 min). Finally, the *N*-terminal Fmoc-group was removed by 20% piperidine in NMP, to afford the linear sidechain-protected azidopeptide **2**.

Cleavage of peptide from solid support and cyclization: The sidechain-protected linear azidopeptide **32a**, **b** or **c** was cleaved from the resin using a solution of TFE in CH_2Cl_2 (2:8 (v/v)), 10 mL for each gram of resin, during 1 hour. The resin beads were removed by filtration and the filtrate was concentrated *in vacuo*. The residue containing crude linear peptide **33a**, **b** or **c** was dissolved in CH_2Cl_2 or DMF, depending on the solubility of the peptide, in a final peptide concentration of ca. 1mM. To this solution 1.2 equivalents of BOP and 2.4 equivalents of DiPEA were added and the reaction mixture was stirred at room temperature. Progress of the cyclization reaction was monitored with analytical HPLC. Depending on the sequence and the solvent, reaction times varied from 16 hours to three days. When full conversion was observed with analytical HPLC, the reaction mixture was concentrated *in vacuo* and the protected cyclic peptide was dissolved in EtOAc. The organic phase was washed with a 1N $KHSO_4$ solution,

water, 5% $NaHCO_3$ solution and brine, dried over Na_2SO_4 and concentrated *in vacuo*.

Side-chain deprotection: The purified sidechain-protected cyclic peptides **34a-c** *(vide infra)* were treated with a solution (10 mL per 0.25 mmol) of TFA/TIS/H_2O (95:2.5:2.5 (v/v/v)). The reaction mixture was stirred during 3 hours, followed by precipitation of the peptides from MTBE/hexane 1:1 (v/v) at -20°C. The precipitates were dissolved in $^tBuOH/H_2O$ 1:1 (v/v) and lyophilized. The purity of the peptides **35a-c** was analyzed with analytical HPLC and the peptides were characterized with mass spectrometry.

Purification of cyclic peptides 35a-c

Compound 35a, loop 1: cyclo(Lys(N_3)-Leu-Thr-Arg-Asp-Gly-Gly-Asn-Gly)
The crude protected cyclic peptide was purified by column chromatography using CH_2Cl_2/EtOH 95:5 (v/v) as an eluent. The product was obtained as a yellow oil. R_f: 0.67 (CH_2Cl_2/EtOH 9:1). Synthesis was performed on 0.5 mmol scale. Yield after deprotection of sidechains: 106 mg (23%).
$[M+H]^+$ monoisotopic calculated for $C_{36}H_{60}N_{16}O_{13}$: 925.4599, $[M+2H]^{2+}$calculated: 463.2336, HRMS, $[M+2H]^{2+}$ found: 463.2316, HPLC: Rt= 13.84 min, purity 94.5%.

Compound 35b, loop 2: cyclo(Ile-Asn-Met-Trp-Gln-Glu-Val-Gly-Lys-Ala-Lys(N_3)-Gly)
The crude protected cyclic peptide was purified by column chromatography in CH_2Cl_2/MeOH 95:5. The product was obtained as a yellow oil. R_f: 0.59 (CH_2Cl_2/MeOH 9:1). Synthesis on 0.25 mmol scale. Yield after deprotection of sidechains: 210 mg (61%). HPLC analysis shows some small impurities, therefore the product was also purified by preparative HPLC. Pure product was obtained as a white powder. Yield: 40 mg (12%).
$[M+H]^+$ monoisotopic calculated for $C_{60}H_{93}N_{19}O_{16}S$: 1368.6841, $[M+2H]^{2+}$calculated: 684.8457, HRMS $[M+2H]^{2+}$ found: 684.8446, HPLC: Rt= 17.51 min, purity= 95.3%

Compound 35c, loop 3: cyclo(Ser-Gly-Gly-Asp-Pro-Glu-Ile-Val-Thr-Lys(N_3)-Gly)
The crude protected cyclic peptide was purified with column chromatography using a gradient of CH_2Cl_2/MeOH 97:3 to 9:1. The product was obtained as colourless oil. R_f: 0.61 (CH_2Cl_2/MeOH 9:1)
The synthesis was carried out on a 0.25 mmol scale. Yield after deprotection of sidechains: 56 mg (21%).
$[M+H]^+$ monoisotopic calculated for $C_{44}H_{70}N_{14}O_{17}$: 1067.5116, $[M+2H]^{2+}$calculated: 534.2594, HRMS $[M+2H]^{2+}$ found: 534.2652, HPLC: Rt= 15.52 min, purity= 100%

References:

(1) Craik, D. J. *Science* **2006**, *311*, 1563–1564.
(2) Clark, R. J.; Craik, D. J. *Biopolymers* **2010**, *94*, 414–422.
(3) White, C. J.; Yudin, A. K. *Nature Chem.* **2011**, *3*, 509–524.
(4) Bock, J. E.; Gavenonis, J.; Kritzer, J. A. *ACS Chem. Biol.* **2013**, *8*, 488–499.
(5) Kessler, H. *Angew. Chem. Int. Ed.* **1982**, *21*, 512–523.
(6) Hruby, V. J. *Life Sciences* **1982**, *31*, 189–199.
(7) Hruby, V. J. *Trends in Pharmacological Sciences* **1985**, *6*, 259–262.
(8) Driggers, E. M.; Hale, S. P.; Lee, J.; Terrett, N. K. *Nature Rev. Drug Discov.* **2008**, *7*, 608–624.
(9) Chen, S.; Morales-Sanfrutos, J.; Angelini, A.; Cutting, B.; Heinis, C. *ChemBioChem* **2012**, *13*, 1032–1038.
(10) Kwong, P. D.; Wyatt, R.; Robinson, J.; Sweet, R. W.; Hendrickson, W. A.; Sodroski, J. *Nature* **1998**, *393*, 648–659.
(11) Kwong, P. D.; Wyatt, R.; Majeed, S.; Robinson, J.; Sweet, R. W.; Joseph Sodroski; Hendrickson, W. A. *Structure* **2000**, *8*, 1329–1339.
(12) Franke, R.; Hirsch, T.; Overwin, H.; Eichler, J. *Angew. Chem. Int. Ed.* **2007**, *46*, 1253–1255.
(13) Zhang, L.; Tam, J. P. *J. Am. Chem. Soc.* **1997**, *119*, 2363–2370.
(14) Gilon, C.; Halle, D.; Chorev, M.; Selincer, Z.; Byk, G. *Biopolymers* **1991**, *31*, 745–750.
(15) McMurray, J. S. *Tetrahedron Lett.* **1991**, *32*, 7679–7682.
(16) Rovero, P.; Quartara, L.; Fabbri, G. *Tetrahedron Lett.* **1991**, *32*, 2639–2642.
(17) Lambert, J. N.; Mitchell, J. P.; Roberts, K. D. *J. Chem. Soc., Perkin Trans. 1* **2001**, 471–484.
(18) Timmerman, P.; Beld, J.; Puijk, W. C.; Meloen, R. H. *ChemBioChem* **2005**, *6*, 821–824.
(19) Cantel, S.; Le Chevalier Isaad, A.; Scrima, M.; Levy, J. J.; DiMarchi, R. D.; Rovero, P.; Halperin, J. A.; D'Ursi, A. M.; Papini, A. M.; Chorev, M. *J. Org. Chem.* **2008**, *73*, 5663–5674.
(20) Kleineweischede, R.; Hackenberger, C. P. R. *Angew. Chem. Int. Ed.* **2008**, *47*, 5984–5988.
(21) Timmerman, P.; Barderas, R.; Desmet, J.; Altschuh, D.; Shochat, S. G.; Hollestelle, M. J.; Höppener, J. W. M.; Monasterio, A.; J Ignacio Casal; Meloen, R. H. *J. Biol. Chem.*, **2009**, *284*, 34126–34134.
(22) Heinis, C.; Rutherford, T.; Freund, S.; Winter, G. *Nature Chem. Biol.* **2009**, *5*, 502–507.
(23) Fluxa, V. S.; Reymond, J.-L. *Bioorganic & Medicinal Chemistry* **2009**, *17*, 1018–1025.
(24) Ingale, S.; Dawson, P. E. *Org. Lett.* **2011**, *13*, 2822–2825.
(25) Smeenk, L. E. J.; Dailly, N.; Hiemstra, H.; van Maarseveen, J. H.; Timmerman, P. *Org. Lett.* **2012**, *14*, 1194–1197.
(26) Londregan, A. T.; Farley, K. A.; Limberakis, C.; Mullins, P. B.; Piotrowski, D. W. *Org. Lett.* **2012**, *14*, 2890–2893.
(27) Zheng, J.-S.; Tang, S.; Guo, Y.; Chang, H.-N.; Liu, L. *ChemBioChem* **2012**, *13*, 542–546.
(28) Montalbetti, C. A. G. N.; Falque, V. *Tetrahedron* **2005**, *61*, 10827–10852.
(29) Albericio, F.; Hammer, R. P.; Garcia-Echeverria, C.; Molins, M. A.; Chang, J. L.; Munson, M. C.; Pons, M. Q.; Barany, G. *Int. J. Pept. Protein Res.* **2009**, *37*, 402–413.
(30) Miller, S. J.; Blackwell, H. E.; Grubbs, R. H. *J. Am. Chem. Soc.* **1996**, *118*, 9606–9614.

(31) Camarero, J. A.; Muir, T. W. *Chem. Commun.* **1997**, *0*, 1369–1370.
(32) Tulla-Puche, J.; Barany, G. *J. Org. Chem.* **2004**, *69*, 4101–4107.
(33) Bock, V. D.; Perciaccante, R.; Jansen, T. P.; Hiemstra, H.; van Maarseveen, J. H. *Org. Lett.* **2006**, *8*, 919–922.
(34) Turner, R. A.; Oliver, A. G.; Lokey, R. S. *Org. Lett.* **2007**, *9*, 5011–5014.
(35) Wagner, M.; Kunz, H. *Synlett* **2000**, *3*, 400–402.
(36) Opatz, T.; Liskamp, R. M. J. *Org. Lett.* **2001**, *3*, 3499–3502.
(37) Fields, G. B. *Int. J. Peptide Protein Res.* **1990**, *35*, 161–214.
(38) Jayalekshmy, P.; Mazur, S. *J. Am. Chem. Soc.* **1976**, *98*, 6710–6711.
(39) Kaiser, E.; Colescott, R. L.; Bossinger, C. D.; Cook, P. I. *Anal. Biochem.* **1970**, *34*, 595.
(40) Rijkers, D. T.; Kruijtzer, J. A.; Killian, J. A.; Liskamp, R. M. *Tetrahedron Lett.* **2005**, *46*, 3341–3345.
(41) Huang, S.; Tour, J. M. *J. Org. Chem.* **1999**, *64*, 8898–8906.
(42) Soucy, P.; Dory, Y. L.; Deslongchamps, P. *Synlett* **2000**, *2000*, 1123–1126.
(43) Malesevic, M.; Strijowski, U.; Bächle, D.; Sewald, N. *J. Biotechnol.* **2004**, *112*, 73–77.
(44) Tornøe, C. W.; Christensen, C.; Meldal, M. *J. Org. Chem.* **2002**, *67*, 3057–3064.
(45) Rostovtsev, V. V.; Green, L. G.; Fokin, V. V.; Sharpless, K. B. *Angew. Chem. Int. Ed.* **2002**, 2596.
(46) Goddard-Borger, E. D.; Stick, R. V. *Org. Lett.* **2007**, *9*, 3797–3800.
(47) Wagner, M.; Heiner, S.; Kunz, H. *Synlett* **2000**, *12*, 1753–1756.
(48) Arx, Von, E.; Faupel, M.; Brugger, M. *J. Chromatography A* **1976**, *120*, 224.
(49) Krchňák, V.; Vágner, J.; Šafář, P.; Lebl, M. *Collect. Czech. Chem. Commun.* **1988**, *53*, 2542–2548.

3

Approaches for attachment of cyclic peptides to the TAC-scaffold

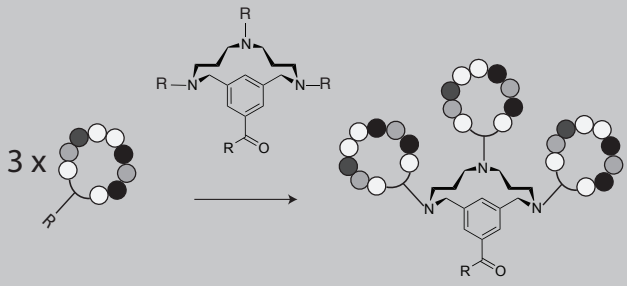

3.1 Introduction

The development of molecular systems that can mimic the properties of natural proteins involves multiple challenges.[1-7] The first challenge, as was described in chapter 2, is controlling the shape or conformation of a particular peptide by its cyclization and developing a reliable synthetic method for those cyclic peptides.[8-11] The remaining challenge now in the design and development of discontinuous epitope mimics, is the organization of multiple individual shapes into a well-defined ensemble that represents a specific molecular recognition surface.[1,2,12] In recent years, various approaches have been reported that describe the attachment of multiple *identical* peptides to a scaffold molecule.[12-17] Although these studies have yielded very active biomolecular constructs and illustrate the importance of molecular scaffolds, the mimicry of discontinuous protein binding sites requires more advanced synthetic methodologies. The development of a synthetic strategy that allows the combination of multiple *different* peptides in one molecule starts with choice of a scaffold molecule. There are many scaffolds that contain a heterobifunctional crosslinker, but relatively few examples of scaffolds that contain three or more orthogonal functionalities are available.[18] A readily available scaffold which contains even four orthogonal synthetic handles is the TriAzaCyclophane scaffold, which was developed in our group (Figure 1).[19] This scaffold molecule has already been used repeatedly for the synthesis or artificial receptors, and also for mimicry of protein binding sites.[20-25]

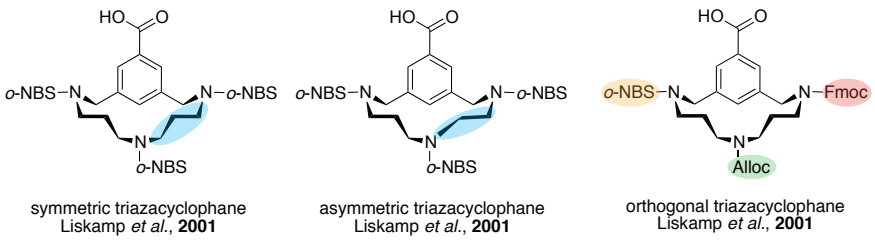

Figure 1 | Different variants of the TriAzaCyclophane scaffold

The most recent work in which the TAC scaffold has been applied involved the conjugation of multiple different cyclic peptides to the scaffold, using a non-stop solid phase synthetic approach.[26] This non-stop solid phase synthesis as depicted in Scheme 1, represents the first synthetic approach that allows the conjugation of up to three different cyclic peptides to one molecule. Even though this non-stop solid phase synthesis method has some obvious, disadvantages, the first successful synthesis of a molecular construct carrying three different cyclic peptides has encouraged us to further explore the possibilities of this system and investigate other and more efficient

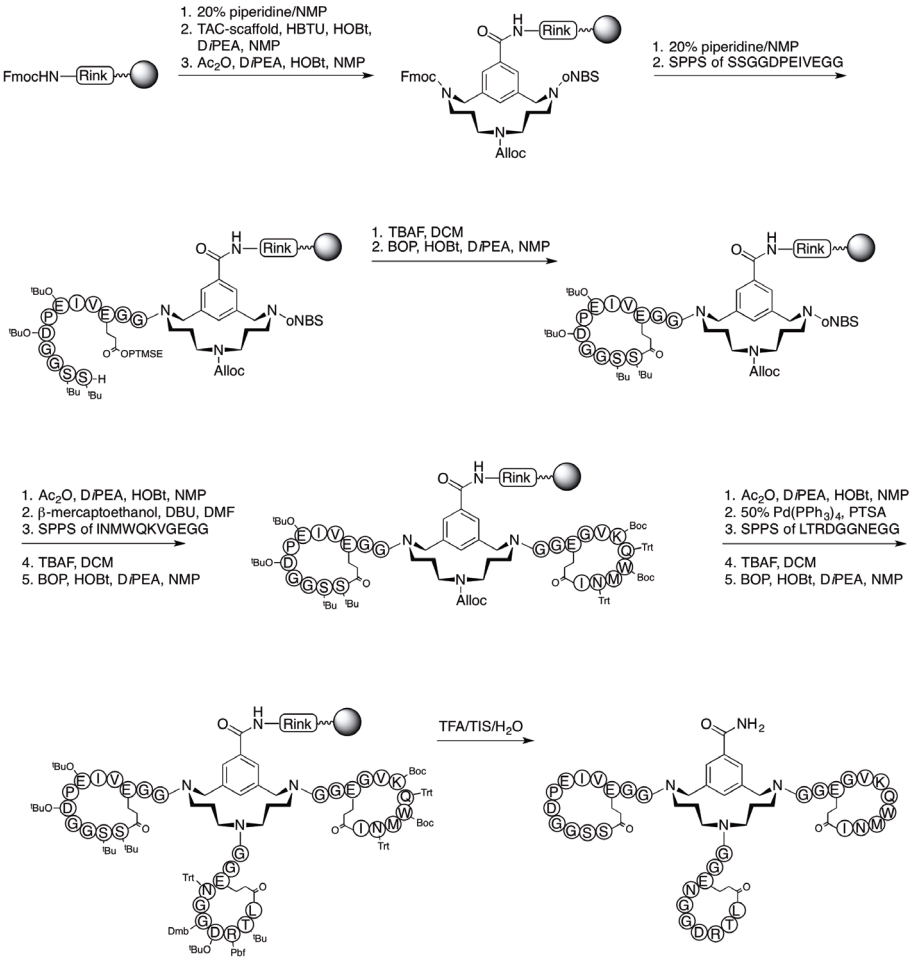

Scheme 1 | Non-stop solid phase synthesis of a discontinuous epitope mimic of HIV gp120[26]

synthetic methods leading to similar discontinuous epitope mimics. The non-stop solid phase method is a promising approach for synthesis of a single compound, however the approach is not ideal when the epitopes still need to be optimized and thus multiple compounds are required. Often multiple variations of peptides need to be evaluated in order to find the optimal compound. For this, it would be highly advantageous to develop a modular approach that allows the introduction of individual different cyclic peptides. In this way, the epitopes can be modified without having to repeat the complete synthesis.

Several methodologies for a modular synthesis of discontinuous epitope mimics have been investigated. The approaches that will be described in this chapter are all based on the use of the TAC-scaffold for conjugation of three different cyclic peptides, representing conserved epitopes of the CD4-binding site of HIV gp120.

3.2 Results and discussion

3.2.1 – Synthesis of the TAC-scaffold

For the construction of discontinuous epitope mimics of HIV gp120, the selectively deprotectable TriAzaCyclophane scaffold was used.[19] This scaffold molecule was synthesized analogous to our earlier developed procedure with some improvements, starting from 3,5-bis-(bromomethyl) benzoic acid methyl ester **5**. Synthesis of the orthogonally protected triamine was initiated with the mono-*o*NBS protection of bis-(3-aminopropyl)amine **1**, using *o*-NBS-Cl and an excess of triamine **1**. Amine **2** was used without any further purification and its primary amine was protected using ethyl trifluoroacetate in the presence of one equivalent of water, to yield TFA-salt **3**. This salt was crystallized from the reaction mixture, and purified by recrystallization. Then, the secondary amine of compound **3** was protected using allylchloroformate, which gave the triply protected triamine **4** in good yield (67%) and this compound can be obtained in large quantities (up to 13 g, 25 mmol).

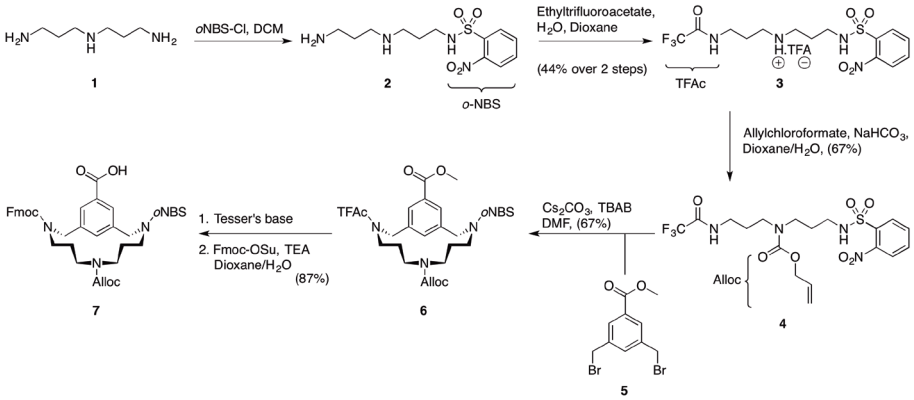

Scheme 2 | Synthesis of a selectively deprotectable TriAzaCyclophane scaffold **7**.

Subsequently, a macrocyclization reaction was performed reacting triamine **4** with 3,5-bis-(bromomethyl) benzoic acid methyl ester **5**, to give monomeric cyclic compound **6.** Formation of a dimeric cyclic species has been observed earlier,[19] but could be prevented here when a more diluted reaction mixture was used (10 mM) and MeCN was substituted by DMF as a solvent. Next, saponification of the methyl ester and cleavage of the trifluoroacetyl group were simultaneously performed using Tesser's base[27] and finally the product was reacted with Fmoc-OSu and triprotected TAC-scaffold **7** was obtained (Scheme 2).

3.2.2 – Attachment of protected cyclic peptides to the TAC scaffold

For further functionalization of TAC-scaffold **7**, it was attached to the solid support (Scheme 3). Firstly, the Fmoc-group of TentaGel S RAM resin was removed by piperidine in NMP and alkyne-functionalized lysine **8** was coupled using BOP, HOBt and DiPEA. This alkyne functionality was introduced in order to have an orthogonal group for further functionalization (e.g. fluorescence, immunization) of the final compound. Then, after Fmoc-deprotection of the α-amine, TAC-scaffold **7** was coupled to afford compound **10.**

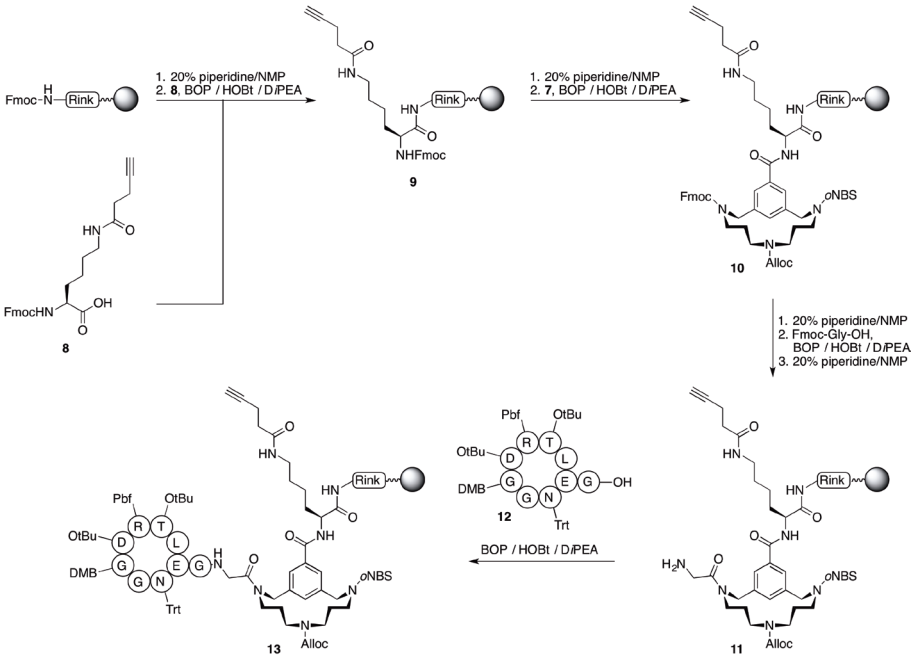

Scheme 3 | Coupling of a protected cyclic peptide to the TAC-scaffold

To avoid possible steric hindrance of the secondary amine upon attachment of the cyclic peptides to the relatively small scaffold molecule, it was decided to introduce a glycine residue as a spacer to the TAC-scaffold prior to attachment of the protected cyclic peptides. The first position to be functionalized on the TAC-scaffold **10** is the secondary amine that is protected with an Fmoc-group. After Fmoc-removal, an Fmoc-glycine residue was coupled to this position followed by removal of this Fmoc-group and coupling of the first protected cyclic peptide **12.** Formation of desired product **13** carrying one cyclic peptide was confirmed with MALDI. (Figure 2 − calculated $[M+H]^{+}$= 1692.672)

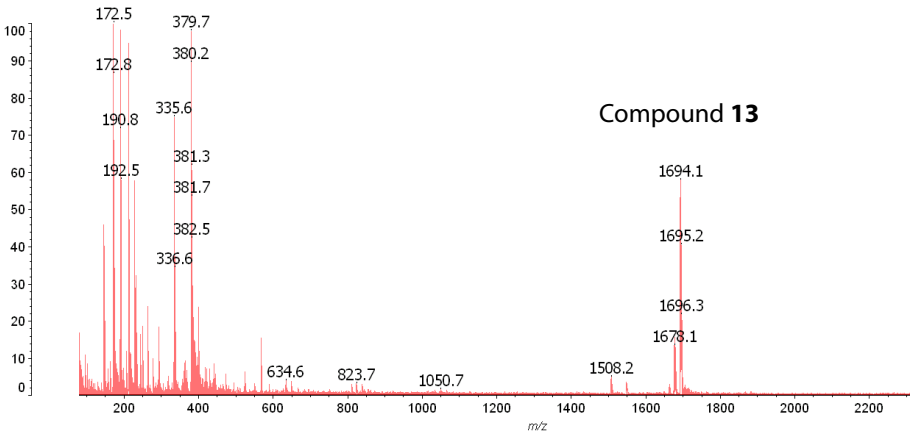

Figure 2 | MALDI of the crude product after coupling of peptide **12** to scaffold **11**

Synthesis towards a discontinuous epitope mimic carrying three cyclic peptides was continued by functionalization of the oNBS-protected secondary amine of **13.** Removal of the oNBS-group was accomplished by treatment with a solution of β-mercaptoethanol and DBU in DMF. Similar to the attachment of the first cyclic peptide, a glycine residue was introduced followed by attempted coupling of a second cyclic peptide **12.** As a proof of principle, the cyclic peptide that was already successfully coupled in the previous step was chosen again for attachment to the second position (Scheme 4).

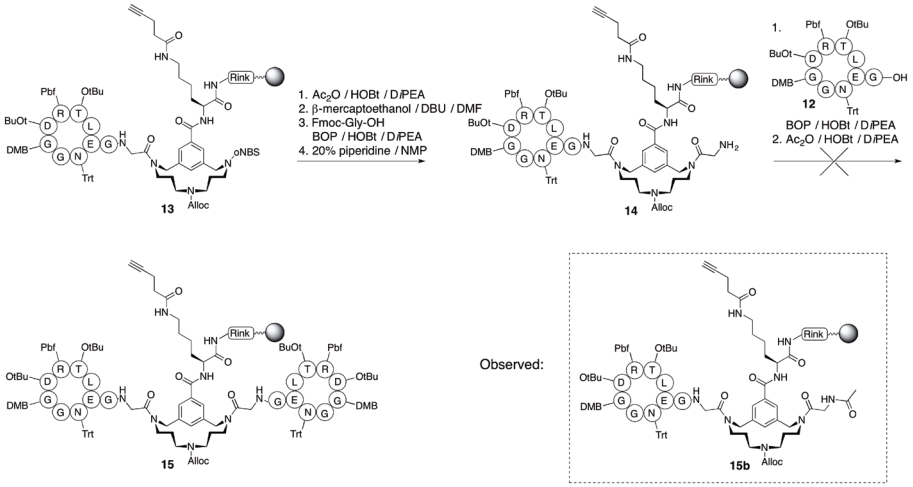

Scheme 4 | Attempted coupling of a second protected cyclic peptide to the TAC-scaffold

After the coupling reaction of the cyclic peptide and acetylation of any remaining unreacted amino functions, a small aliquot of the resin was taken for cleavage and analysis. Unfortunately, instead of the desired product **15** carrying two cyclic peptides only the acetylated product **15b** containing only one cyclic peptide was observed ($[M+H]^+ = 1607.220$).

Variation of the coupling reagent did not improve the result of this coupling reaction, and since no attachment at all of the second cyclic peptide was observed at this intermediate stage of the synthesis, it was decided to develop an alternative synthetic approach.

3.2.3 – Coupling of cyclic peptides to the TAC-scaffold via click chemistry

Since not only the coupling of protected cyclic peptides to the TAC-scaffold was troublesome but also their synthesis and purification was sub-optimal, it was decided to design a strategy for the synthesis of discontinuous epitope mimics that allowed the use of *unprotected* peptides. However, attachment of unprotected cyclic peptides to a scaffold molecule requires the use of an orthogonal conjugation technique. It was decided to use the Cu(I)-catalyzed azide-alkyne cycloaddition (CuAAC)[28,29] for the attachment of unprotected cyclic peptides to the TAC-scaffold, because of its successful application in various chemoselective (bio)conjugation reactions, its high efficiency and versatility, as well as the relatively straightforward incorporation of the required functional groups into synthetic molecules.[30] For this purpose, the TAC-scaffold was equipped with three alkyne functionalities, while an azide-moiety was incorporated in the cyclic peptides (chapter 2 and Scheme 5).

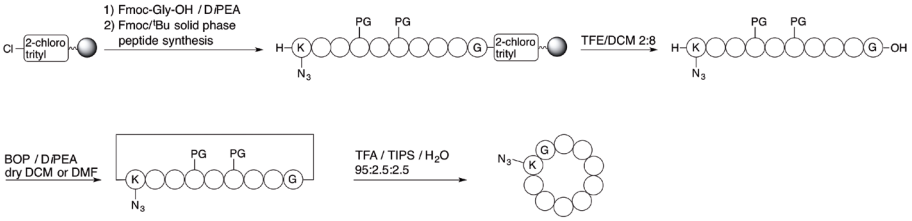

Scheme 5 | Synthesis of cyclic azidopeptides as described in chapter 2.

Synthesis of the required alkyne-functionalized TAC-scaffold was initiated by attachment of tris-o-NBS-protected TAC-scaffold **16** to TentaGel S RAM resin (Scheme 6). The resulting resin-bound product **17** was treated with a solution of β-mercaptoethanol and DBU in DMF to remove all oNBS-protecting groups, followed by HBTU-mediated coupling of three 4-pentynoic acid residues to the secondary amines. The resulting resin-bound TAC-scaffold **18** was now used to carry out the CuAAC-reaction.

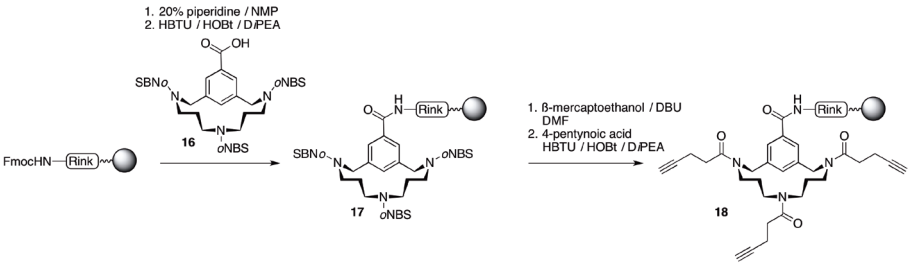

Scheme 6 | Synthesis of TAC-scaffold equipped with three alkynes

Because of the ease of purification of solid phase synthesized compounds and the highly efficient Cu(I)-catalyzed click reactions on the solid phase that were reported in literature,[28,31-34] it was decided to perform the CuAAC-reactions on the solid-supported scaffold **18**. Test reactions were performed with scaffold **18** and benzylazide **20** to find optimal conditions, trying different catalytic systems, temperatures, reaction times and (microwave) heating. Full conversion of benzyl azide was observed, after only 15 minutes of microwave heating at 80°C and using CuI as copper(I) source and 20% piperidine in NMP as a base. However, when these conditions were applied to (linear) azidopeptide **21**, hardly any conversion was observed and no desired cycloaddition products could be identified with LC-MS. Although a variety of reaction conditions were attempted, none of them led to formation of the desired product. Thus, addition of a reducing agent, increasing the amount of catalyst, increasing reaction temperature and/or reaction time or the use of a different base did not yield the desired product (Table 1). Since this CuAAC approach on the solid phase was unsuccessful, it was decided to cleave the scaffold molecule from the solid support and continue synthesis in solution.

Table 1 | Study of conditions for the CuAAC reaction between scaffold **18** and peptide **21**

Eq. CuI	Base (eq)	Reducing agent (eq)	Substrate conc. (mM)	Solvent	Conditions	Reaction time	Conversion (%)[a]
0.5	-	-	1	20% pip./NMP	Microwave 80°C	15 min	0
0.5	-	-	1	20% pip./NMP	Microwave 80°C	30 min	0
0.5	-	-	1	20% pip./NMP	r.t.	overnight	0
5	DiPEA (10)	-	1	DMF	Microwave 80°C	15 min	0
5	-	Ascorbic acid (5)	1	DMF	Microwave 80°C	15 min	0
5	DiPEA (10)	Ascorbic acid (5)	1	DMF	Microwave 80°C	15 min	0
5	DiPEA (10)	Ascorbic acid (5)	5	DMF	Microwave 80°C	15 min	0
5	DiPEA (10)	Ascorbic acid (5)	5	20% pip./NMP	Microwave 80°C	15 min	0

[a] Conversion was determined by LC-MS analysis after cleavage of the product from te resin. pip.= piperidine

Alkyne-functionalized scaffold **18** was cleaved from the resin and the resulting crude product **19** was purified by column chromatography. Subsequently, scaffold **19** was reacted with different azides (Figure 3) to investigate the reactivity of the scaffold towards both small molecules and larger peptides. Many sources of Cu(I) have been described for CuAAC in solution.[35] The most common and original conditions would be an aqueous solution of $CuSO_4$ and sodium ascorbate as a reducing agent. These conditions were used here as a starting point for optimization of the microwave assisted click cycloaddition reaction between scaffold **19** and azides **20-22**. Since click chemistry of three ligands on the relatively small TAC-scaffold appeared not to be a routine effort, also in this solution-based approach the first CuAAC attempt involved conjugation of benzylazide **20**. Using 0.2 equivalents of $CuSO_4$ and 0.4 equivalents Na-ascorbate per alkyne in $^tBuOH/H_2O$ (3:2 v/v), complete conversion of starting materials was observed with LC-MS after 10 minutes of microwave heating at 80ºC. Mass spectrometry analysis showed that the triple-clicked product was the main product (>90%) of this reaction. ($[M+H]^+$ found: 916.42)

So far, research on TAC-scaffolded protein mimics[23,25] or artificial receptors[24] only involved the attachment of small molecules to the scaffold molecule. The possibility

to incorporate larger peptide fragments would be an important improvement in the synthesis of TAC-scaffolded protein mimics, since this would allow a faster, modular synthesis. Therefore, as a proof of concept, CuAAC between linear peptide **21** (1 eq per alkyne) and scaffold **19** was performed in the presence of 0.2 equivalents of $CuSO_4$ and 0.4 equivalents Na-ascorbate per alkyne-functionality.

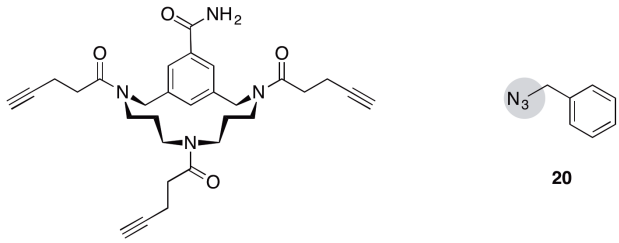

19

20

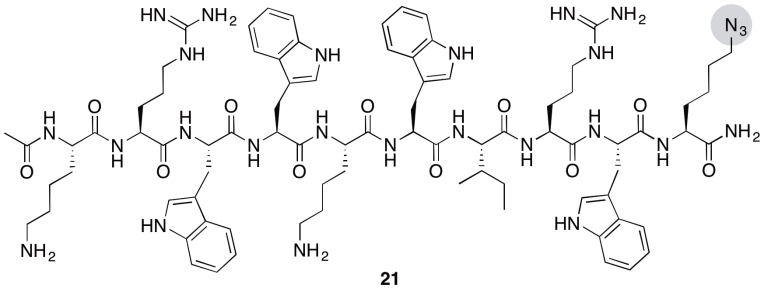

21

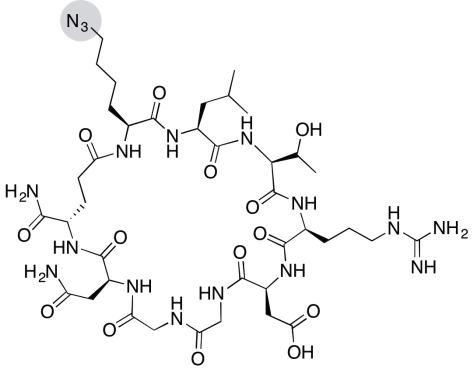

22

Figure 3 | Model compounds for microwave assisted CuAAC on scaffold **19**.

Partial conversion of the scaffold molecule was observed with peptide **21** by LC-MS after 10 minutes of microwave irradiation at 80°C, and a broad new peak was formed. MALDI analysis of the reaction mixture revealed that mono, double and triple clicked products were formed, as can be seen in Figure 4. Although no complete conversion with azidopeptide **21** was observed, these results demonstrated the possibility to introduce larger peptide fragments to the TAC scaffold and these findings provided important information about the reactivity of the system for further research involving the attachment of cyclic peptides.

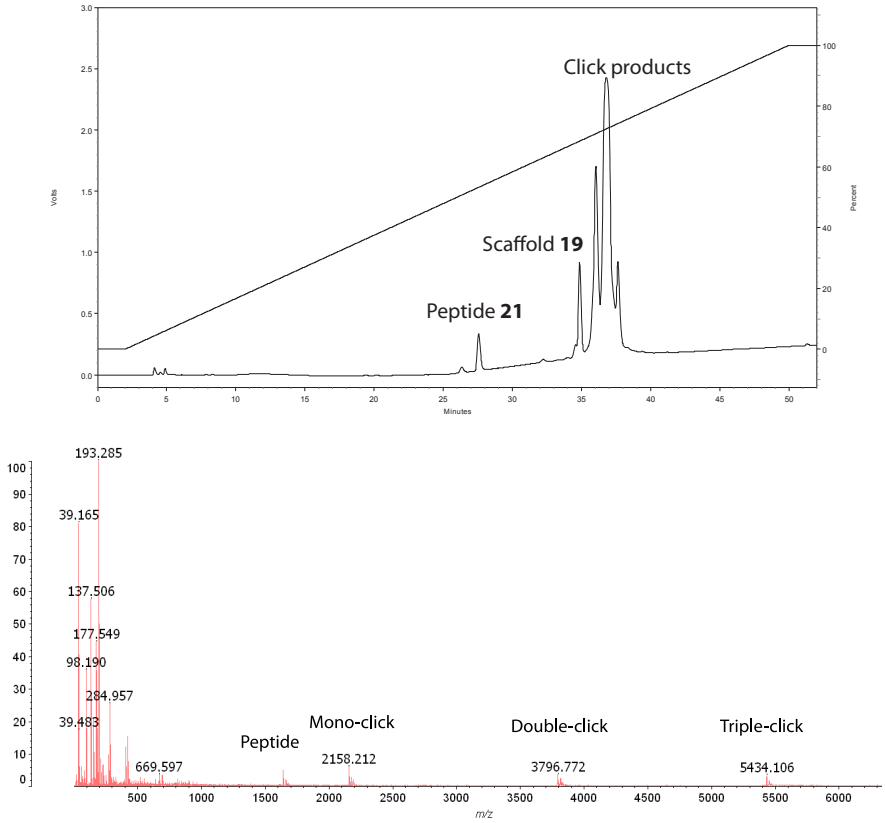

Figure 4 | HPLC chromatogram (top) and MALDI spectrum (bottom) of reaction products resulting from CuAAC between scaffold **19** and peptide **21**

Analogous to conjugation of linear peptide **21**, now three equivalents of cyclic azidopeptide **22** were reacted with TAC scaffold **19** under microwave irradiation at 80°C. Since peptide **22** was not soluble in ^{t}BuOH, DMF was used instead. After 10

minutes of microwave irradiation, an aliquot was taken and analyzed with analytical HPLC and MALDI. The resulting chromatograms and mass spectrum are shown in Figure 5 and 6. HPLC analysis showed that starting materials were not completely converted into products, and a very broad product-peak was observed which indicates the presence of multiple products. This suggestion was confirmed with MALDI analysis, which showed that indeed all possible click products (mono, di- and trivalent click) were formed.

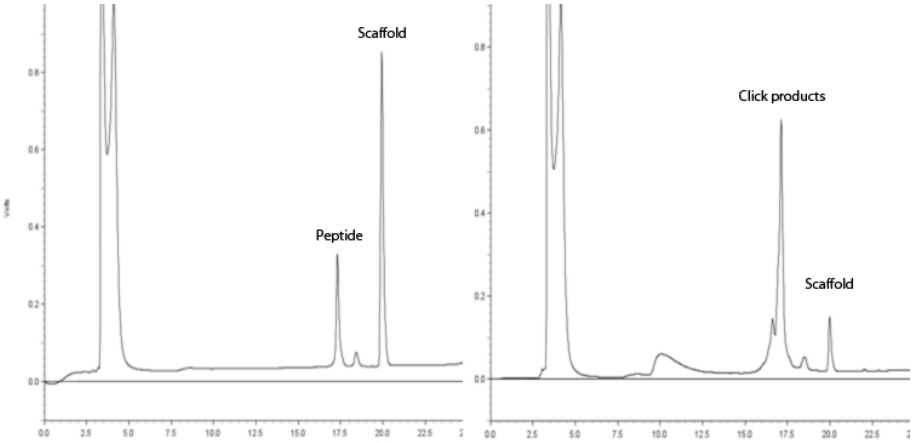

Figure 5 | HPLC chromatograms of CuAAC between TAC scaffold **19** and cyclic azidopeptide **22**. Left: t=0 sample before microwave irradiation. Right: sample after 10 minutes microwave irradiation.

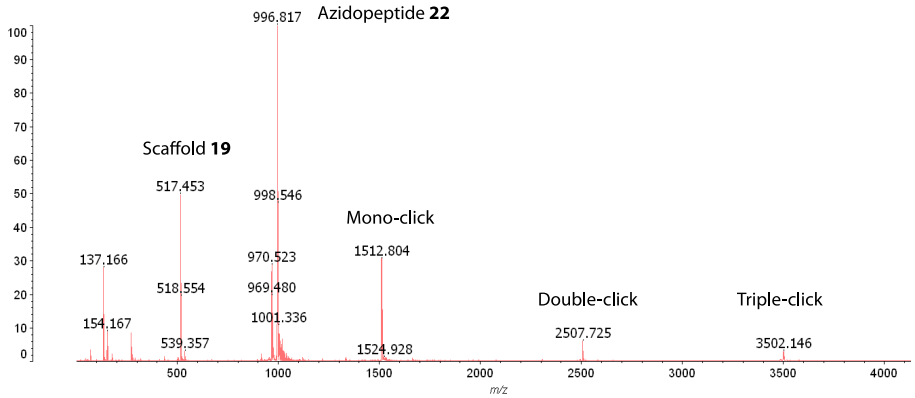

Figure 6 | MALDI spectrum of CuAAC between TAC scaffold **19** and cyclic azidopeptide **22** after 10 minutes of microwave irradiation

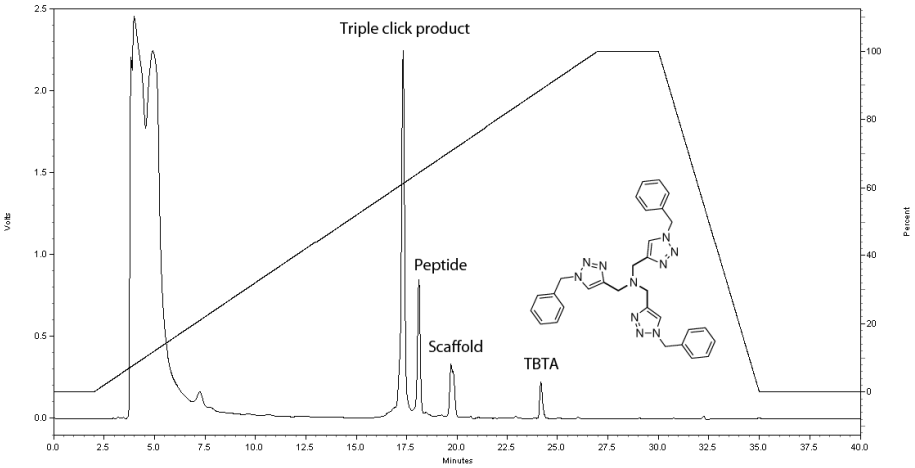

Figure 7 | HPLC chromatograms of CuAAC between TAC scaffold **19** and cyclic azidopeptide **22** using optimized reaction conditions including the use of TBTA.

In order to attempt to improve the conversion of this reaction, the amount of catalyst and the reaction time were increased but this did not lead to significant improvement of the conversion. Further optimization studies were performed, including the addition of TBTA to the reaction mixture. This ligand (shown in Figure 7) is known to maintain the catalytically active state of Cu(I), by binding tightly to it and thereby stabilizing this oxidation state of the metal.[36,37] Optimization studies showed that using cyclic peptide **22** (1 eq per alkyne) in the presence of 0.2 equivalents of $CuSO_4$, 0.4 equivalents Na-

ascorbate and 0.05 equivalents of TBTA per alkyne-functionality and microwave irradiation at 80ºC for 15 minutes resulted in a much cleaner reaction mixture, and gave selective formation of the "triple-click" product **23** (Figure 8). Although still no full conversion of starting materials was observed, the triple-click product was obtained in 56% isolated yield (3.8 mg).

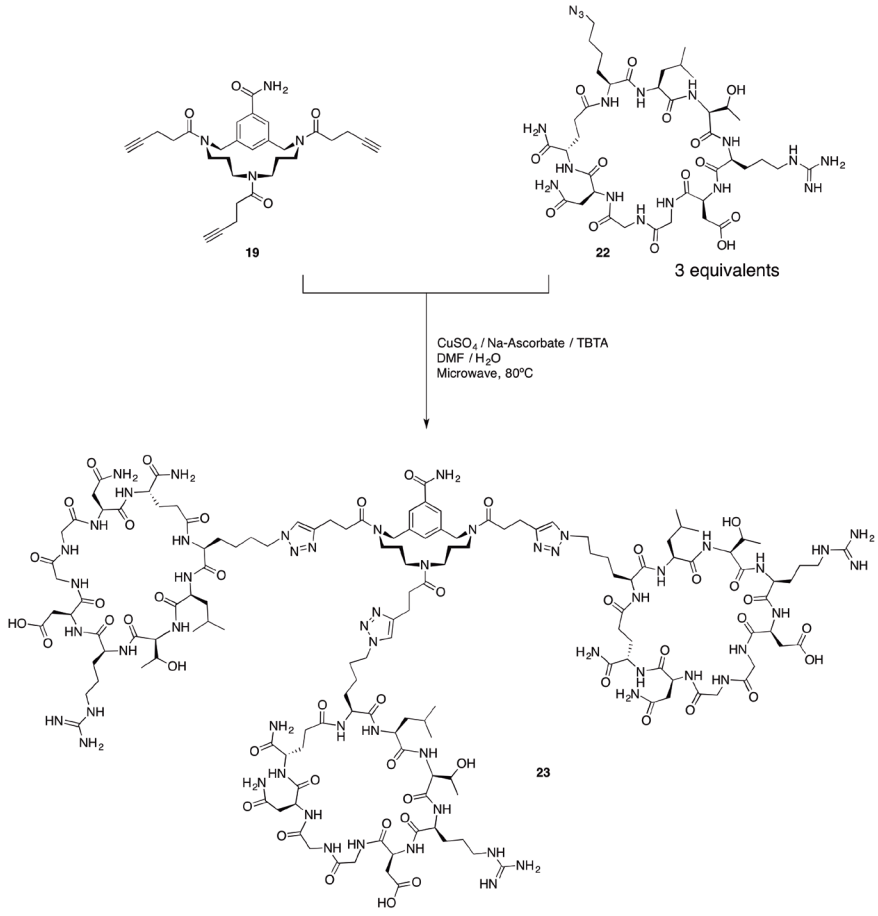

Figure 8 | Conjugation of cyclic peptide **22** to scaffold **19** via CuAAc

Although the conversion of this reaction shown in Figure 7 was not yet optimal, the use of TBTA was clearly beneficial and promoted formation of the triple-clicked product. Since compound **23** was only a model compound, no further optimization studies were performed here to drive the reaction to completion.

3.3 Conclusions

The development of a modular synthetic approach for the attachment of three identical cyclic peptides to a small scaffold molecule was outlined in this chapter.
The work shows that the best approach involved the attachment of *unprotected* cyclic peptides to the TAC-scaffold. Coupling of protected cyclic peptides to the TAC-scaffold was troublesome, the desired products could not be obtained using standard coupling reagents and analysis of the resulting products was troublesome.
A consequence of the use of unprotected cyclic peptides was that conjugation to a scaffold molecule required the use of an orthogonal ligation reaction. The attachment of three identical cyclic peptides to the TAC-scaffold was successfully achieved using the copper catalyzed azide alkyne cycloaddition reaction (CuAAC)[28,29] using TBTA[37] to maintain the catalytically active state of Cu(I) in combination with microwave heating.
In the next chapter this synthetic approach will be applied for the attachment of three different cyclic peptides to the TAC-scaffold, leading to the synthesis of a mimic of the discontinuous epitope of HIV gp120.

3.4 Experimental methods

Reagents, materials and analysis methods
Unless stated otherwise, chemicals were obtained from commercial sources and used without further purification. Peptide grade DiPEA, CH_2Cl_2, NMP, TFA and HPLC grade solvents were purchased from Biosolve B.V. (Valkenswaard, The Netherlands). Fmoc-protected amino acids were purchased from GL Biochem Ltd. (Shanghai, China). Sidechain protecting groups for amino acids were as follows: Ser(tBu), Asp(OtBu), Glu(OtBu), Thr(tBu), Asn(Trt), Trp(Boc), Gln(Trt), Lys(Boc), Arg(Pbf). TentaGel S RAM resin functionalized with a Rink linker (particle size 90μm, capacity 0.20-0.27 mmol/g) was purchased from Rapp Polymere GmbH (Tübingen, Germany). 2-Chlorotrityl chloride resin (100-200 mesh, 1% DVB, 1.0-1.6 mmol/g) was purchased from Iris Biotech GmbH. Solid phase peptide synthesis was carried out in plastic syringes with a polyethylene frit (20 μm) obtained from Screening Devices B.V. The resin loading was determined by measuring the UV absorbance of the piperidine-dibenzofulvene adduct (λ_{max} 300 nm).[38] Special amino acids were coupled manually, following the standard procedure for Fmoc/tBu solid phase peptide synthesis as described in chapter 2. Peptides containing commercially available amino acids were synthesized automatically on an Applied Biosystems 433A peptide synthesizer with a UV-monitoring system, which was used to monitor the Fmoc-removal step *i.e.* formation

of the dibenzofulvene-piperidine adduct at 301 nm. Reactions were performed at room temperature unless stated otherwise. Solution phase reactions were monitored by TLC analysis and R_f-values were determined on Merck pre-coated silica gel 60 F-254 (0.25 mm) plates. Spots were visualized with UV-light, and by heating plates dipped in ninhydrine, Cl_2/N,N,N,N'-tetramethyl-4,4'-diaminodiphenylmethane (TDM)[39] or a $KMnO_4$ solution. Column chromatography was performed using Silica-P Flash silica gel (60 Å, particle size 40-63 μm; Silicycle). Microwave reactions were performed in a Biotage Initiator (300 W) reactor in sealed vessels suitable for reaction volumes of 0.5-2 mL. ^{1}H NMR experiments were conducted on a 300 MHz Varian G-300 spectrometer, and chemical shifts are given in ppm (δ) relative to TMS (0.00 ppm). ^{13}C NMR spectra were recorded at 75 MHz at a Varian G-300 spectrometer and chemical shifts are given in ppm (δ) relative to $CDCl_3$ (77 ppm). In the synthesis of TAC, all NMR spectra were in accordance with previously published structures.[19] Therefore, for these compounds only ^{1}H-NMR spectra are reported here. Analytical HPLC was accomplished on a Shimadzu-10Avp (Class VP) system using UV-detector operating at 214 and 254 nm. The mobile phase was 0.1% TFA in CH_3CN/H_2O 5:95 (buffer A) and 0.1% TFA in CH_3CN/H_2O 95:5 (buffer B). For analysis of protected (cyclic) peptides the mobile phase was 0.1% TFA in CH_3CN/H_2O 20:80 (buffer A) and 0.1% TFA in CH_3CN/iPrOH/H_2O 50:45:5 (buffer B). A Phenomenex Gemini C18 column (110 Å, 5 μm, 250×4.60 mm) was used at a flow rate of 1 mL min^{-1} using the following protocol: 100% buffer A for 1 min, then a linear gradient of buffer B (0-100% in 30 min for a 40 min program or 0-100% in 50 min for a 60 min program). Purification of the peptides was performed on a Prep LCMS-QP8000α HPLC system (Shimadzu) using a Phenomenex Gemini C18 column (10 μm, 110 Å, 250×21.2 mm) at a flow rate of 12.5 mL min^{-1} using a standard protocol: 100% buffer A for 5 min followed by a linear gradient of buffer B (0-100% in 100 min) using the same buffers as described for analytical HPLC. Electrospray ionization mass spectrometry (ESI-MS) was performed on a Shimadzu LCMS-QP8000 single quadrupole bench-top mass spectrometer operating in a positive ionization mode or a Thermo-Finnigan LCQ Deca XP Max ion trap mass spectrometer. Analytical LC-MS was preformed on Thermo-Finnigan LCQ Deca XP Max coupled to a on a Shimadzu-10Avp (Class VP) system using UV-detector operating at 254 nm. MALDI-TOF-MS spectra were recorded on a Kratos Analytical (Shimadzu) AXIMA CFR mass spectrometer using α-cyano-4-hydroxycinnamic acid (CHCA) or sinapic acid as a matrix and human ACTH (18-39) or bovine insulin oxidized B chain as references. High resolution electrospray ionization (ESI) mass spectra were measured on a Micromass LCT mass spectrometer calibrated with CsI. All reported mass values are monoisotopic.

Mono-o-NBS protected bis(3-aminopropyl)amine

A solution of o-NBS-Cl (34.3 g, 150 mmol) in dry DCM (500 mL) was added dropwise to a cooled (ice/water, 0°C) solution of bis(3-aminopropyl)amine **1** (212 mL, 1.5 mol, 10 equiv) in dry DCM (600 mL). The mixture was allowed to react at room temperature overnight. After that, the reaction mixture was concentrated to a total volume of approximately 500 mL and the organic fraction was washed with a combination of

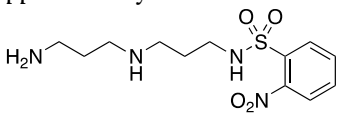

200 mL water and 270 mL 1N HCl. The organic layer was collected and to the aqueous layer 125 g NH_4Cl was added. The aqueous layer was extracted three times with 400 mL DCM. The organic layers were combined and concentrated to a volume of 500 mL, washed with brine, dried over Na_2SO_4 and concentrated *in vacuo*. The resulting mono-*o*-NBS protected bis(3-aminopropyl)amine **2** was analyzed with TLC and used without purification. Yield: 55 g (150 mmol, quantitative). R_f = 0.44 ($CHCl_3$/MeOH/25% NH_4OH (aq) – 8:4:1.5 v/v/v).

^{1}H-NMR (300 MHz, DMSO-d_6, TMS): δ 1.40-1.54 (d of quintets, 4H, $CH_2CH_2CH_2$), 2.40-2.47 (q, 4H, $NHCH_2CH_2$), 2.51-2.56 (t, 2H, NH_2CH_2), 2.91-2.95 (t, 2H, *o*-NBS-$NHCH_2$), 3.23-3.29 (q, 2H, TFAc- $NHCH_2$), 7.81-7.99 (m, 4H, C^{AR}-*H*).

***o*-NBS,TFAc-protected triamine 3**

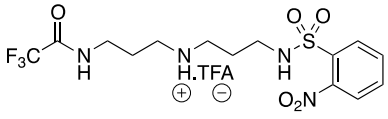

Crude mono-*o*-NBS protected bis(3-aminopropyl)amine **2** (55 g, 150 mmol) was suspended in dry dioxane (500 mL). To the resulting suspension, ethyl trifluoroacetate (2.5 eq, 45 mL, 375 mmol) and water (1 eq, 2.7 mL, 150 mmol) were added, after which the mixture was stirred overnight under reflux. The resulting mixture was concentrated *in vacuo* resulting in a very viscous yellow oil which slowly crystallized. The product was purified by recrystallization, by dissolving the product in boiling EtOAc (50 mL) and slowly adding DCM (300-400 mL), followed by storage overnight at 4°C. The yellow crystals were filtered, washed with cold DCM and dried *in vacuo*. *o*-NBS/TFAc-protected triamine **3** was obtained as a light yellow crystalline solid. Yield: 29.7 g (57 mmol, 38% from compound **2**). R_f = 0.20 (CH_2Cl_2/MeOH/TEA 90:10:1 v/v/v).

^{1}H-NMR (300 MHz, DMSO-d_6, TMS): δ 1.75-1.83 (d of quintets, 4H, $CH_2CH_2CH_2$), 2.90 (br. s, 4H, $NHCH_2CH_2$), 2.96-2.99 (q, 2H, *o*-NBS-$NHCH_2$), 3.23-3.29 (q, 2H, TFAc- $NHCH_2$), 7.87-8.03 (m, 4H, C^{AR}-*H*), 8.27 (t, 1H, *o*-NBS-N*H*), 8.59 (br s, 2H, NH_2), 9.56 (t, 1H, TFAc-N*H*).

o-NBS,Alloc,TFAc-protected triamine 4

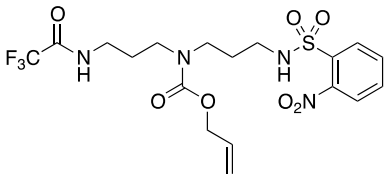

Protected triamine **3** (20 g, 38 mmol) was dissolved in a mixture of dioxane (160 mL) and water (160 mL). A solution of $NaHCO_3$ (12.8 g, 152 mmol) in water (120 mL) was added and the resulting mixture was cooled on ice. To this cooled (0ºC, ice/water) mixture, a solution of Alloc-Cl (4.8 mL, 46 mmol) in dioxane (80 mL) was added dropwise under stirring. The reaction mixture was allowed to reach room temperature and was stirred overnight. After that, the mixture was concentrated to remove dioxane, water (400 mL) was added and the aqueous phase was extracted three times with DCM (400 mL and 2 × 200 mL). The combined organic layers were dried over Na_2SO_4 and concentrated *in vacuo*, yielding the crude product as a yellow oil. Purification by column chromatography (EtOAc/hexanes 45:55 v/v) afforded triamide **4** as a yellow oil. Yield: 12.8 g (26 mmol, 67%). R_f = 0.30 (EtOAc/hexanes 1:1 v/v).

^{1}H-NMR (300 MHz, $CDCl_3$, TMS): δ 1.75-1.84 (m, 4H, $CH_2CH_2CH_2$), 3.09-3.16 (q, 2H, *o*-NBS-NHCH_2), 3.31-3.35 (br s, 6H, NCH_2CH_2), 4.60-4.64 (d, 2H, OCH_2), 5.22-5.28 (m, 2H, CH=CH_2), 5.34 + 6.05 (2 br s, 2 × 0.5 H, *o*-NBS-N*H*), 5.88-5.97 (m, 1H, C*H*=CH_2), 6.58 (br s, 0.5 H, TFAc-N*H*), 7.75 (m, 2H, C^{AR}-*H*), 7.85 (m, 1H, C^{AR}-*H*), 7.87 (br s, 0.5 H, TFAc- NHCH_2), 8.12 (m, 1H, C^{AR}-*H*).

MeOC(O)-TAC(*o*-NBS,Alloc,TFAc) 6

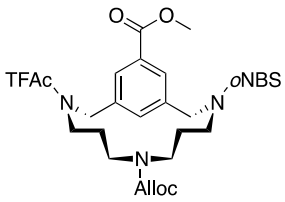

o-NBS/Alloc/TFAc-protected triamine **4** (2.50 g, 5.03 mmol) was dissolved in dry DMF (500 mL, 4Å molsieves). To this solution, bisbromide **5**[19] (1.62 g, 5.03 mmol), Cs_2CO_3 (6.56 g, 20.1 mmol) and TBAB (1.62 g, 5.03 mmol) were added and the solution was stirred overnight at room temperature. The reaction mixture was concentrated *in vacuo* and the residue was dissolved in DCM. The organic phase was washed with $KHSO_4$ (400 mL 1 N + 100 mL 2N) and the aqueous phase was extracted again with DCM (500 mL). The combined organic layers were washed with brine, dried over Na_2SO_4 and concentrated *in vacuo* which afforded the crude product as a yellow oil. Purification by column chromatography (DCM/EtOAc/hexanes, 79:5:6 v/v/v) afforded the product as a light yellow foam. Yield: 2.2 g (3.35 mmol, 67%). R_f = 0.55 (EtOAc/hexanes 2:1 v/v)

^{1}H-NMR (300 MHz, $CDCl_3$, TMS): δ 1.35 (m, 2.5H, $CH_2CH_2CH_2$), 1.62 (m, 1.5H, $CH_2CH_2CH_2$), 2.92-3.11 (m, 4H, NCH_2CH_2), 3.23-3.45 (m, 4H, NCH_2CH_2), 3.93, 3.95 (2 s, 3H, OCH_3), 4.45-4.51 (m, 4H, Ar-CH_2N + OCH_2), 4.66 (s, 1H, Ar-CH_2N), 4.77 (s, 1H, Ar-CH_2N), 5.15-5.24 (m, 2H, CH=CH_2) 5.83 (m, 1H, C*H*=CH_2) 7.67-8.08 (m, 7H, C^{AR}-*H*).

HOC(O)-TAC (o-NBS,Alloc,Fmoc) 7

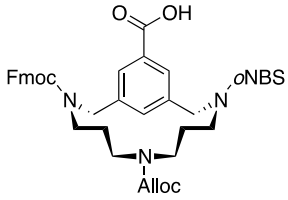

Fully protected TAC-scaffold **6** (1.97 g, 3.0 mmol) was suspended in Tesser's base (105 mL, dioxane/MeOH/4N NaOH 14:5:1 v/v/v). The reaction mixture was stirred overnight at room temperature. The resulting clear solution was neutralized by the addition of 1N HCl, concentrated *in vacuo* and resuspended in 100 ml dioxane/water (1:1 v/v). Triethylamine was added to the reaction mixture until a pH of 9.5 was obtained. A solution of Fmoc-OSu (1.11 g, 3.3 mmol) in dioxane (10 mL) was added to the reaction mixture. Triethylamine was added dropwise to maintain a pH of 8.5-9 and the reaction mixture was stirred at room temperature for 2 h. Subsequently, the reaction mixture was concentrated *in vacuo* to remove dioxane, and the aqueous residue was acidified with 1N $KHSO_4$ to pH 2. The aqueous layer was extracted with EtOAc (3 × 100 mL) and the combined organic layers were washed with brine, dried over Na_2SO_4 and concentrated *in vacuo*. The crude product was purified by column chromatography in EtOAc/hexanes/AcOH 10:40/0.5 v/v/v. This afforded compound **7** as a white solid. Yield: 2.21 g (2.9 mmol, 87%). R_f = 0.14 (EtOAc/hexanes 1:4 (v/v) + 0.5% AcOH)

^{1}H-NMR (300 MHz, $CDCl_3$, TMS): δ 0.89-1.05 + 1.19-1.51 (br m, 4H, $CH_2CH_2CH_2CH_2$), 2.3-2.5 + 2.8-3.1 + 3.2-3.4 (br m, 8H, NCH_2CH_2), 4.2-4.5, 4.6-4.8 (br m, 9H, Fmoc-OCH_2CH, Alloc- OCH_2, Ar-CH_2N) 5.16-5.23 (br m, 2H, $CH{=}CH_2$), 4.45-4.51 (m, 4H, Ar-CH_2N + OCH_2), 5.85 (m, 1H, $CH{=}CH_2$), 7.14-7.40, 7.54-7.80, 7.86-8.10 (m, 7H, C^{AR}-*H*).

Fmoc-Lys(1-pentynoyl)-OH 8

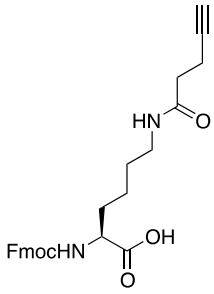

4-Pentynoic acid (1.96 g, 20 mmol), DCC (4.13 g, 20 mmol) and *N*-hydroxysuccinimide (2.3 g, 20 mmol) were dissolved in 200 mL CH_2Cl_2. The reaction mixture was stirred for 2 h at room temperature. The mixture was filtered to remove DCU and the filtrate was concentrated *in vacuo*. Fmoc-Lys-OH.HCl (8.1 g, 20 mmol) was suspended in 300 mL CH_2Cl_2 and Et_3N (5.62 mL, 40 mmol) was added to the solution. The pre-activated 4-pentynoic acid was added to the reaction mixture and the resulting mixture was stirred at room temperature. Upon completion of the reaction, the mixture was concentrated *in vacuo* and the residue was dissolved in 300 mL EtOAc. The organic layer was washed with 1N $KHSO_4$ (300 mL), saturated $KHCO_3$ (300 mL), H_2O (300 mL), dried over Na_2SO_4 and concentrated *in vacuo*. The crude product was purified by column chromatography in EtOAc/hexanes 3:7 v/v. This afforded compound **8** as a white solid. Yield: 7.62 g (17 mmol, 85%). R_f = 0.70 ($CHCl_3$/MeOH/AcOH 95:20:3 v/v/v.

1H-NMR (300 MHz, DMSO-$_{d6}$, TMS): δ 1.37 (br. s., 4H, Lys-$^{\delta}CH_2$ and Lys-$^{\gamma}CH_2$),

1.67-1.80 (m, 2H, Lys-$^{\beta}CH_2$), 2.25 (m, 2H, CH_2C-CH), 2.34 (d, 2H, NHCOCH_2), 2.50 (s, 1H, C-C*H*), 3.03 (d, 2H, $^{\varepsilon}CH_2$), 3.92 (m, 1H, $^{\alpha}CH$) 4.25-4.27 (m, 3H, Fmoc-C*H*CH_2), 7.31-7.91 (m, 10H, Fmoc-ARC*H* and N*H*). 13C-NMR (75 MHz, DMSO-$_{D6}$): δ 14.3, 23.1, 28.7, 30.5, 34.3, 38.3, 46.7, 53.8, 65.5, 71.2, 120.1, 125.3, 127.1, 127.7, 140.7, 143.9, 156.2, 170.1, 174.0

Protected cyclic peptide 12: cyclo(Leu-Thr(tBu)-Arg(Pbf)-Asp(OtBu)-*N*(DMB)Gly-Gly-Asn(Trt)-γGln)-Gly-OH

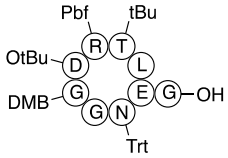

Cyclic peptide **12** was synthesized on 2 chlorotrityl chloride resin. The resin was loaded with Fmoc-Gly-OH, following the procedure described in chapter 2. As a second amino acid, Fmoc-Glu(OPTMSE)-OH was coupled using 2 equivalents of amino acid (1.53 g, 2.81 mmol), 2 equivalents of HBTU and HOBt and 4 equivalents D*i*PEA in NMP. The mixture was allowed to react overnight, and completion of the reaction was confirmed with a Kaiser test.[40] Synthesis of the remaining peptide sequence was performed on 0.25 mmol scale, on an automatic ABI 433A Peptide Synthesizer. An adapted protocol was used which after deprotection of the final Fmoc-group performed automatic deprotection of the PTMSE-protecting group using TBAF in DCM, and sidechain-to-tail cyclization of the peptide. The resulting cyclic peptide was cleaved from the resin by treatment with TFE/DCM (10 mL, 2:8 v/v) followed by precipitation in MTBE/hexanes (1:1 v/v) and centrifugation. The resulting pellets were dissolved in tBuOH/H_2O (1:1 v/v) and lyophilized. The crude product was obtained as a white powder (480 mg, >100%), which was purified by preparative HPLC, using a buffer system for hydrophobic peptides: 0.1% TFA in CH_3CN/H_2O 20:80 (buffer A) and 0.1% TFA in CH_3CN/iPrOH/H_2O 50:45:5 (buffer B). Yield: 48 mg (0.039 mmol, 12%). The purity of peptide **12** was established with analytical HPLC, R_t = 28.88 min, purity > 90%. Monoisotopic mass calculated for $C_{84}H_{113}N_{13}O_{20}S$ $[M+H]^+$ 1656.79, found 1656.52

Compound 13

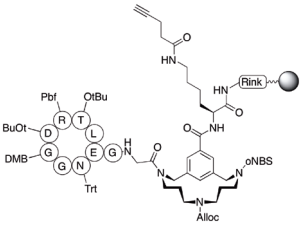

Analysis was performed after a micro cleavage of compound **13** from the resin. During this process also acid-labile sidechain protecting groups of the peptide were cleaved. 5 mg resin was treated with 1 mL TFA/TIS/H_2O for 1 h. After this, the solution was filtered, concentrated *in vacuo* and the residue was dissolved in MeCN/H_2O (1:1 v/v).

HPLC: R_t = 27.87 min. Monoisotopic mass calculated for $C_{73}H_{105}N_{21}O_{24}S$ $[M+H]^+$ 1692.74, found 1692.67

Compound 15b

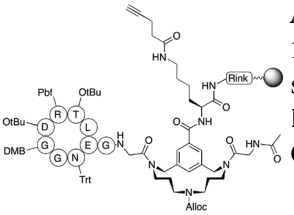

Analysis was performed after micro cleavage of compound **15b** from the resin. During this process also acid-labile sidechain protecting groups of the peptide were cleaved. HPLC: Rt = 26.39 min. Monoisotopic mass calculated for $C_{71}H_{107}N_{21}O_{22}$ $[M+H]^+$ 1606.79, found 1607.22

Peptide 21 Ac-Lys-Arg-Trp-Trp-Lys-Trp-Ile-Arg-Trp-Lys(N_3)-NH_2
Azidopeptide **21** was synthesized on Tentagel S RAM resin (0.24 mmol/g) following the standard procedure as described in chapter 2. Synthesis was performed on a 0.6 mmol scale (2.5 g resin). The thus obtained peptide was deprotected and cleaved from the resin using TFA/TIS/H_2O (15 mL, 95:2.5:2.5 v/v/v) followed by precipitation in MTBE/hexanes (1:1 v/v) and centrifugation. The resulting pellets were dissolved in tBuOH/H_2O (1:1 v/v) and lyophilized, affording the crude azidopeptide **21** as a white powder (1.2 g, >100%). 210 mg of this crude product was purified by preparative HPLC. The mobile phase was 0.1% TFA in CH_3CN/H_2O 5:95 (buffer A) and 0.1% TFA in CH_3CN/H_2O 95:5 (buffer B). Yield: 81 mg (0.051 mmol 49%).
The purity of peptide **21** was established with analytical HPLC. R_t= 41.27 min, purity >95%. Monoisotopic mass calculated for $C_{82}H_{114}N_{26}O_{11}$ $[M+H]^+$ 1639.92, found 1639.48

***N,N,N*-tris(pent-4-ynoyl)-triazacyclophane scaffold 19**

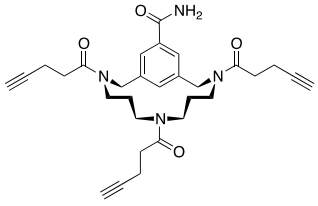

Tentagel S RAM resin (4 g, 0.24 mmol/g) was swelled in NMP (3 × 10 mL per gram of resin, 2 min). For all subsequent reactions also 10 mL solvent per gram of resin was used. The *N*-terminal Fmoc protecting group was removed using 20% piperidine in NMP (3 × 8 min) followed by washing steps with NMP (3 × 2 min), CH_2Cl_2 (3 × 2 min) and NMP (3 × 2 min). *N*,*N*,*N*-tris(2-nitrophenylsulfonamido)-triazacyclophane scaffold **16**[8-11,41] (1.60 g, 1.92 mmol, 2 eq), 2 equivalents of HOBt and HBTU and 4 equivalents of DiPEA were dissolved in NMP, added to the resin and coupled overnight. After coupling, the resin **17** was washed with NMP (3 × 2 min), CH_2Cl_2 (3 × 2 min) and DMF (3 × 2 min) followed by treatment with 15 eq (14.4 mmol, 2.15 mL) DBU and 30 eq β-mercaptoethanol (28.8 mmol, 2.02 mL) in DMF. After 30 min, the solution was drained and the procedure was repeated once. The resin was washed with DMF (3 × 2 min), CH_2Cl_2 (3 × 2 min) and NMP (3 × 2 min), followed by coupling of 4-pentynoic acid (3 eq per amine, 847 mg, 8.64 mmol) using 3 equivalents of HOBt and HBTU and 6 equivalents of DiPEA in NMP. The mixture was allowed to react for two h followed by the standard washing procedure (see chapter 2). Resin **18** (2.17 g, 0.5 mmol) was treated with 40 mL TFA/TIS/H_2O (95:2.5:2.5 v/v/v)

during 2.5 h, after which the mixture obtained after filtration was concentrated *in vacuo* and applied to a silica column and eluted with a gradient of CH_2Cl_2/MeOH/acetone (93:2:5 to 90:5:5 v/v/v). After solvent removal the product was obtained as a white foam. (131 mg, 51%). R_f: 0.46 (CH_2Cl_2/MeOH/acetone 90:5:5 v/v/v).
HRMS monoisotopic calcd for $C_{30}H_{36}N_4O_4$ $[M+H]^+$, 517.2809, found 517.2785.
HPLC: R_t= 23.87 min, purity= 99%.

Cyclic peptide 22: cyclo(Lys(N_3)-Leu-Thr-Arg-Asp-Gly-Gly-Asn-γGln)-NH_2
Cyclic azidopeptide **22** was synthesized on Tentagel S RAM resin (0.24 mmol/g). The first amino acid, Fmoc-Glu(OPTMSE)-OH, was coupled manually using 3 equivalents of amino acid, HBTU and HOBt and 6 equivalents of D*i*PEA. From this point onwards, the protocol for automatic synthesis of cyclic peptides that was described for the synthesis of cyclic peptide **12** was followed. Synthesis was performed on 0.25 mmol scale, and resulted in 179 mg crude peptide **22** (72%). The crude cyclic azidopeptide was purified with preparative HPLC, affording 29 mg pure compound **22** (12%).
The purity of peptide **22** was established with analytical HPLC. R_t = 18.05 min, purity >99%. Monoisotopic mass calculated for $C_{39}H_{65}N_{17}O_{14}$ $[M+H]^+$ 996.49, found 996.44.

Click compound 23
10-fold stock solutions of $CuSO_4$ (12.0 µmol, 2.9 mg in 1 mL H_2O) and sodium ascorbate (24.0 µmol, 4.8 mg in 1 mL H_2O) were prepared. TBTA (0.15 mg, 0.29 µmol) was dissolved in 100 µL DMF. Peptide **22** was dissolved in DMF (4Å mol sieves, 200 µL).
TAC scaffold **19** (1.9 µmol, 1 mg) was added to the microwave vessel (0.5-2 mL) followed by addition of the peptide-solution. 100 µL of the $CuSO_4$ stock solution (1.2 µmol, 0.29 mg) and 100 µL of the sodium ascorbate stock solution (0.48 µmol, 0.48 mg) were added to the mixture, followed by addition of the TBTA solution (0.29 µmol, 0.15 mg). The microwave vessel was sealed and the reaction mixture was allowed to react in the microwave reactor at 80ºC during 15 min.
After reaction, a sample was taken from the reaction mixture for LC-MS analysis. Based on this analysis, the triple clicked compound **23** was isolated by preparative HPLC. Yield: 3.8 mg (56%).
Rt = 17.37 min, purity >99%. Monoisotopic mass calculated for $C_{147}H_{231}N_{55}O_{46}$ $[M+H]^+$ 3503.74, found 3501.99.

References

(1) DeGrado, W. F.; Wasserman, Z. R.; Lear, J. D. *Science* **1989**, *243*, 622–628.
(2) Mutter, M.; Vuilleumier, S. *Angew. Chem. Int. Ed.* **1989**, *28*, 535–554.
(3) Altmann, K. H.; Mutter, M. *Int. J. Biochem.* **1990**, *22*, 947.
(4) Ma, B.; Elkayam, T.; Wolfson, H.; Nussinov, R. *Proc. Natl. Acad. Sci.* **2003**, *100*, 5772–5777.
(5) Yin, H.; Hamilton, A. D. *Angew. Chem. Int. Ed.* **2005**, *44*, 4130–4163.
(6) Rosenzweig, B. A.; Ross, N. T.; Tagore, D. M.; Jayawickramarajah, J.; Saraogi, I.; Hamilton, A. D. *J. Am. Chem. Soc.* **2009**, *131*, 5020–5021.
(7) Ghosh, P. S.; Hamilton, A. D. *J. Am. Chem. Soc.* **2012**, *134*, 13208–13211.
(8) Gokhale, A.; Weldeghiorghis, T. K.; Taneja, V.; Satyanarayanajois, S. D. *J. Med. Chem.* **2011**, *54*, 5307–5319.
(9) Bock, J. E.; Gavenonis, J.; Kritzer, J. A. *ACS Chem. Biol.* **2013**, *8*, 488–499.
(10) Chen, S.; Morales-Sanfrutos, J.; Angelini, A.; Cutting, B.; Heinis, C. *ChemBioChem* **2012**, *13*, 1032–1038.
(11) White, C. J.; Yudin, A. K. *Nature Chem.* **2011**, *3*, 509–524.
(12) Singh, Y.; Dolphin, G. T.; Razkin, J.; Dumy, P. *ChemBioChem* **2006**, *7*, 1298–1314.
(13) Thumshirn, G.; Hersel, U.; Goodman, S. L.; Kessler, H. *Chem. Eur. J.* **2003**, *9*, 2717–2725.
(14) Dijkgraaf, I.; Rijnders, A. Y.; Soede, A.; Dechesne, A. C.; van Esse, G. W.; Brouwer, A. J.; Corstens, F. H. M.; Boerman, O. C.; Rijkers, D. T. S.; Liskamp, R. M. J. *Org. Biomol. Chem.* **2007**, *5*, 935.
(15) Yim, C.-B.; Dijkgraaf, I.; Merkx, R.; Versluis, C.; Eek, A.; Mulder, G. E.; Rijkers, D. T. S.; Boerman, O. C.; Liskamp, R. M. J. *J. Med. Chem.* **2010**, *53*, 3944–3953.
(16) Foillard, S.; Jin, Z.-H.; Garanger, E.; Boturyn, D.; Favrot, M.-C.; Coll, J.-L.; Dumy, P. *ChemBioChem* **2008**, *9*, 2326–2332.
(17) Galibert, M.; Dumy, P.; Boturyn, D. *Angew. Chem. Int. Ed.* **2009**, *48*, 2576–2579.
(18) Beal, D. M.; Jones, L. H. *Angew. Chem. Int. Ed.* **2012**, *51*, 6320–6326.
(19) Opatz, T.; Liskamp, R. M. J. *Org. Lett.* **2001**, *3*, 3499–3502.
(20) Opatz, T.; Liskamp, R. M. J. *J. Comb. Chem.* **2002**, *4*, 275–284.
(21) Chamorro, C.; Hofman, J.-W.; Liskamp, R. M. J. *Tetrahedron* **2004**, *60*, 8691–8697.
(22) Monnee, M. C. F.; Brouwer, A. J.; Liskamp, R. M. J. *QSAR Comb. Sci.* **2004**, *23*, 546–559.
(23) van Zoelen, D.-J.; Egmond, M. R.; Pieters, R. J.; Liskamp, R. M. J. *ChemBioChem* **2007**, *8*, 1950–1956.
(24) Albada, H. B.; Liskamp, R. M. J. *J. Comb. Chem.* **2008**, *10*, 814–824.
(25) Hijnen, M.; van Zoelen, D. J.; Chamorro, C.; van Gageldonk, P.; Mooi, F. R.; Berbers, G.; Liskamp, R. M. J. *Vaccine* **2007**, *25*, 6807–6817.
(26) Chamorro, C.; Kruijtzer, J. A. W.; Farsaraki, M.; Balzarini, J.; Liskamp, R. M. J. *Chem. Commun.* **2009**, 821.
(27) Tesser, G. I.; Balvert-Geers, I. C. *Int. J. Pept. Protein Res.* **1975**, *7*, 295–305.
(28) Tornøe, C. W.; Christensen, C.; Meldal, M. *J. Org. Chem.* **2002**, *67*, 3057–3064.
(29) Rostovtsev, V. V.; Green, L. G.; Fokin, V. V.; Sharpless, K. B. *Angew. Chem. Int. Ed.* **2002**, 2596–2597.
(30) Holub, J. M.; Kirshenbaum, K. *Chem. Soc. Rev.* **2010**, *39*, 1325.

(31) Zhang, Z.; Fan, E. *Tetrahedron Lett.* **2006**, *47*, 665–669.
(32) Kümin, M.; Sonntag, L.-S.; Wennemers, H. *J. Am. Chem. Soc.* **2007**, *129*, 466–467.
(33) Angelo, N. G.; Arora, P. S. *J. Org. Chem.* **2007**, *72*, 7963–7967.
(34) Ingale, S.; Dawson, P. E. *Org. Lett.* **2011**, *13*, 2822–2825.
(35) Meldal, M.; Tornøe, C. W. *Chem. Rev.* **2008**, *108*, 2952–3015.
(36) Wang, Q.; Chan, T. R.; Hilgraf, R.; Fokin, V. V.; Sharpless, K. B.; Finn, M. G. *J. Am. Chem. Soc.* **2003**, *125*, 3192–3193.
(37) Chan, T. R.; Hilgraf, R.; Sharpless, K. B.; Fokin, V. V. *Org. Lett.* **2004**, *6*, 2853–2855.
(38) Fields, G. B. *Int. J. Peptide Protein Res.* **1990**, *35*, 161–214.
(39) Arx, Von, E.; Faupel, M.; Brugger, M. *J. Chromatogr. A* **1976**, *120*, 224.
(40) Kaiser, E.; Colescott, R. L.; Bossinger, C. D.; Cook, P. I. *Anal. Biochem.* **1970**, *34*, 595.
(41) Monnee, M. C. F.; Brouwer, A. J.; Verbeek, L. M.; van Wageningen, A. M. A.; Liskamp, R. M. J. *Bioorg. Med. Chem. Lett.* **2001**, *11*, 1521–1525.

4

A combinatorial approach toward smart libraries of discontinuous epitopes of HIV gp120 on a TAC synthetic scaffold

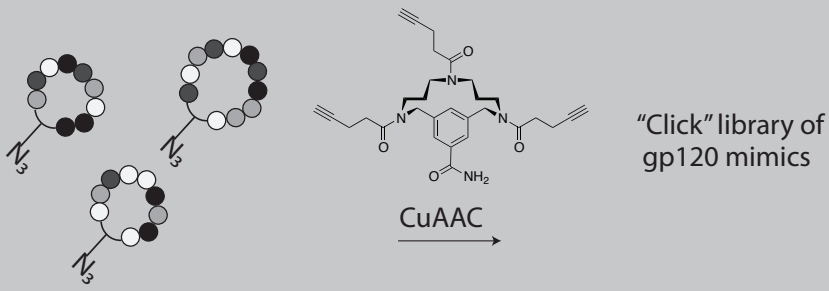

Part of the work described in this chapter has been published: G.E. Mulder, J.A.W. Kruijtzer, R.M.J. Liskamp, *Chem Commun.* **2012**, 10007-10009.

4.1 Introduction

One of the greatest challenges in the construction of protein mimics is mimicry of the discontinuous epitope nature of the large surfaces of proteins. This mimicry is difficult to achieve, since linear peptides usually do not adopt the correct 3D-folded structure of these epitopes. For mimicry of discontinuous epitopes, the challenge is not only the proper folding of individual peptide segments but also the combination of several different peptides into a single molecule. In previous chapters, methods were described for the efficient synthesis of cyclic peptides, and for the coupling of multiple cyclic peptides to relatively small scaffold molecules. The research presented in chapters two and three clearly pointed at the necessity of using unprotected cyclic peptides for these purposes. These findings could now be used for the synthesis of a mimic of the discontinuous CD4-binding site of HIV gp120.

Among the many protein-protein interactions involving discontinuous epitopes, we are especially interested in the interaction of HIV gp120 with the CD4 receptor, since this interaction is a potential target for HIV-vaccine design.[1,2] Therefore, mimicry of the gp120 discontinuous epitopes in a (much) smaller protein mimic may possibly lead to a synthetic vaccine.

Numerous methods have been described for the determination of key binding regions of proteins, also called functional epitopes or hot spots. Crystal structure analysis,[3,4] site-directed mutagenesis and epitope-mapping studies[5] have shown that amino acids which are essential for correct binding of HIV gp120 to CD4 are located in three regions far removed from each other in the primary sequence of gp120. The primary contact residues, D368, E370, W427, and D457 of gp120 which are involved in interaction with CD4 could be identified by X-ray crystallography[3] and mutagenesis studies[5], and are located in conserved domains of the otherwise highly variable protein.

Based on the X-ray crystal structure of protein complexes, in this case the gp120-CD4 complex,[3] it was possible to decide which interacting peptide segments might be most effective for inclusion in a discontinuous epitope mimic to be synthesized (Figure 1).

Indeed, we[6] and others[7] have followed this approach. For this purpose we have devised a conveniently accessible (TAC, triazacyclophane) scaffold, to which three different peptide sequences can be attached.[8] In order to obtain the best possible mimicry of epitope *loops*, previously we have developed a general approach for the non-stop solid phase synthesis of subsequently three *different cyclic peptides* onto a TAC scaffold.[6]

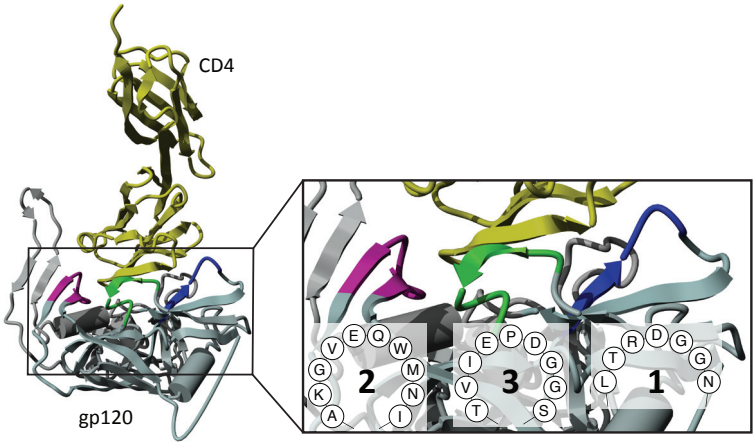

Figure 1 | Conserved epitopes in the CD4 binding site on gp120. These loop-shaped epitopes were selected for inclusion in a gp120 discontinuous epitope mimic.

inhibition of infection was observed in tissue culture. Although such an inhibition is difficult to realize, this result pointed at the potential problem of whether the right or best mimic has been synthesized.

With respect to this, crucial issues related to designing and synthesizing the optimal discontinuous epitope mimics are: (i) do the cyclic peptides mimicking the discontinuous epitope loops have the right size? (ii) is the arrangement of the cyclic peptides in the mimic an adequate representation of the situation in the protein complex? (iii) does the scaffold provide the proper flexibility or rigidity? (iv) does the scaffold provide a good platform for the relative involvement of the different loops of the discontinuous epitope?

In this chapter, an approach is provided for solutions of several of these issues. Current trends in biological approaches towards finding actives in peptide- and protein-based drug research include the screening of many combinations of peptides often from large libraries –obtained for example from phage display– before finding a hit. Two recent approaches point at the importance of the introduction of cyclic peptides or loops in peptide libraries, and the use of these to find active hits. In the approach by Timmerman et al.[9,10] in principle collections of especially mono- and bicyclic peptides can rapidly be prepared. The alkylation agent used for this purpose was also employed in the approach by Heinis et al.[11] for the preparation of bicyclic peptides from phage-encoded peptides. Here, a reproducible combinatorial approach is described for the

introduction of up to three cyclic peptides onto a scaffold, leading to clean collections or libraries of scaffolded loops, which can be unambiguously characterized by MS, conveniently separated by HPLC and screened as mixtures or as single compounds for binding to the CD4-receptor. This convergent approach as compared to the earlier described non-stop solid phase approach[6] allowed a much faster accessibility to several protein mimics for screening purposes. In addition, the approach permitted variation of the structural inputs such as scaffold, ring size, identity and position of the cyclic peptides, thereby addressing the issues raised above for designing and synthesizing optimal discontinuous epitope mimics.

4.2 Results and discussion

4.2.1 – Synthetic approach

For the the assembly of multiple (unprotected) peptides on a scaffold molecule, a wide variety of bioorthogonal ligation methods are available.[12-14] However, when libraries are screened for actives, it is crucial that no unknown contaminations or impurities are present. These could give rise to false positives that cannot be re-synthesized. Our approach utilizes the Cu(I)-catalyzed azide alkyne cycloaddition (CuAAC)[15,16] reaction, which is known to be fast, highly selective and leads to full conversion of starting materials and to highly stable products. We have introduced the triazacyclophane (TAC) scaffold as a template, which could lead to considerable pre-organization of the attached peptide ligands with respect to each other.[6,17-21] For CuAAC the TAC-scaffold was outfitted with three pentynoic acid residues leading to **1** (Scheme 1). A detailed description of the synthetic procedure for **1** can be found in chapter 3.

As was discussed above and described in chapter 2, the best mimicry of epitope *loops* can probably be achieved using cyclic peptides. Although widely used in every conceivable branch of chemistry and biology, synthesis and purification of cyclic peptides, irrespective of their size and amino acid composition, turned out to be a major hurdle.[22-24] Various synthetic procedures were employed, and the method shown in Scheme 2 proved to be most efficient. Briefly, first the linear peptide containing an azidolysine residue for CuAAC was synthesized on 2-chlorotrityl chloride resin (**2**).

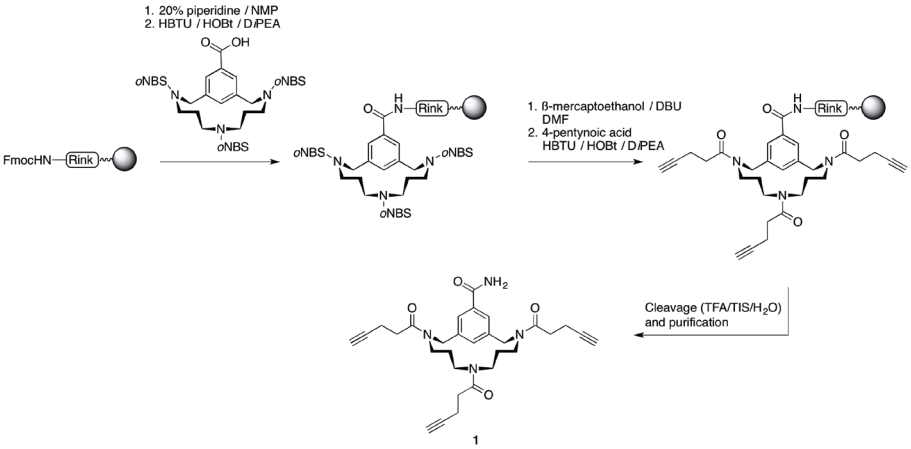

Scheme 1 | Synthesis of the the alkyne-functionalized TAC-scaffold **1**

This resin allowed cleavage of the peptide from the resin while its side chain protecting groups remained unaffected, and cleavage from this resin yielded the peptide with a C-terminal carboxylic acid **4**. Next, the protected peptide **3** was cleaved from the resin, followed by head-to-tail cyclization of this sidechain-protected linear peptide in solution.

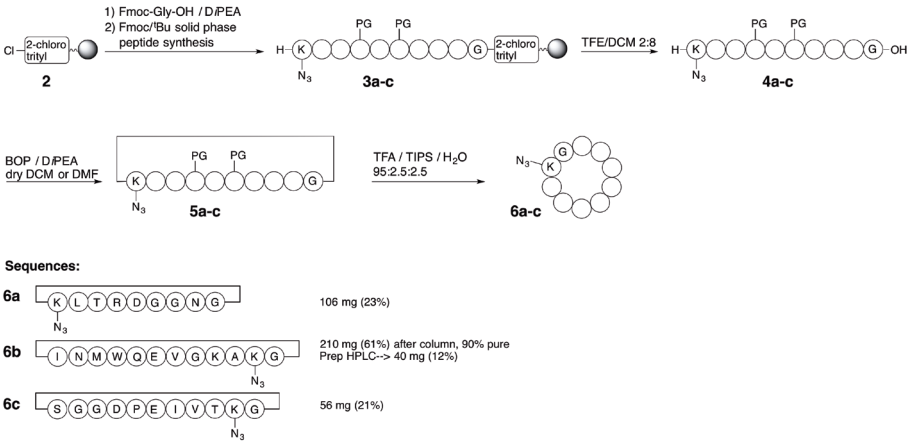

Scheme 2 | Synthesis of head to tail cyclized azidopeptides

Because of the presence of a number of (lipophilic) protecting groups, normal (pressure) column chromatography could be carried out on silica. This facilitated the purification of large quantities of cyclic peptides in one single run, leading to pure protected cyclic peptides **5** in high yields. As was described in chapter 3, cyclic peptides **6a-6c** could now be attached to the TAC-scaffold using CuAAC.

Since the exact desired conformation of the cyclic peptides on the scaffold is unknown and usually large collections of compounds have to be screened for finding actives, an approach was developed which generated a small library of discontinuous epitope mimics of HIV gp120. Thus, an equimolar mixture of the three cyclic peptides **6a-6c** mimicking the three conserved loops of the CD4-binding site of gp120, was conjugated to the TAC scaffold by CuAAC.

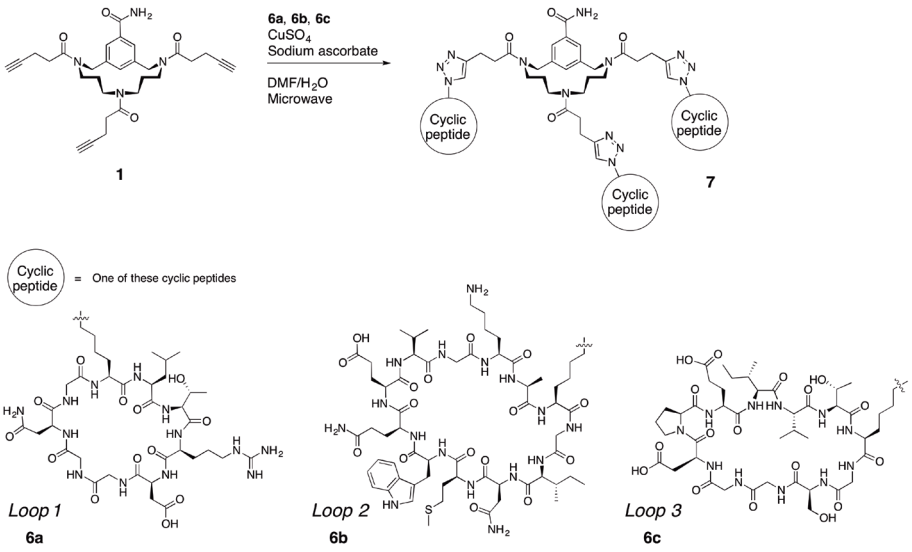

Scheme 3 | Synthesis of libraries of discontinuous epitope mimics by conjugation of cyclic peptides to the TAC-scaffold via CuAAC.

Since CuAAC is orthogonal to all amino acid sidechain functionalities, protecting groups were removed before performing CuAAC. Whereas "clicking" of protected cyclic peptides resulted in incomplete couplings and intractable mixtures (see chapter 3), clicking of deprotected cyclic peptides appeared to be an ideal approach

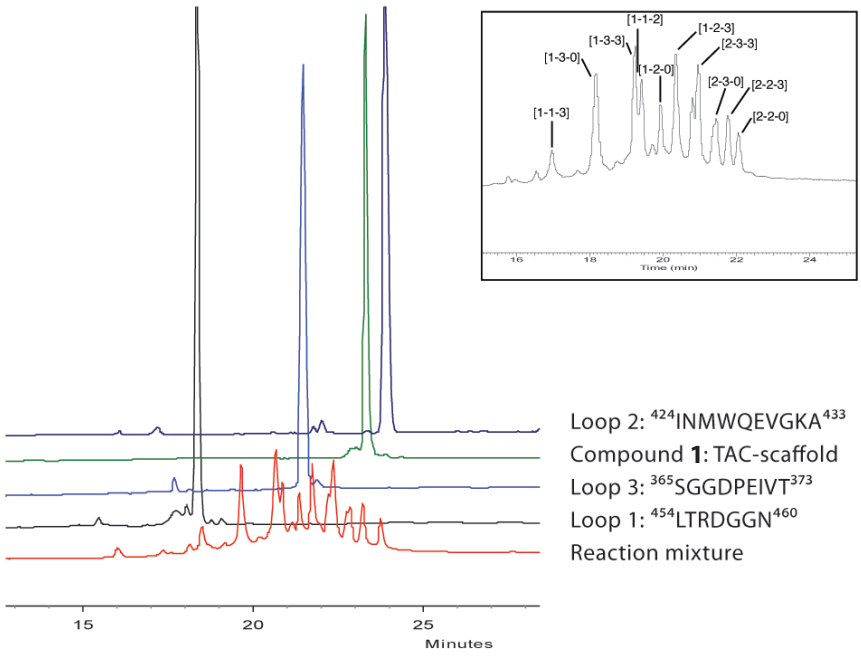

Figure 2 | HPLC chromatogram of cyclic azidopeptides containing the conserved epitopes, TAC-scaffold **1** and reaction products of the CuAAC reaction depicted in Scheme 3.

for obtaining libraries of TAC-scaffolded cyclic peptides. The most efficient reaction conditions involved the use of $CuSO_4$, in the presence of TBTA.[25,26] The reaction mixture was allowed to react during 25 minutes, under microwave irradiation at 80ºC. HPLC analysis revealed full conversion of all staring materials and very defined and clean reaction mixtures containing libraries of discontinuous epitope mimics of HIV gp120 were obtained (Figure 2). With LC-MS practically all combinations of cyclic peptide loops on the TAC-scaffold could be identified based on their mass value.

LC-MS-analysis revealed that no by-products were formed during CuAAC and reaction mixtures solely containing the desired discontinuous epitope mimics were obtained. Thus, this approach provided access to "clean" collections or libraries. In addition, the synthetic method described here was highly reproducible, since very similar HPLC-patterns were observed upon repeating the procedure. Most importantly, when the experiment was repeated on a larger scale (5-10 mg per peptide), the individual library members could be isolated from the mixture by preparative HPLC. Using a gradient of

0-55% buffer B in 100 minutes, the library of epitope mimics was purified in a single run. Fractions were analyzed with LC-MS, lyophilized and up to mg (!) quantities of practically all individual pure epitope mimics were obtained. Since with LC-MS the $[M+3H]^{3+}$ signal was observed for the TAC-scaffolded discontinuous epitope mimics, MALDI was performed on the purified compounds to confirm the mass value observed by LC-MS. This is illustrated for two different epitope mimics in Figure 3. In Table 1, characteristics of the obtained discontinuous epitope mimics are given.

Table 1 | Characteristics of TAC-scaffolded discontinuous epitope mimics **7**

Loop combination	Bruto formula	$[M+H]^+$ calculated	$[M+H]^+$found	R_t(min)
1-1-2	$C_{162}H_{249}N_{55}O_{48}S$	3733.86	3732.15	14.87
1-2-2	$C_{186}H_{282}N_{58}O_{49}S_2$	4177.08	4176.55	15.59
1-1-3	$C_{146}H_{226}N_{50}O_{47}$	3432.69	3432.11	14.42
1-3-3	$C_{154}H_{236}N_{48}O_{51}$	3574.74	3574.59	14.94
1-2-3	$C_{170}H_{259}N_{53}O_{50}S$	3875.91	3874.51	15.32
2-2-3	$C_{194}H_{292}N_{56}O_{53}S_2$	4319.13	4318.95	16.17
2-3-3	$C_{178}H_{269}N_{51}O_{54}S$	4017.96	4017.14	15.97

4.2.2 – Investigation of binding of the discontinuous epitope mimics to CD4

The thus prepared libraries enabled evaluation of the biological activity of the gp120 discontinuous epitope mimics. More importantly, because of the presence of practically all combinations of epitope mimics, firstly the relative importance of each epitope mimicking cyclic peptide could be evaluated, and secondly, if mimics containing just one or two out of three different loop-mimicking cyclic peptides were still biologically active.

To evaluate the binding of the discontinuous epitope mimics to CD4, a competitive gp120-capture ELISA experiment was performed.[27] An ELISA setup was used here, since this technique is well suited for the rapid screening of multiple discontinuous epitope mimics and does not require any modification or surface immobilization of the mimics.

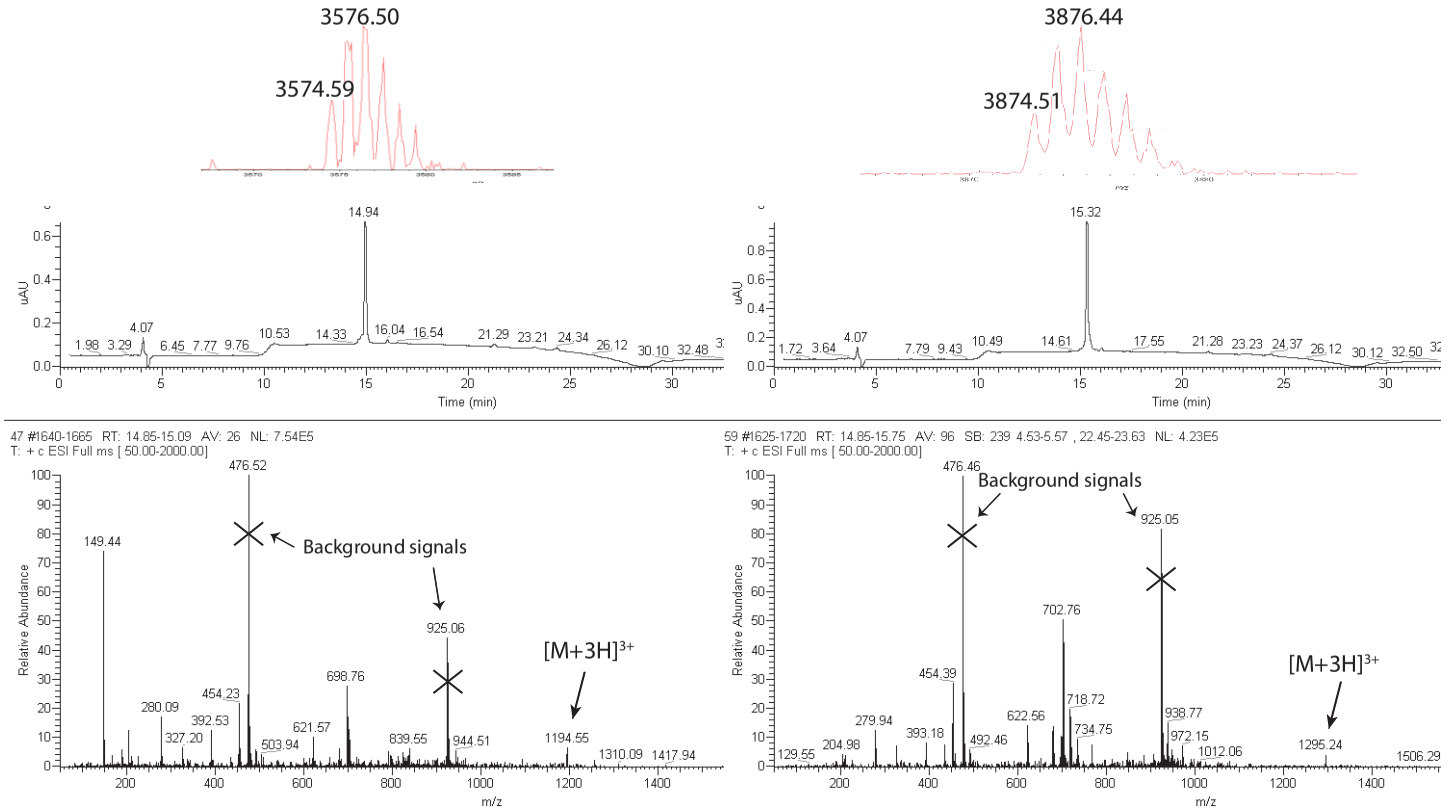

Figure 3 | MALDI (top) and LC-MS (bottom) analysis of TAC-scaffolded discontinuous epitope mimics. Analyses for mimics carrying loop combinations 1-3-3 (left) and 1-2-3 (right) are shown.

Several concentrations of the discontinuous epitope mimics were added to 96-wells plates coated with recombinant CD4 (sCD4), in the presence of recombinant monomeric gp120(IIIB) (rgp120). Subsequently, the amounts of rgp120 bound to the plate were detected using horseradish peroxidase (HRP)-conjugated murine anti-gp120 mAb and visualization of antibody binding was performed using 3,3',5,5'-tetramethylbenzidine (TMB) as a substrate. This substrate yields a blue color when detecting HRP. In this thesis, the potency of the discontinuous epitope mimics was determined relative to binding of rgp120 in absence of any mimic (maximum OD_{450}-signal). Binding-properties were expressed in percentage inhibition of the maximum OD_{450}-signal.

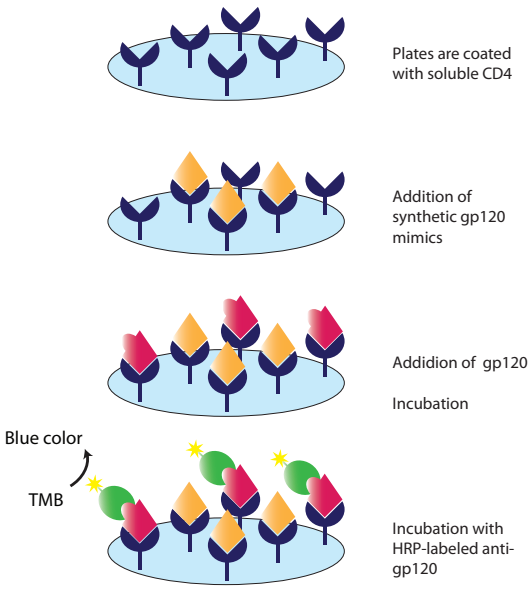

Figure 4 | Schematic representation of the gp120-capture ELISA experiment.

Not only the libraries of discontinuous epitope mimics (Figure 6) were tested for CD4-binding, but also the individual cyclic peptides **6a-6c** and an unscaffolded mixture of these cyclic peptides were tested. In addition a known inhibitor of the CD4-gp120 interaction, the naphthalene sulfonic acid dye Chicago Sky Blue (Figure 4), was tested evaluated in the same assay to compare the results and confirm the efficacy of the assay.

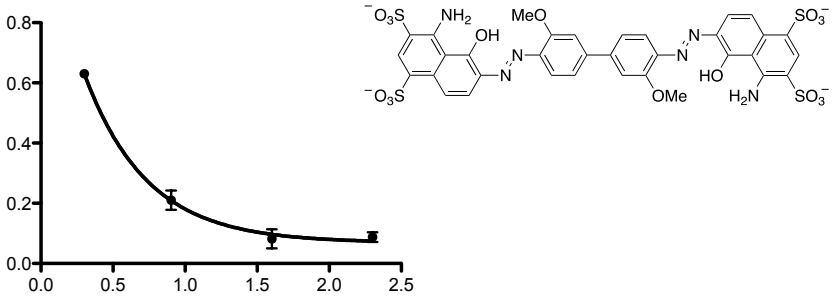

Figure 5 | Chicago Sky Blue (CSB, right) and results of this compound in the gp120 capture ELISA (left). 50% reduction of gp120 binding was observed at a CSB concentration of 4.2 μM.

In a first experiment, the "clean" mixture of all combinations of epitope mimics showed significant decreases in OD_{450}-values, indicating that these mimics reduced the amounts of rgp120 captured on solid-phase CD4. Pre-incubation of the epitope mimics with rgp120 prior to addition of the mixture to the sCD4-coated plates did not influence the outcome of the experiment, indicating that the epitope mimics compete with rgp120 for binding to CD4 rather than binding to rgp120 itself.

In contrast to the mixture of epitope mimics, none of the individual cyclic peptides was able to compete significantly with rgp120 for CD4-binding at concentrations up to 2 mg/mL, which corresponds to 1.5-2 mM. In addition, no competition was observed when an unscaffolded mixture of the cyclic peptides was added to the CD4-coated plate in concentrations equal to the active epitope mimics (Table 2). This clearly indicates a synergistic effect of combining multiple epitopes in one molecule, and demonstrates the importance of the TAC scaffold.

Table 2 | Inhibition of rgp120 binding to CD4 at 1 mg/mL concentration

Compound (1mg/mL)	Inhibition of rgp120-binding (%)
'Clean' mixture **7**	89
Unscaffolded mixture of **6a**, **6b** and **6c**	0
6a	18
6b	12
6c	0

After this first indication of activity, the individual purified discontinuous epitope mimics were tested in an identical competition experiment at a single concentration (Figure 6). From this experiment, several trends were apparent.

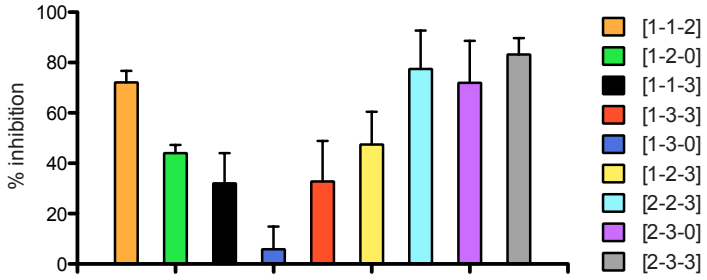

Figure 6 | Results of the competitive gp120(IIIB)-CD4 ELISA for all pure epitope mimics. Inhibition of rgp120 binding to CD4 at 1 mg/mL mimic concentration.

First of all, in contrast to the individual cyclic peptides, the combination of just two cyclic peptides onto a scaffold already led to a molecule that can compete with gp120 for CD4-binding. Moreover, all discontinuous epitope mimics carrying a combination of the cyclic peptides mimicking loops 2 and 3 were stronger competitors than the other combinations. Also, the combination of these cyclic peptides exhibited a slightly higher affinity for its target than a previously synthesized epitope mimic carrying the linear peptide fragments.[7]

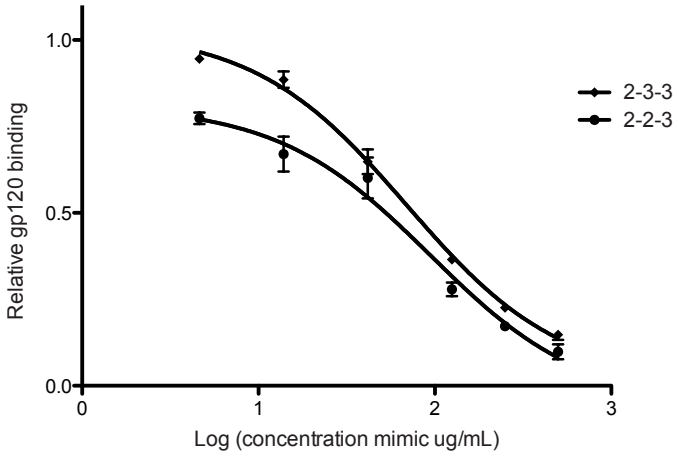

Figure 7 | Competition of the most potent mimics with gp120(IIIB) for CD4-binding. (IC_{50} 2-2-3: 16.8 µM ± 5.7).

The importance of these two epitopes is in agreement with the information that can be derived from the crystal structure of the gp120-CD4 complexes.[3,6] In particular amino acid residues in CD4 showed multiple contacts with amino acid residues Asp 368 and Glu 370 in gp120 epitope ^{365}SGGDPEI^{371} –corresponding to loop 3– and with Trp 427 in epitope ^{425}NMWQEV^{430}, corresponding to loop 2.[3] Moreover, it has been shown that changes in gp120 epitope ^{454}LTRDGGN^{460}, corresponding to loop 1, did not affect the binding to CD4 significantly, since these residues are located in a relatively flexible portion of gp120.[4] Still, one would have expected that a molecular construct containing all three loops capable of interacting with CD4 should have been the best interacting construct. Explanations of this lack of increased affinity may be found in a non-optimal cyclic peptide ring size or positioning of the individual cyclic peptides.

4.3 Conclusions

In this chapter, a combinatorial approach was described for the generation of libraries of discontinuous epitope mimics of HIV gp120. The approach presented here showed that libraries of complex cyclic peptide containing molecular constructs could be conveniently and reproducibly generated after which the library members could be separated and screened. Alternatively, different libraries with varying peptide ring size, linker length or scaffold can be generated and screened as such, followed by separation of the library members to uncover the best hit in a particular library. In the delineated approach, the best hits (i.e. [2-3-3] and [2-2-3]) will be starting points for libraries with varied cyclic peptide ring size and variation of the scaffold. Ultimately, the best library member can be re-synthesized using our earlier developed non-stop solid phase synthesis allowing evaluation of the relative positioning of the cyclic peptide on the scaffold, since for example a [2-3-2] molecular construct is not identical to a [2-2-3] construct.

In summary, CuAAc of a mixture of cyclic peptides to a scaffold molecule provided rapid access to a diversity of peptide biomolecular constructs as a clean smart library for mimicry of the discontinuous protein surface. Using this method, for the first time up to three different cyclic peptides were incorporated into a single molecule in a convergent synthetic manner employing a TAC-scaffold. In addition, the individual epitopes and scaffold molecules required for this molecular construct were conveniently accessible by chemical synthesis. The library members were separated and evaluated for binding to CD4. Appreciable binding was found for certain molecular constructs and these can be used as starting points for the preparation of focused libraries. Ultimately, these compounds might be employed as inhibitors of attachment of HIV or, more importantly, applied as synthetic vaccines for the generation of antibodies capable of binding to HIV. This approach is very promising for the generation of mimics of other proteins containing discontinuous epitopes, possibly ultimately leading to synthetic antibodies.

4.4 Experimental procedures

General

2-Chlorotrityl chloride resin (100-200 mesh, 1% DVB, 1.0-1.6 mmol/g) was purchased from Iris Biotech GmbH and was used for synthesis of the cyclic peptides. Solid phase peptide synthesis was carried out in plastic syringes with a polyethylene frit (20 μm) obtained from Screening Devices B.V. The resin loading was determined by measuring the UV absorbance of the piperidine-dibenzofulvene adduct (λ_{max} 300 nm).[28] All components used in gp120-capture ELISA experiments were purchased from ImmunoDiagnostics, Inc. (Woburn, MA).

Reactions were performed at room temperature unless stated otherwise. Microwave reactions were performed in a Biotage Initiator (300W) reactor in sealed vessels suitable for reaction volumes of 0.5-2 mL. Analytical LC-MS was preformed on Thermo-Finnigan LCQ Deca XP Max coupled to a on a Shimadzu-10Avp (Class VP) system using UV-detector operating at 254 nm. A Phenomenex Gemini C18 column (110 Å, 5 μm, 250×4.6 mm) was used at a flow rate of 1 mL min^{-1} using a standard protocol: 100% buffer A for 1 min, then a linear gradient of buffer B (0-100% in 30 min). The mobile phase was 0.1% TFA in CH_3CN/H_2O 5:95 (buffer A) and 0.1% TFA in CH_3CN/H_2O 95:5 (buffer B). For analysis of protected (cyclic) peptides the mobile phase was 0.1% TFA in CH_3CN/H_2O 20:80 (buffer A) and 0.1% TFA in CH_3CN/iPrOH/H_2O 50:45:5 (buffer B). Purification of cyclic peptide **6b** and the discontinuous epitope mimics was performed on a Prep LCMS-QP8000α HPLC system (Shimadzu) using a Phenomenex Gemini C18 column (10 μm, 110 Å, 250×21.2 mm) at a flow rate of 12.5 mL min^{-1}. For **6b** a standard protocol was used: 100% buffer A for 5 min followed by a linear gradient of buffer B (0-100% in 100 min). For purification of the discontinuous epitope mimics, an adapted protocol was used: 100% buffer A for 5 min followed by a linear gradient of buffer B (0-55% in 100 min). Electrospray ionization mass spectrometry (ESI-MS) was performed on a Shimadzu LCMS-QP8000 single quadrupole bench-top mass spectrometer operating in a positive ionization mode or a Thermo-Finnigan LCQ Deca XP Max ion trap mass spectrometer. MALDI-TOF-MS spectra were recorded on a Kratos Analytical (Shimadzu) AXIMA CFR mass spectrometer using α-cyano-4-hydroxycinnamic acid (CHCA) or sinapic acid as a matrix and human ACTH (18-39) or bovine insulin oxidized B chain as references. All reported mass values are monoisotopic. The microtiterplate reader used in the ELISA experiments was a BioTek μQuant (Beun de Ronde, Abcoude, The Netherlands). Software used for data analysis was the Full Mode-KC4 version 3.4.

Synthesis of TAC-scaffold and cyclic azidopeptides

The synthesis of alkyne-functionalized TAC-scaffold TAC-scaffold **1** has been described in chapter 3. The syntheses of cyclic azidopeptides **6a**, **6b** and **6c** have been described in chapter 2.

General procedure for scaffold conjugation of cyclic peptides by optimized CuAAc. 10-fold stock solutions of $CuSO_4$ (44.9 µmol, 11.2 mg in 1 mL H_2O) and sodium ascorbate (89.9 µmol, 17.8 mg in 1 mL H_2O) were prepared. TBTA[25,26] was dissolved in 100 µL DMF. Peptides were dissolved individually in the smallest possible amount (100-500 µL) of DMF (4Å molsieves).

Solutions of three peptides in DMF were prepared: loop 1 (compound **6a**, 7.49 µmol, 6.93 mg), loop 2 (compound **6b**, 7.49 µmol, 10.25 mg) and loop 3 (compound **6c**, 7.49 µmol, 7.99 mg). TAC scaffold **1** (7.49 µmol, 3.97 mg) was added to the microwave vessel and dissolved in 100 µL DMF (4Å). 100 µL of the $CuSO_4$ stock solution (4.49 µmol, 1.12 mg) and 100 µL of the sodium ascorbate stock solution (8.99 µmol, 1.78 mg) were added to the solution, followed by addition the TBTA solution (1.10 µmol, 0.60 mg). The peptide solutions were combined and added to the reaction mixture. Depending on the amount of DMF that was used to dissolve the peptides, H_2O was added to obtain a 3:2 DMF/H_2O ratio and 1-1.5 mL total volume. The microwave vessel was sealed and allowed to react in the microwave at 80°C during 25 min.

After reaction, a sample was taken from the reaction mixture for LC-MS analysis. Based on this analysis, the individual components were purified by preparative HPLC. Fractions were analyzed and epitope mimics were identified with LC-MS, and lyophilized. Fractions containing pure epitope mimics were used for gp120-capture ELISA.

HIV-1 gp120 capture ELISA

Recombinant HIV-1IIIB gp120 protein (referred to as rgp120 hereafter unless otherwise noted) capture ELISA was performed according to the manufacturer's instructions (ImmunoDiagnostics, Inc., Woburn, MA). Firstly, various concentrations of free ligand rgp120 (up to 2 µg/ml, in a 2-fold dilution series) in sample buffer (50 µL 0.1% BSA in PBS) were added to a CD4-coated plate in the absence of test compounds. After a 60-min incubation at room temperature, the amounts of captured rgp120 were detected by peroxidase-conjugated murine anti-gp120 MAb. It was determined that the best S/N-ration and optimal OD_{450}-values were obtained when an rgp120 concentration of 1 µg/ml was used.

When optimal concentrations were determined, competition experiments were performed. Test compounds diluted in sample buffer and 2% DMSO were added to the CD4-coated plate, immediately followed by addition of 50 µL 2 µg/ml rgp120 (final concentration 1 µg/mL). After 4 h of incubation at room temperature, the plate was washed with wash buffer (0.1% Tween 20 in PBS) followed by incubation with peroxidase-conjugated murine anti-gp120 MAb to detect the amounts of captured rgp120. Any unbound material was washed away using wash buffer, and plates were developed by adding 100 µL/well substrate solution (0.1 mg/mL TMB in 0.1 N NaOAc buffer pH 5.5, containing 0.003% H_2O_2). The reaction was stopped after 10 min by

adding 100 µL 4N sulfuric acid. Absorbances (ODs) were read at 450 nm using a microtiterplate reader. The OD_{450}-value obtained after incubation with 1 µg/ml rgp120 without addition of any epitope mimics was used as a maximum reference, and the OD_{450}-value when no epitope mimic or rgp120 was added was used as a background value. Binding-properties of epitope mimics were corrected for this background signal, and were expressed in percentage of the maximum OD_{450}-signal. All assays were performed in duplicate and were independently repeated at least three times.

References:

(1) Gilbert, P.; Wang, M.; Wrin, T.; Petropoulos, C.; Gurwith, M.; Sinangil, F.; D'Souza, P.; Rodriguez Chavez, I. R.; DeCamp, A.; Giganti, M.; Berman, P. W.; Self, S. G.; Montefiori, D. C. *J. Infect. Dis.* **2010**, *202*, 595–605.

(2) Schellinger, J. G.; Danan-Leon, L. M.; Hoch, J. A.; Kassa, A.; Srivastava, I.; Davis, D.; Gervay-Hague, J. *J. Am. Chem. Soc.* **2011**, *133*, 3230–3233.

(3) Kwong, P. D.; Wyatt, R.; Robinson, J.; Sweet, R. W.; Hendrickson, W. A.; Sodroski, J. *Nature* **1998**, *393*, 648–659.

(4) Kwong, P. D.; Wyatt, R.; Majeed, S.; Robinson, J.; Sweet, R. W.; Sodroski, J.; Hendrickson, W. A. *Structure* **2000**, *8*, 1329–1339.

(5) Pantophlet, R.; Ollmann Saphire, E.; Poignard, P.; Parren, P. W. H. I.; Wilson, I. A.; Burton, D. R. *J. Virol.* **2003**, *77*, 642–658.

(6) Chamorro, C.; Kruijtzer, J. A. W.; Farsaraki, M.; Balzarini, J.; Liskamp, R. M. J. *Chem. Commun.* **2009**, 821.

(7) Franke, R.; Hirsch, T.; Overwin, H.; Eichler, J. *Angew. Chem. Int. Ed.* **2007**, *46*, 1253–1255.

(8) Monnee, M. C. F.; Brouwer, A. J.; Verbeek, L. M.; van Wageningen, A. M. A.; Liskamp, R. M. J. *Bioorg. Med. Chem. Lett.* **2001**, *11*, 1521–1525.

(9) Timmerman, P.; Beld, J.; Puijk, W. C.; Meloen, R. H. *ChemBioChem* **2005**, *6*, 821–824.

(10) Timmerman, P.; Barderas, R.; Desmet, J.; Altschuh, D.; Shochat, S. G.; Hollestelle, M. J.; Höppener, J. W. M.; Monasterio, A.; J Ignacio Casal; Meloen, R. H. *J. Biol. Chem.* **2009**, *284*, 34126–34134.

(11) Heinis, C.; Rutherford, T.; Freund, S.; Winter, G. *Nature Chem. Biol.* **2009**, *5*, 502–507.

(12) Beal, D. M.; Jones, L. H. *Angew. Chem. Int. Ed.* **2012**, *51*, 6320–6326.

(13) Tiefenbrunn, T. K.; Dawson, P. E. *Biopolymers* **2010**, *94*, 95–106.

(14) Holub, J. M.; Kirshenbaum, K. *Chem. Soc. Rev.* **2010**, *39*, 1325.

(15) Rostovtsev, V. V.; Green, L. G.; Fokin, V. V.; Sharpless, K. B. *Angew. Chem. Int. Ed.* **2002**, 2596–2597.

(16) Tornøe, C. W.; Christensen, C.; Meldal, M. *J. Org. Chem.* **2002**, *67*, 3057–3064.

(17) Opatz, T.; Liskamp, R. M. J. *J. Comb. Chem.* **2002**, *4*, 275–284.

(18) Chamorro, C.; Hofman, J.-W.; Liskamp, R. M. J. *Tetrahedron* **2004**, *60*, 8691–8697.

(19) Monnee, M. C. F.; Brouwer, A. J.; Liskamp, R. M. J. *QSAR Comb. Sci.* **2004**, *23*, 546–559.

(20) van Zoelen, D.-J.; Egmond, M. R.; Pieters, R. J.; Liskamp, R. M. J. *ChemBioChem* **2007**, *8*, 1950–1956.

(21) Albada, H. B.; Liskamp, R. M. J. *J. Comb. Chem.* **2008**, *10*, 814–824.

(22) Lambert, J. N.; Mitchell, J. P.; Roberts, K. D. *J. Chem. Soc., Perkin Trans. 1* **2001**, 471–484.

(23) Wu, Z.; Guo, X.; Guo, Z. *Chem. Commun.* **2011**, *47*, 9218.

(24) Smeenk, L. E. J.; Dailly, N.; Hiemstra, H.; van Maarseveen, J. H.; Timmerman, P. *Org. Lett.* **2012**, *14*, 1194–1197.

(25) Wang, Q.; Chan, T. R.; Hilgraf, R.; Fokin, V. V.; Sharpless, K. B.; Finn, M. G. *J. Am. Chem. Soc.* **2003**, *125*, 3192–3193.

(26) Chan, T. R.; Hilgraf, R.; Sharpless, K. B.; Fokin, V. V. *Org. Lett.* **2004**, *6*, 2853–2855.

(27) Yang, Q.-E.; Stephen, A. G.; Adelsberger, J. W.; Roberts, P. E.; Zhu, W.; Currens, M. J.; Feng, Y.; Crise, B. J.; Gorelick, R. J.; Rein, A. R.; Fisher, R. J.; Shoemaker, R. H.; Sei, S.

J. Virology **2005**, *79*, 6122–6133.
(28) Fields, G. B. *Int. J. Peptide Protein Res.* **1990**, *35*, 161–214.

5

Scaffold optimization in discontinuous epitope containing protein mimics of gp120 using smart libraries

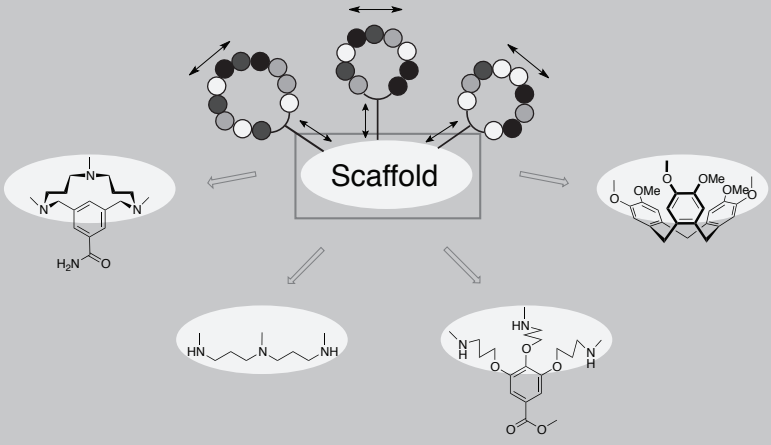

Part of the work described in this chapter has been published: G.E. Mulder, H.C. Quarles van Ufford, J. van Ameijde, A.J. Brouwer, J.A.W. Kruijtzer and R.M.J. Liskamp, *Org. Biomol. Chem.* **2013**, 2676-2684.

5.1 Introduction

One of the great challenges of this decade in drug discovery is development of protein mimics to be obtained by chemosynthesis, biosynthesis or a combination of both.[1] In order to be successful in protein mimicry and in the generation of molecular constructs that can interact with for example a partner protein, in many cases two characteristics of protein mimics will be important. Firstly, binding has to occur to relatively large and structurally complex surface areas in many protein-protein interfaces. Secondly, these surfaces often have a modular architecture, and consist of multiple epitopes within the protein.[2]

In our research we are particularly interested in the development of protein mimics containing discontinuous epitopes that are capable of interacting with these modular protein surfaces. Previously, we have described protein mimics of cystatin B[3] and the whooping cough protein pertactin[4], which contained different *linear* peptide sequences as mimics of the corresponding discontinuous epitopes. However, peptide cyclization is likely to improve the affinity of discontinuous epitope mimics.[5-11]

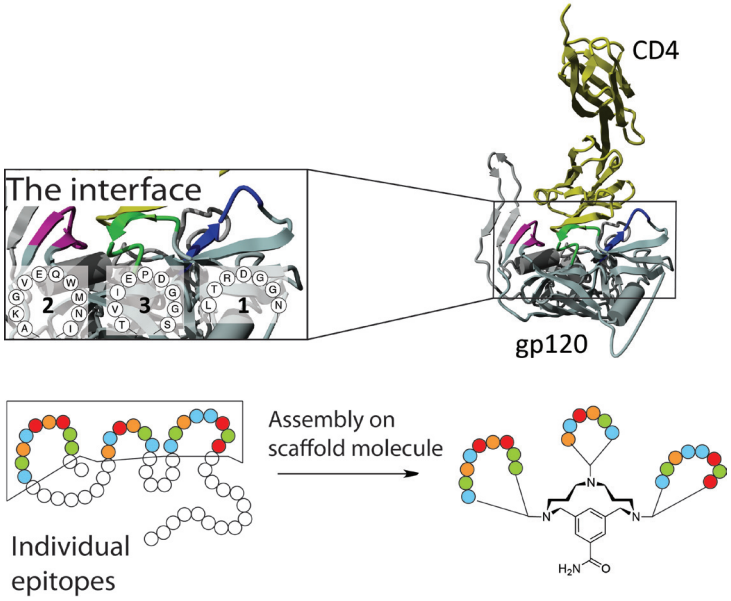

Figure 1 | Detailed view of the discontinuous CD4 binding site of HIV gp120, and schematic representation of a possible method to mimic this binding site using cyclic peptides on a molecular scaffold.

In addition, cyclic peptides are chemically and enzymatically more stable than their linear counterparts.[5,6] Therefore, we have focused on the introduction of cyclic peptides onto suitable scaffold molecules.[12,13]

Although we have developed a method for the sequential introduction of discontinous epitopes onto a suitable (TAC) scaffold, the question arises then whether the ideal protein mimic has been synthesized. Important issues to be addressed include: (i) are the cyclic peptides, which mimic the epitope loops, of the right size? (ii) is the arrangement of the cyclic peptides in the mimic an adequate representation of the situation in the protein complex? (iii) does the scaffold provide the proper flexibility or rigidity? (iv) does the scaffold provide a good platform for the relative involvement of the different loops of the discontinuous epitope? Some of these issues were addressed in the method that is reported in the previous chapter for the preparation of "smart" libraries.[13] Libraries of TAC-scaffolded cyclic peptides mimicking the discontinuous epitopes of HIV-gp120 were synthesized, resulting in protein mimics that can interact with the CD4 receptor (Figure 1). From this library, the best member can be selected followed by re-synthesis.[13]

In the research described in this chapter, we report results on the investigations of the influence of the scaffold. In our research we aim at the development of protein mimics of gp120 to be used to prevent (a) attachment of HIV-gp120 to the CD4-receptors of cells and (b) using this mimic as a synthetic vaccine.[14,15] Based on the X-ray crystal structure of the gp120-CD4 protein complex,[16] we[12] and others[17] have determined which interacting peptide segments may be most effective for inclusion in a synthetic discontinuous epitope mimic. From the very start of this project, we realized that in view of size and complexity, prediction and/or modelling of the molecular constructs aimed at, is very difficult. Therefore, generation of collections or libraries of protein mimics is an attractive avenue, if not an essential approach, to uncover potentially promising molecules. In chapter four, we have described a method for conjugation of up to three different cyclic peptides onto a TriAzaCyclophane (TAC) scaffold using the Cu(I)-catalyzed azide-alkyne cycloaddition (CuAAC) to afford clean and reproducible ("smart") libraries.[13] The resulting protein mimics were evaluated in a competitive ELISA with HIV gp120 at micromolar concentrations. The most potent gp120 mimic was capable of competing with HIV-gp120 for CD4-binding with an IC_{50}-value of 16.8 μM. In the research described in this chapter, we have selected three alternative trivalent

scaffold molecules that all differ in flexibility/rigidity. These scaffold molecules were all used for the preparation of smart libraries and investigation of the ability of the resulting protein mimics to compete with HIV-gp120 for CD4-binding. Finally, cyclic peptides on the scaffold molecule that resulted in the most potent protein mimics were varied, thereby obtaining an additional improvement of activity.

Since the short half life of peptides is often a limiting factor in the development of peptide leads into drugs[18], this chapter will be concluded with a stability-study of one of the most potent discontinuous epitope mimics in human serum.

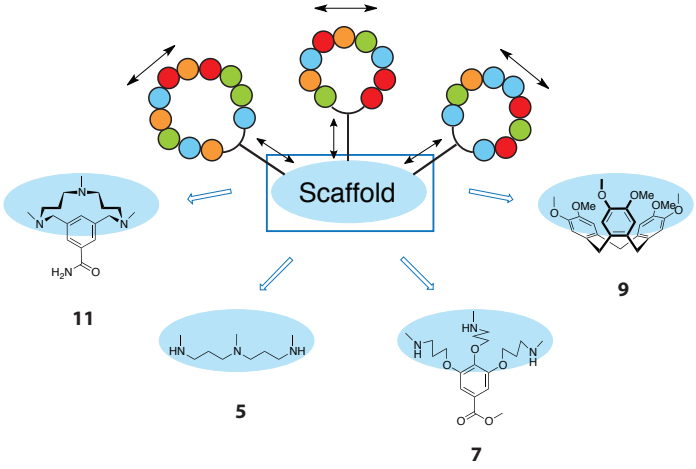

Figure 2 | Preorganization of epitopes by different scaffold molecules.

5.2 Results and discussion

5.2.1 – Scaffold selection

Three additional scaffold molecules were selected for synthesis of protein mimics containing discontinuous epitopes of HIV gp120. Since up to three different cyclic peptides have to be introduced onto the scaffold molecule, all selected scaffolds were trivalent and equipped with alkyne functionalities for conjugation to the cyclic peptides using CuAAC. As is schematically indicated in Figure 2 by arrows indicating the relative movements of the peptide loops, their orientation and extent of pre-organization is clearly dependent on the character of the scaffold. Alkyne containing triamine **5** may

be considered as the flexible/open analogue of the TAC-scaffold, and should reveal the (dis)advantage of a more organized (TAC)scaffold. Alkyne containing dendrimer building block[19] **7** allows in principle organization of the peptide loops roughly in one plane, which is not the case with the TAC or triamine scaffold. Alkyne-functionalised CycloTriVeratrylene (CTV) **9** will furnish the most pre-organized system, which is indicative from the use of CTV for the organization of peptide chains into a triple helix mimic and parallel organization of other ligands.[20]

5.2.2 – Epitope selection and synthesis of cyclic peptide loops containing an azido handle

The HIV gp120 epitopes that were selected for this and previous studies[12,13,17] - ^{365}SGGDPEI^{371}, ^{425}NMWQEV^{430} and ^{454}LTRDGGN^{460} - represent conserved regions of the otherwise highly variable gp120. In addition, these sequences contain the primary contact residues of gp120 (D368, E370, W427, and D457) for its interaction with CD4, as was determined from the crystal structure of core gp120 in complex with an extracellular two-domain fragment of CD4.[16,21] Although the interacting loops are located relatively far away in the primary structure of the protein, the crystal structure clearly shows the proximity of the selected epitopes in the folded, receptor-bound state. These epitopes are therefore suitable candidates for preparation of the corresponding peptide loops followed by their attachment to a scaffold in order to mimic the protein binding site.

Synthesis of cyclic azidopeptides containing these epitopes was performed on 2-chlorotrityl chloride resin, since peptides can be cleaved from this resin without affecting their side chain protecting groups. Moreover, cleavage of peptides from this resin yields a peptide with a C-terminal carboxylic acid that subsequently can be used for head-to-tail cyclization. To avoid racemization during the cyclization reaction, glycine was chosen as the C-terminal amino acid for preparation of each peptide loop. The azide handle for CuAAC was introduced by incorporation of Fmoc-azidolysine (chapter 2). After completion of their synthesis (Scheme 1) and removal of the N-terminal Fmoc-group, peptides were cleaved from the resin and cyclized in solution using BOP as a coupling reagent (Scheme 1).

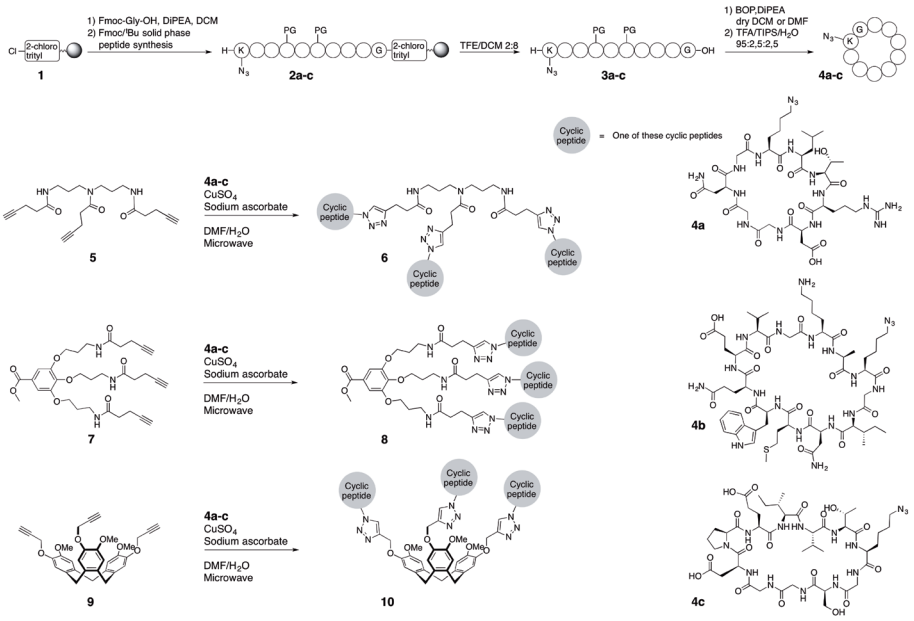

Scheme 1 | Synthesis of cyclic azidopeptides and click chemistry to form gp120 discontinuous epitope mimics

Cyclization reactions were performed in high dilution at 1 mM concentration and monitored by analytical HPLC. After aqueous workup, the protected cyclic peptides could be purified using normal silica gel column chromatography. This was highly advantageous compared to preparative HPLC as a purification method, since yields were much higher and larger quantities could be purified in a single run. The purity of the cyclic peptides was assessed after removal of the side chain protecting groups, and was very good (>95%) for two of the three peptides. The largest cyclic peptide **4b** and an elongated version of peptide **4c** (see experimental section) were purified by preparative HPLC to ensure a high quality precursor for subsequent attachment to the scaffolds.

5.2.3 – Library synthesis of the discontinuous epitope containing protein mimics

Libraries of discontinuous epitope containing protein mimics **6**, **8** and **10** were synthesized using CuAAC reactions. Scaffold molecules **5**, **7** or **9** were incubated with equimolar mixtures of cyclic azidopeptides **4a-c** and subjected to CuAAC following the

procedure that was described previously for conjugation of cyclic peptides to the TAC scaffold.[13] Reaction conditions involved the use of $CuSO_4$ and sodium ascorbate in the presence of TBTA, as was described in detail in chapter 4.

Full conversion of starting materials was observed for reactions on all three scaffold molecules after only 20 minutes reaction time in the microwave reactor, and very clean reaction mixtures containing only desired products were obtained, as was confirmed with LC-MS. This clearly demonstrates the general applicability and reliability of this method for generation of smart libraries of discontinuous epitope mimics. The resulting reaction mixtures were purified with preparative HPLC to isolate the individual pure epitope mimics.[13] Preparative HPLC was performed using standard H_2O/MeCN buffers (see experimental section) and a slow gradient over 100 minutes starting at 100% buffer A and going to 55% buffer B. In this way, in a single click experiment followed by one HPLC run, a library containing practically all combinations of epitope mimics was obtained. Characteristics of the pure isolated epitope mimics are shown in tables 1-3. Typically, click experiments were performed on 5-10 µmol scale and 0.5-1 mg of the pure epitope mimics was obtained.

Table 1 | Characteristics of triamine-scaffolded compounds **6**

Loop combination	Bruto formula	$[M+H]^+$ calculated	$[M+H]^+$found	R_t(min)
1-1-2	$C_{153}H_{242}N_{54}O_{45}S$	3588.80	3587.57	14.66
1-2-2	$C_{177}H_{275}N_{57}O_{48}S_2$	4032.03	4030.21	15.69
1-1-3	$C_{137}H_{219}N_{49}O_{46}$	3287.63	3286.89	13.97
1-3-3	$C_{145}H_{229}N_{47}O_{50}$	3429.68	3428.99	14.41
1-2-3	$C_{161}H_{252}N_{52}O_{49}S$	3730.85	3729.11	15.29
2-2-3	$C_{185}H_{285}N_{55}O_{52}S_2$	4174.08	4173.43	16.26
2-3-3	$C_{169}H_{262}N_{50}O_{53}S$	3872.91	3872.12	15.89

Table 2 | Characteristics of dendrimer-scaffolded compounds **8**

Loop combination	Bruto formula	$[M+H]^+$ calculated	$[M+H]^+$found	R_t(min)
1-1-2	$C_{164}H_{254}N_{54}O_{50}S$	3812.88	3813.62	15.12
1-2-2	$C_{188}H_{287}N_{57}O_{53}S_2$	4255.10	4256.01	15.92
1-1-3	$C_{148}H_{231}N_{49}O_{51}$	3511.70	3511.14	14.68
1-3-3	$C_{156}H_{241}N_{47}O_{55}$	3653.76	3654.66	15.30
1-2-3	$C_{172}H_{264}N_{52}O_{54}S$	3954.93	3955.97	15.67
2-2-3	$C_{196}H_{297}N_{55}O_{57}S_2$	4398.15	4397.44	16.48
2-3-3	$C_{180}H_{274}N_{50}O_{58}S$	4096.98	4097.66	16.29

Table 3 | Characteristics of CTV-scaffolded compounds **10**. Typical yields are given for a synthesis performed on 4.4 µmol scale.

Loop combination	Bruto formula	$[M+H]^+$ calculated	$[M+H]^+$found	R_t(min)	Yield (mg)
1-1-2	$C_{165}H_{243}N_{51}O_{48}S$	3738.79	3739.16	16.21	0.41
1-2-2	$C_{189}H_{276}N_{54}O_{51}S_2$	4183.01	4181.57	16.85	0.57
1-1-3	$C_{148}H_{220}N_{46}O_{49}$	3438.61	3438.39	16.10	0.53
1-3-3	$C_{157}H_{230}N_{44}O_{53}$	3580.67	3580.33	16.74	0.48
1-2-3	$C_{173}H_{253}N_{49}O_{52}S$	3881.84	3881.01	16.77	0.59
2-2-3	$C_{197}H_{286}N_{52}O_{55}S_2$	4325.06	4323.22	17.63	0.72
2-3-3	$C_{181}H_{263}N_{47}O_{56}S$	4023.89	4022.43	17.41	0.49
1-1-3*	$C_{157}H_{233}N_{49}O_{53}$	3653.71	3654.15	16.06	0.87
1-3*-3*	$C_{173}H_{256}N_{50}O_{61}$	4010.85	4010.87	16.44	0.63

5.2.4 – Evaluation of binding affinity of the gp120 protein mimics

To evaluate the relative capacity of the scaffold molecules for positioning and pre-organizing the discontinuous epitopes of HIV gp120, the three different libraries of protein mimics were screened for activity in a competitive ELISA experiment. CD4-

coated plates were used, and the ability of gp120 mimics to compete with recombinant monomeric gp120(IIIB) for binding to CD4 was assessed. The amounts of captured gp120 were detected by peroxidase-conjugated murine anti-gp120 mAb. The maximum signal was determined by detection of only gp120 without addition of any protein mimic, and the background absorption was determined by performing the assay without addition of gp120 or a protein mimic. The latter values were subtracted from the competition experiment values and the activity was expressed as a percentage of the maximum attainable effect.

In addition to evaluation of the library members of the discontinuous epitope protein mimics, binding of the individual unscaffolded cyclic peptides was investigated. At the highest concentration (1 mg/mL) tested, no inhibition of gp120-binding was observed by any of the separate cyclic peptides. This clearly demonstrated the necessity of the presence of at least two peptide loops in one molecular construct.

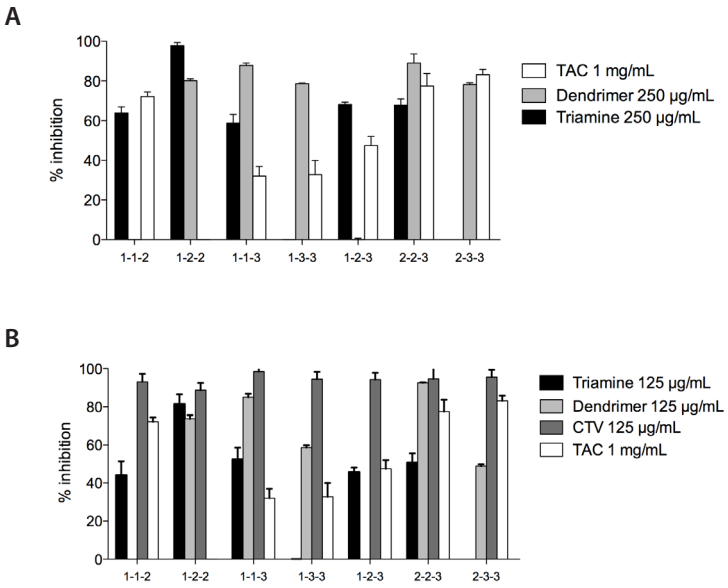

Figure 3 | Inhibition of gp120 binding of gp120 discontinuous epitope protein mimics in competitive ELISA. Libraries of protein mimics based on four different scaffold molecules were evaluated. a) Two newly synthesized libraries **6** and **8** were tested at 250 µg/mL and were compared to the results of the previously published TAC-scaffolded library evaluated at a concentration of 1 mg/mL. b) Evalution of all newly synthesized libraries **6**, **8** and **10**, at a concentration of 125 µg/mL. For comparison, the results of the TAC-based library at 1 mg/mL were included.

Moreover, an unscaffolded equimolar mixture of the three peptide loops did not show any binding to CD4, which unambiguously confirmed the requirement of a molecular scaffold for assembly of the different epitope loops leading to an effective discontinuous epitope containing protein mimic. For evaluation of the activity of the libraries, libraries **6**, **8**, and **10** of gp120 discontinuous epitope protein mimics, were screened at 125 and 250 µg/mL in an initial ELISA experiment. This first experiment revealed significant inhibitory activity differences between the libraries based on different scaffold molecules (Figure 3).

At a concentration of 250 µg/mL most protein mimics were able to inhibit binding of gp120 by more than 60%. At a concentration of 125 µg/mL however, the activity of especially the triamine-scaffolded protein mimics dropped, while all CTV-scaffolded protein mimics still showed almost complete inhibition at this concentration.

Based on these results, the library of CTV-scaffolded protein mimics was tested in higher dilutions to identify the most active individual library member. Results of this experiment are shown in Figure 4 and IC_{50} values of the most potent protein mimics are displayed in Table 1. The experiment showed that the [1-1-3]-construct was most potent protein mimic in binding to CD4 with an IC_{50} value of 2.2 µM, which corresponds to an almost tenfold increased activity compared to the most potent TAC-scaffolded mimic.[13]

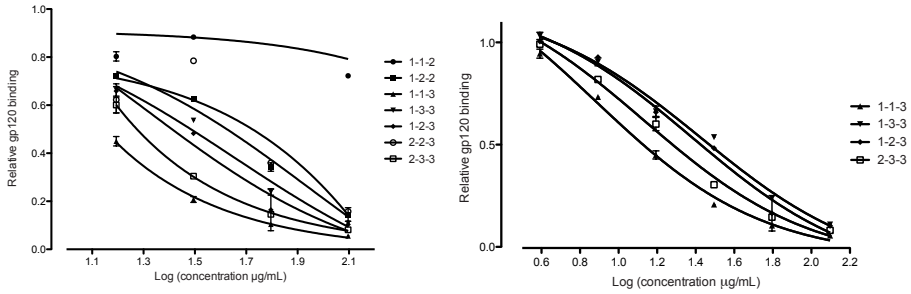

Figure 4 | Results of competitive ELISA for all CTV-based mimics. Normalized values for inhibition of gp120-binding to CD4 are displayed, where 0 is full inhibition and 1 is no inhibition. Left: All obtained mimics were screened at four concentrations in twofold serial dilutions, starting at 125 µg/mL. Right: The four most potent mimics were tested in higher dilutions in order to determine IC_{50} values.

Table 4 | IC_{50}-values and mass values found for the most active CTVscaffolded mimics

Loop combination	IC_{50} (μM)	$[M+H]^+$ calculated	$[M+H]^+$found
1-1-3	2.20 ± 0.35	3438.6210	3438.39
1-3-3	7.49 ± 1.42	3580.6728	3580.33
1-2-3	6.20 ± 1.72	3881.8453	3881.01
2-3-3	3.39 ± 0.54	4023.8970	4022.43

Also, this most potent CTV-scaffolded mimic carries a different combination of cyclic peptides, that is [1-1-3] than the most active TAC-scaffolded protein mimic, that is [2-2-3]. This shows that not only the character, that is the nature of the amino acid residues in the peptide loops is important, but also their orientation in space is of crucial importance and has to be taken into consideration when designing an optimal discontinuous epitope protein mimic.

5.2.5 – Optimization of cyclic peptides

It was decided to investigate if the peptide loops of the most successful CTV-protein mimic could be further optimized leading to an even better discontinuous epitope mimic. Perusal of the crystal structure of the gp120-CD4 complex showed that epitopes ^{454}LTRDGGN^{460} (loop 1, Figure 5) and ^{365}SGGDPEIVT^{373} (loop 3, Figure 5) are part of larger loop-like structures. This suggested that enlargement of the cyclic peptides and conjugation to the CTV-scaffold leading to additional gp120 protein mimics (Figure 5) might lead to an improved activity of these compounds. Based on the crystal structure the epitope ^{454}LTRDGGN^{460} (loop 1) was extended at its C-terminus with five amino acids, resulting in ^{454}LTRDGGNSNNEI^{465}. Loop 3 ^{365}SGGDPEIVT^{373} was extended with two amino acids on its N-terminus, giving ^{363}QSSGGDPEIVT^{373}(Figure 5).

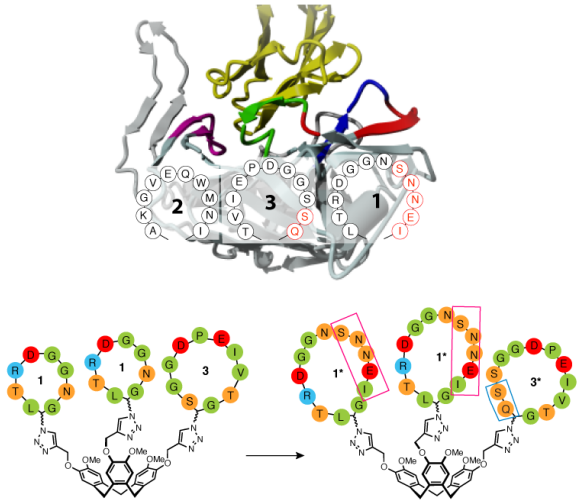

Figure 5 | Top: Crystal structure of HIV gp120. Epitopes for mimicry indicated in blue (loop 1), pink (loop 2), and green (loop 3). The amino acids that were selected for extension of the loops are indicated in red. Bottom: CTV scaffold carrying initial (left) and extended (right) loops.

The modified cyclic peptides were synthesized according to the procedure described above and depicted in Scheme 1, starting with a C-terminal glycine residue incorporation of an azidolysine residue for attachment to the scaffold molecule. Since we specifically wanted to investigate the influence of the enlarged loops 1 and 3, that is loops 1* and loops 3*, only these were introduced onto the CTV-scaffold **9** and a library of discontinuous epitope protein mimics was generated by CuAAC. In a first experiment, a combination of loop 1 and loop 3* was conjugated to CTV. Subsequently, a combination of loop 1* and loop 3 was attached to the CTV scaffold. Finally, both enlarged loops 1* and 3* were introduced. The resulting collections of discontinuous epitope mimics, together with the original CTV-scaffolded protein mimics carrying combinations of loop 1 and 3, were evaluated with competitive ELISA. This experiment revealed that elongation of loop 1 did not affect the binding of the [1*-1*-3] or [1*-3-3] mimics in any way. Substitution of loop 3 with its enlarged version however, modestly improved the activity of the resulting CTV-scaffolded protein mimics (Figure 6).

The clean synthesis of these discontinuous epitope protein mimics, now containing further modified loops, demonstrates the potential of this approach for screening and optimizing the activity of protein mimics.

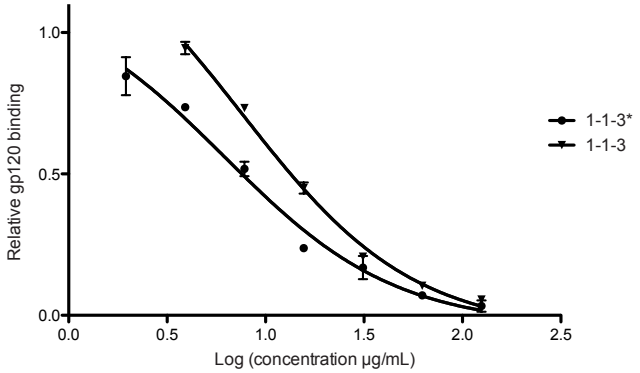

Figure 6 | Comparison of CTV-scaffolded mimics carrying 'original' and elongated cyclic peptides. IC_{50} value of [1-1-3*] 1.7 µM ± 0.48.

5.2.6 – Serum stability

The serum stability of a CTV-scaffolded discontinuous epitope mimic containing three different cyclic peptides was determined in 25% (vol/vol) aqueous human serum. CTV-scaffolded compound was dissolved in serum at a final concentration of 150 µg/mL and incubated at 37ºC. Aliquots were taken and serum proteins were precipitated. After centrifugation the supernatant was lyophilized and analysed with HPLC to determine the peak area of the CTV-scaffolded compound. After 25 hours of incubation time still 62% of intact mimic was detected.

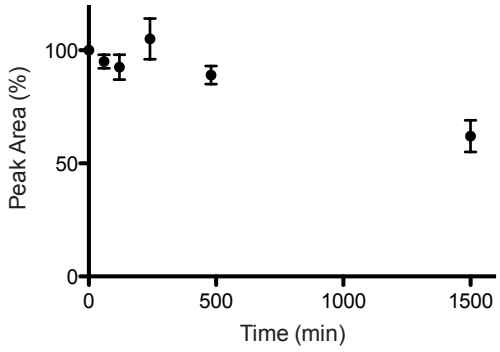

Figure 7 | Stability in human serum of CTV-scaffolded discontinuous epitope mimic carrying three different cyclic peptides.

5.3 Conclusions

In summary, we have developed a rapid, versatile and reproducible method for the generation of libraries of discontinuous epitope protein mimics. CuAAc of a mixture of up to three cyclic peptides was successfully applied on three different trivalent scaffold molecules, resulting in clean collections (6, 8 and 10) of HIV-gp120 discontinuous epitope protein mimics, in order to investigate the necessity of orientation and extent of pre-organization. Screening for their ability to compete with HIV-gp120 for binding to CD4 led to CTV-scaffold protein mimic [1-1-3] having an IC_{50} value of 2.2 μM. An additional improvement of this activity to an IC_{50} value of 1.7 μM could be reached for [1-1-3*] by enlargement of peptide loop 3 to 3*. This shows that both the orientation of the cyclic peptides, as well as the conformation of the individual peptides significantly influence the binding properties of the resulting protein mimics.

Results were highly reproducible and the synthetic approach is reliable and broadly applicable, since it allows variation of each of components of the protein mimics. In our opinion, this demonstrates the potential of this approach for the generation of protein mimics of other proteins containing discontinuous binding sites, possibly ultimately leading to the generation of synthetic antibodies.

5.4 Experimental section

General information

Unless stated otherwise, chemicals were obtained from commercial sources and used without further purification. Peptide grade DiPEA, CH_2Cl_2, NMP, TFA and HPLC grade solvents were purchased from Biosolve B.V. (Valkenswaard, The Netherlands). Fmoc-protected amino acids were purchased from GL Biochem Ltd. (Shanghai, China). Sidechain protecting groups for amino acids were as follows: Ser(tBu), Asp(OtBu), Glu(OtBu), Thr(tBu), Asn(Trt), Trp(Boc), Gln(Trt), Lys(Boc), Arg(Pbf). 2-Chlorotrityl chloride resin (100-200 mesh, 1% DVB, 1.0-1.6 mmol/g) was purchased from Iris Biotech GmbH and was used for synthesis of the cyclic peptides. Solid phase peptide synthesis was carried out in plastic syringes with a polyethylene frit (20 μm) obtained from Screening Devices B.V. The resin loading was determined by measuring the UV absorbance of the piperidine-dibenzofulvene adduct (λ_{max} 300 nm).[22] All components used in gp120-capture ELISA experiments were purchased from ImmunoDiagnostics, Inc. (Woburn, MA). Reactions were performed at room

temperature. Solution phase reactions were monitored by TLC analysis and R_f-values were determined on Merck pre-coated silica gel 60 F-254 (0.25 mm) plates. Spots were visualized with UV-light, and by heating plates dipped in ninhydrine, Cl_2/N,N,N,N'-tetramethyl-4,4'-diaminodiphenylmethane (TDM)[23] or a $KMnO_4$ solution. Column chromatography was performed using Silica-P Flash silica gel (60 Å, particle size 40-63 μm; Silicycle). Microwave reactions were performed in a Biotage Initiator (300 W) reactor in sealed vessels suitable for reaction volumes of 0.5-2 mL. ^{1}H NMR experiments were conducted on a 300 MHz Varian G-300 spectrometer, and chemical shifts are given in ppm (δ) relative to TMS (0.00 ppm). ^{13}C NMR spectra were recorded at 75 MHz at a Varian G-300 spectrometer and chemical shifts are given in ppm (δ) relative to $CDCl_3$ (77 ppm). Analytical HPLC was accomplished on a Shimadzu-10Avp (Class VP) system using UV-detector operating at 214 and 254 nm. The mobile phase was 0.1% TFA in CH_3CN/H_2O 5:95 (buffer A) and 0.1% TFA in CH_3CN/H_2O 95:5 (buffer B). For analysis of protected (cyclic) peptides the mobile phase was 0.1% TFA in CH_3CN/H_2O 20:80 (buffer A) and 0.1% TFA) in CH_3CN/iPrOH/H_2O 50:45:5 (buffer B). A Phenomenex Gemini C18 column (110 Å, 5 μm, 250×4.60 mm) was used at a flow rate of 1 mL min^{-1} using a standard protocol: 100% buffer A for 1 min, then a linear gradient of buffer B (0-100% in 30 min). Purification of the peptide-containing compounds was performed on a Prep LCMS-QP8000α HPLC system (Shimadzu) using a Phenomenex Gemini C18 column (10 μm, 110 Å, 250×21.2 mm) at a flow rate of 12.5 mL min^{-1} using a standard protocol: 100% buffer A for 5 min followed by a linear gradient of buffer B (0-55% in 100 min) using the same buffers as described for analytical HPLC. Electrospray ionization mass spectrometry (ESI-MS) was performed on a Shimadzu LCMS-QP8000 single quadrupole bench-top mass spectrometer operating in a positive ionization mode or a Thermo-Finnigan LCQ Deca XP Max ion trap mass spectrometer. Analytical LC-MS was preformed on Thermo-Finnigan LCQ Deca XP Max coupled to a Shimadzu- 10Avp (Class VP) system using UV-detector operating at 254 nm. MALDI-TOF-MS spectra were recorded on a Kratos Analytical (Shimadzu) AXIMA CFR mass spectrometer using α-cyano-4-hydroxycinnamic acid (CHCA) or sinapic acid as a matrix and human ACTH (18-39) or bovine insulin oxidized B chain as references. High resolution electrospray ionization (ESI) mass spectra were measured on a Micromass LCT mass spectrometer calibrated with CsI. All reported mass values are monoisotopic. The microtiterplate reader used in the ELISA experiments was a BioTek μQuant (Beun de Ronde, Abcoude, The Netherlands). Software used for data analysis was the Full Mode-KC4 version 3.4.

Peptide synthesis

Purification of cyclic peptides 4a-c

The syntheses of Fmoc-L-ε-azidolysine and cyclic azidopeptides **4a**, **4b** and **4c** have been described in chapter 2.

Cyclic peptide cyclo(Leu-Thr-Arg-Asp-Gly-Gly-Asn-Ser-Asn-Asn-Glu-Ile-Lys(N_3)-Gly), **loop 1***

The crude protected cyclic peptide was purified with column chromatography using a gradient of CH_2Cl_2/EtOH 95:5 to 9:1. The product was obtained as colorless oil. R_f: 0.56 (CH_2Cl_2/EtOH 9:1). Synthesis was performed on 0.25 mmol scale. Yield after deprotection of sidechains: 48 mg (13%). $[M+H]^+$ monoisotopic calculated for $C_{58}H_{95}N_{23}O_{23}$: 1482.70, found 1483.01. HPLC: R_t= 15.33 min, purity= 100%

Cyclic peptide cyclo(Gln-Ser-Ser-Gly-Gly-Asp-Pro-Glu-Ile-Val-Thr-Lys(N_3)-Gly), **loop 3***

The crude protected cyclic peptide was purified with column chromatography in CH_2Cl_2/MeOH 95:5. The product was obtained as a yellow oil. R_f: 0.54 (CH_2Cl_2/MeOH 9:1). Synthesis on 0.25 mmol scale. Yield after deprotection of side chains: 190 mg (42%). HPLC analysis shows some small impurities, therefore the product is further purified with preparative HPLC. Pure product was obtained as a white powder. Yield: 9.8 mg (3%). $[M+H]^+$ monoisotopic calculated for $C_{52}H_{83}N_{17}O_{21}$: 1282.60, found 1282.49. HPLC: R_t= 14.68 min, purity= 100%

Synthesis of the scaffold molecules

The synthesis of alkyne-functionalized TAC-scaffold **1** has been described in chapter 3.

Linear triamine scaffold 5

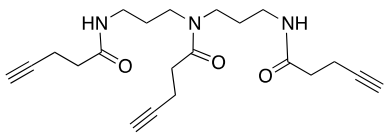

4-Pentynoic acid (2.47 g, 25.15 mmol) was dissolved in 30 mL CH_2Cl_2. The solution was stirred and cooled with an ice bath. BOP (11.12 g, 25.15 mmol) and DiPEA (8.56 mL, 50.30 mmol) were added to the solution, followed by addition of bis(3-aminopropylamine (1.08 mL, 7.6 mmol). The reaction mixture was allowed to warm up to room temperature and was stirred overnight, after which the mixture was concentrated *in vacuo*. The residue was dissolved in EtOAc and washed three times with 1 M $KHSO_4$, with water, three times with 1N $NaHCO_3$ and with brine. The organic phase was dried over Na_2SO_4 and concentrated *in vacuo*. The product was purified by column chromatography using 3% MeOH in DCM. When the product started to elute, 10% MeOH in CH_2Cl_2 was used. Pure product **5** was obtained as a yellow oil that slowly crystallized into a light yellow solid. Yield: 2.71 g (93%). R_f: 0.61 (CH_2Cl_2/MeOH 9:1). ^{1}H-NMR (300 MHz, $CDCl_3$, TMS): δ 1.62-1.68 (m, 2H, CH_2*CH_2*CH_2), 1.80-1.85 (m, 2H, CH_2*CH_2*CH_2), 1.98 (t, 2H, alkyne-*H*), 2.04 (t, 1H, alkyne-*H*), 2.39-2.44 (m, 4H, C(O)CH_2*CH_2*), 2.50-2.56 (m, 8H, C(O)CH_2 and C(O)CH_2*CH_2*), 3.16-3.22 (q, 2H, NHC*H*$_2$), 3.30-3.35 (m, 4H, NHC*H*$_2$ and NC*H*$_2$), 3.42 (t, 2H, NC*H*$_2$), 5.98 (s, 1H, N*H*), 6.77 (s, 1H, N*H*).

^{13}C-NMR (75 MHz, $CDCl_3$): δ 14.7, 14.9, 27.4, 29.3, 31.8, 35.4, 35.8, 36.9, 42.5, 45.4, 69.2, 82.9, 171.1, 171.4, 171.6

Dendrimer building block 7

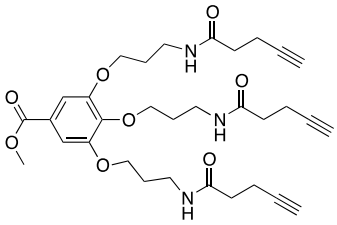

Dendrimer building block **7** was synthesized starting from its hydrochloric acid salt precursor, which was prepared following a previously described procedure.[24]

To a suspension of this hydrochloride salt precursor (930 mg, 2.0 mmol), 4-pentynoic acid (588 mg, 6.0 mmol) and BOP (2.93 g, 6.6 mmol) in CH_2Cl_2 (20 mL) was added D*i*PEA (3.39 mL, 19.5 mmol). The mixture was stirred at room temperature for 16h and concentrated *in vacuo*. The residue was dissolved in EtOAc and washed with 1 M $KHSO_4$ (twice), 1 M NaOH (twice) and brine. The organic layer was dried over Na_2SO_4 and concentrated *in vacuo* to a volume of approximately 20 mL. Precipitation after addition of hexanes, followed by filtration afforded the product as a white solid (951 mg, 80%). R_f = 0.44 (MeOH/CH_2Cl_2, 5/95). Mp = 133 ºC. ^{1}H NMR (500 MHz, $CDCl_3$): δ = 2.04 (m, 9H, 3× OCH_2CH_2, 3× º-H), 2.43 (m, 6H, 3× C(O)CH_2), 2.52 (m, 6H, 3× C(O)CH_2CH_2), 3.50 (m, 6H, 3× $NHCH_2$), 3.89 (s, 3H, OCH_3), 4.11 (m, 6H, 3× OCH_2), 6.69, 6.85 (2bt, 3H, 3× NH), 7.25 (s, 2H, Ph-C^{2,6}-H).
^{13}C NMR (125 MHz, $CDCl_3$): δ = 14.8, 14.9 (C(O)CH_2CH_2), 29.0, 30.1 (OCH_2CH_2), 35.1, 35.2 (C(O)CH_2), 37.0, 37.1 ($NHCH_2$), 52.2 (OCH_3), 66.8, 71.7 (OCH_2), 69.1, 69.2 (C^{o}*C*-H), 83.0 (*C*^{o}C-H), 107.7 (Ph-C^{2,6}), 125.3 (Ph-C^{1}), 141.0 (Ph-C^{4}), 152.2 (Ph-C^{3,5}), 166.4 (CO_2Me), 171.3, 171.4 (NHC=O). $[M+H]^+$ monoisotopic calculated for $C_{32}H_{41}N_3O_8$: 596.2966, found: 596.45.

CTV-derivative 9

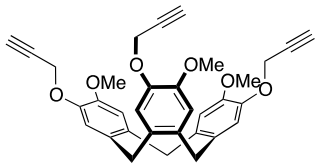

CTV derivative **9** was prepared in two steps starting from vanillyl alcohol, by alkylation with propargyl bromide followed by conversion into the CTV-derivative.

1-O-propargyl-vanillylalcohol: Vanillyl alcohol (3.08 g, 20.0 mmol) and propargyl bromide (80 % in toluene, 2.16 mL, 20 mmol) was dissolved in acetone (40 mL). After addition of K_2CO_3 (4.15 g, 30 mmol) the reaction mixture was stirred at reflux temperature overnight. Evaporation of the solvent was followed by addition of water (75 mL) and DCM (75 mL), separation of the layers, drying of the organic phase (Na_2SO_4) and evaporation of the solvent. The alkylated vanillylalcohol was obtained in 93% (3.57 g) as a white solid and used without further purification. ^{1}H-NMR (300 MHz, $CDCl_3$) δ 1.73 (br. s, 1H, O*H*), 2.50 (t, 1H, ^{3}*J* 2.3 Hz, propargyl-C*H*), 3.88 (s, 3H, CH_3), 4.63 (2H, CH_2OH), 4.76 (d, 2H, ^{3}*J* 2.3 Hz, propargyl-CH_2), 6.88 (m, 1H, Ar*H*), 6.95 (d, 1H, ^{3}*J* 2.0 Hz, Ar*H*), 7.01 (d, 1H, ^{3}*J* 8.3Hz, Ar*H*)

^{13}C-NMR (75 MHz, $CDCl_3$) δ 55.7 (OCH_3), 56.7 (propargyl-CH), 65.0 (CH_2OH), 75.7 (propargyl-CH_2), 78.5 (propargyl-C^q), 110.8, 114.3, 119.0, 135.0, 146.1, 149.7 (ArC)

(O-propargyl)$_3$-CTV 9: After dissolving 1-*O*-propargyl-vanillylalcohol (3.57 g, 18.6 mmol) in methanol (20 mL), the reaction mixture was cooled to 0°C and perchloric acid (11.0 mL) was added dropwise and then stirred overnight at room temperature. DCM (100 mL) was added and the crude material was washed with 1M NaOH (aq) until the organic layer was no longer acidic. After drying on Na_2SO_4 and evaporation of the solvents, the crude material was triturated with Et_2O, yielding **9** (2.01 g, 21%) as an off-white solid. ^{1}H-NMR (300 MHz, DMSO-d_6) δ 3.42 (3H, s, propargyl-CH), 3.50 (3H, d, ^3J=13.5 Hz, Ar-C*H*H'), 3.74 (9H, s, OCH_3), 4.71 (9H, m, Ar-CH*H'* + propargyl-CH_2), 7.11 (6H, 2 x s, ArH).

^{13}C-NMR (75 MHz, DMSO-d_6) δ 35.4 (Ar-CH_2), 56.0 (OCH_3), 56.3 (propargyl-CH), 78.0 (propargyl-CH_2), 79.9 (propargyl-C^q), 114.1, 116.1, 131.8, 133.3, 145.1, 148.0 (ArC).

General procedure for scaffold conjugation of cyclic peptides by optimized CuAAc. 10-fold stock solutions of $CuSO_4$ (44.9 µmol, 11.2 mg in 1 mL H_2O) and sodium ascorbate (89.9 µmol, 17.8 mg in 1 mL H_2O) were prepared. TBTA was dissolved in 100 µL DMF. Peptides were dissolved individually in the smallest possible amount (100-500 µL) of DMF (4Å, molsieves).

Solutions of three peptides in DMF were prepared: loop 1 (compound **4a**, 7.49 µmol, 6.93 mg), loop 2 (compound **4b**, 7.49 µmol, 10.25 mg) and loop 3 (compound **4c**, 7.49 µmol, 7.99 mg). Scaffold **5**, **7** or **9** (7.49 µmol) was added to the microwave vessel and dissolved in 100 µL DMF (4Å, molsieves). 100 µL of the $CuSO_4$ stock solution (4.49 µmol, 1.12 mg) and 100 µL of the sodium ascorbate stock solution (8.99 µmol, 1.78 mg) were added to the solution, followed by addition of the TBTA solution (1.10 µmol, 0.60 mg in 100 µL). The peptide solutions were combined and added to the reaction mixture. Depending on the amount of DMF that was used to dissolve the peptides, H_2O was added to obtain a 3:2 DMF/H_2O ratio and 1-1.5 mL total volume. The microwave vessel was sealed and allowed to react in the microwave reactor at 80°C during 25 minutes. After reaction, a sample was taken from the reaction mixture for LC-MS analysis. Based on this analysis, the individual components were purified with preparative HPLC. Typically, preparative HPLC was performed using standard H_2O/MeCN buffers and a slow gradient over 100 minutes starting at 100% buffer A and going to 55% buffer B.

TAC-scaffolded compounds **12**

Loop combination	Bruto formula	[M+H]+ calculated	[M+H]+ found	Rt (min)
1-1-2	$C_{162}H_{249}N_{55}O_{46}S$	3733.86	3732.15	14.87
1-2-2	$C_{186}H_{282}N_{58}O_{49}S_2$	4177.08	4176.55	15.59
1-1-3	$C_{146}H_{226}N_{50}O_{47}$	3432.69	3432.11	14.42
1-3-3	$C_{154}H_{236}N_{48}O_{51}$	3574.74	3574.59	14.94
1-2-3	$C_{170}H_{259}N_{53}O_{50}S$	3875.91	3874.51	15.32
2-2-3	$C_{194}H_{292}N_{56}O_{53}S_2$	4319.13	4318.95	16.17
2-3-3	$C_{178}H_{269}N_{51}O_{54}S$	4017.96	4017.14	15.97

HIV-1 gp120 capture ELISA

Recombinant HIV-1IIIB gp120 protein capture ELISA was performed according to the manufacturer's instructions (ImmunoDiagnostics, Inc., Woburn, MA). Firstly, various concentrations of free ligand rgp120 in sample buffer (up to 2 µg/ml, in a 2-fold dilution series) were added to a CD4-coated plate in the absence of test compounds. After a 60-min incubation at room temperature, the amounts of captured rgp120 were detected by peroxidase-conjugated murine anti-gp120 mAb.[25] We determined that optimal OD_{450}-values were obtained when a final rgp120 concentration of 1 µg/ml was used. When optimal concentrations were determined, competition experiments were performed. Test compounds diluted in sample buffer (50 µL 0.1% BSA in PBS) and 2% DMSO were added to the CD4-coated plate, immediately followed by addition of 50 µL 2 µg/ml rgp120 (final concentration 1 µg/mL). After 4 h of incubation at room temperature, the plate was washed with wash buffer (0.1% Tween 20 in PBS) followed by incubation with peroxidase-conjugated murine anti-gp120 mAb to detect the amounts of captured rgp120. Any unbound material was washed away using wash buffer, and plates were developed by adding 100 µL/well 3,3',5,5'-tetramethylbenzidine (TMB) substrate solution (0.1 mg/mL TMB in 0.1 N NaOAc buffer pH 5.5, containing 0.003% H_2O_2). The reaction was stopped by adding 100 µL 4N sulphuric acid. Absorbances (ODs) were read at 450 nm using a microtiterplate reader. All assays were performed in duplicate and were independently repeated at least two times.

Serum-stability study[26]

The following procedure was performed in duplicate:

250 µL pooled human serum (Sanquin blood supply) was taken and diluted with 500 µL milliQ. The solution was centrifuged and the supernatant was taken.

0.15 mg CTV-scaffolded discontinuous epitope mimic was dissolved in 2 µL DMSO and 248 µL milliQ was added. To this solution, the human serum supernatant was added to obtain a final compound concentration of of 150 µg/mL in 25% (v/v) human serum. The resulting solution was incubated 37ºC. Aliquots of 95 µL were taken after

0, 60, 120, 240 and 480 minutes and after 25 hours and the proteins were precipitated with 300 µL MeCN/H_2O/formic acid (89:10:1). After 45 minutes of storage on ice, the sample was centrifuged (10 min, 12000 rpm at 4°C). The supernatants were lyophilized and dissolved in 200 µL MeCN/H_2O (1:1 (v/v)) for analysis. The peak area of the CTV-scaffolded discontinuous epitope mimic was determined with analytical HPLC, and was found to be 62% of the initial value after 25 h incubation time at 37°C.

References

(1) Yin, H.; Hamilton, A. D. *Angew. Chem. Int. Ed.* **2005**, *44*, 4130–4163.

(2) Robinson, J. A.; DeMarco, S.; Gombert, F.; Moehle, K.; Obrecht, D. *Drug Discov. Today* **2008**, *13*, 944–951.

(3) van Zoelen, D.-J.; Egmond, M. R.; Pieters, R. J.; Liskamp, R. M. J. *ChemBioChem* **2007**, *8*, 1950–1956.

(4) Hijnen, M.; van Zoelen, D. J.; Chamorro, C.; van Gageldonk, P.; Mooi, F. R.; Berbers, G.; Liskamp, R. M. J. *Vaccine* **2007**, *25*, 6807–6817.

(5) Heinis, C.; Rutherford, T.; Freund, S.; Winter, G. *Nature Chem. Biol.* **2009**, *5*, 502–507.

(6) Angelini, A.; Cendron, L.; Chen, S.; Touati, J.; Winter, G.; Zanotti, G.; Heinis, C. *ACS Chem. Biol.* **2012**, *7*, 817–821.

(7) Baeriswyl, V.; Rapley, H.; Pollaro, L.; Stace, C.; Teufel, D.; Walker, E.; Chen, S.; Winter, G.; Tite, J.; Heinis, C. *ChemMedChem* **2012**, *7*, 1173–1176.

(8) Chen, S.; Morales-Sanfrutos, J.; Angelini, A.; Cutting, B.; Heinis, C. *ChemBioChem* **2012**, *13*, 1032–1038.

(9) Bock, J. E.; Gavenonis, J.; Kritzer, J. A. *ACS Chem. Biol.* **2013**, *8*, 488–499.

(10) Gokhale, A.; Weldeghiorghis, T. K.; Taneja, V.; Satyanarayanajois, S. D. *J. Med. Chem.* **2011**, *54*, 5307–5319.

(11) Craik, D. J.; Swedberg, J. E.; Mylne, J. S.; Cemazar, M. *Expert Opin. Drug Discov.* **2012**, *7*, 179–194.

(12) Chamorro, C.; Kruijtzer, J. A. W.; Farsaraki, M.; Balzarini, J.; Liskamp, R. M. J. *Chem. Commun.* **2009**, 821.

(13) Mulder, G. E.; Kruijtzer, J. A. W.; Liskamp, R. M. J. *Chem. Commun.* **2012**, *48*, 10007.

(14) Gilbert, P.; Wang, M.; Wrin, T.; Petropoulos, C.; Gurwith, M.; Sinangil, F.; D'Souza, P.; Rodriguez Chavez, I. R.; DeCamp, A.; Giganti, M.; Berman, P. W.; Self, S. G.; Montefiori, D. C. *J. Infect. Dis.* **2010**, *202*, 595–605.

(15) Schellinger, J. G.; Danan-Leon, L. M.; Hoch, J. A.; Kassa, A.; Srivastava, I.; Davis, D.; Gervay-Hague, J. *J. Am. Chem. Soc.* **2011**, *133*, 3230–3233.

(16) Kwong, P. D.; Wyatt, R.; Robinson, J.; Sweet, R. W.; Hendrickson, W. A.; Sodroski, J. *Nature* **1998**, *393*, 648–659.

(17) Franke, R.; Hirsch, T.; Overwin, H.; Eichler, J. *Angew. Chem. Int. Ed.* **2007**, *46*, 1253–1255.

(18) Pollaro, L.; Heinis, C. *Med. Chem. Commun.* **2010**.

(19) Brouwer, A. J.; Liskamp, R. M. J. *Eur. J. Org. Chem.* **2005**, 487–495.

(20) Rump, E. T.; Rijkers, D. T. S.; Hilbers, H. W.; de Groot, P. G.; Liskamp, R. M. J. *Chemistry* **2002**, *8*, 4613–4621.

(21) Kwong, P. D.; Wyatt, R.; Majeed, S.; Robinson, J.; Sweet, R. W.; Sodroski, J.; Hendrickson, W. A. *Structure* **2000**, *8*, 1329–1339.

(22) Fields, G. B. *Int. J. Peptide Protein Res.* **1990**, *35*, 161–214.

(23) Arx, Von, E.; Faupel, M.; Brugger, M. *J. Chromatogr. A* **1976**, *120*, 224.

(24) Brouwer, A. J.; Mulders, S. J. E.; Liskamp, R. M. J. *Eur. J. Org. Chem.* **2001**, 1903–1915.

(25) Yang, Q.-E.; Stephen, A. G.; Adelsberger, J. W.; Roberts, P. E.; Zhu, W.; Currens, M. J.; Feng, Y.; Crise, B. J.; Gorelick, R. J.; Rein, A. R.; Fisher, R. J.; Shoemaker, R. H.; Sei, S. *J. Virology* **2005**, *79*, 6122–6133.

(26) Knappe, D.; Henklein, P.; Hoffmann, R.; Hilpert, K. *Antimicrob. Agents Chemother.* **2010**, *54*, 4003–4005.

6

Summary and outlook

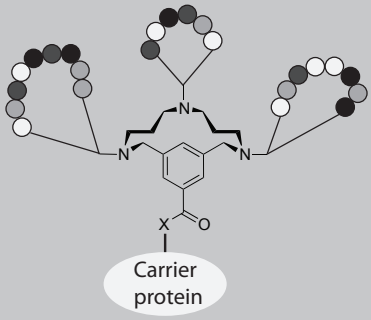

6.1 Summary

The research described in this thesis aimed at the development of a generally applicable and reliable method for the mimicry of discontinuous protein binding sites, based on scaffolded cyclic peptides. Although this class of compounds has increasingly gained interest in recent years, only limited information about the synthesis of scaffolded cyclic peptides is available. Some successful examples of especially bicyclic peptides have been described[1], however a general method for the *modular* synthesis of protein mimics containing up to three different *cyclic* peptides was not available at the start of this research project.

The development of such an approach involves three main aspects: 1) the synthesis of cyclic peptides which contain a linker for conjugation, 2) a molecular scaffold for conjugation of up to three cyclic peptides and 3) a fast and efficient conjugation method to attach the cyclic peptides to this scaffold molecule. These aspects were studied in this thesis.

Chapter 1 presents a literature overview of the various attempts towards the mimicry of complex protein binding sites that have been published over the past few decades. A multitude of methods for the synthesis of cyclic peptides has been described, a large variety of molecular scaffolds is available, and the number of synthetic constructs containing multiple *linear* peptides is growing rapidly. However, a general method for the synthesis of these complex molecules was still not available, and especially a robust method for the assembly of multiple cyclic peptides is highly desired.

In **chapter 2**, a number of methods are described for the synthesis of cyclic peptides carrying a linker for conjugation to a molecular scaffold. Since cyclic peptides are only intermediate products in the synthesis of discontinuous protein binding site mimics, their synthesis should be very efficient and result in significant amounts of highly pure products (preferably 20-50 mg). In addition, multiple different cyclic peptides are required and therefore the synthetic method should preferably be sequence-independent. Both solid-supported and solution phase cyclization methods have been attempted, involving various cyclization strategies. The most important conclusion from this chapter was that peptide cyclization should be performed in solution, on partially protected peptides. The resulting protected cyclic peptides could be purified by normal phase chromatography, which allows the rapid purification of large quantities

of cyclic peptides. Subsequently, The resulting cyclic peptides have to be deprotected, since *unprotected* cyclic peptides are required for conjugation to the scaffold.

The attachment of the resulting cyclic peptides to the TAC-scaffold is described in **chapter 3**. Classical amide-bond formations were performed using protected cyclic peptides, but in this way only one cyclic peptide could be attached to the TAC-scaffold. Therefore an orthogonal ligation method, the copper-catalysed azide alkyne cycloaddition reaction (CuAAC), was applied and an optimization study was performed to find the optimal conditions for conjugation of unprotected cyclic peptides to the relatively small TAC-scaffold. For the formation of trivalent peptide-conjugates on the TAC-scaffold, the addition of the Cu(I)-stabilising ligand TBTA proved to be essential.

Chapter 4 combines the results of the previous two chapters for the reliable synthesis of a library of TAC-scaffolded cyclic peptides. A mixture of three different cyclic peptides, representing important conserved binding domains of the CD4 binding site of HIV-1 gp120, was attached to the TAC-scaffold. The resulting library of gp120 mimics was evaluated in a gp120-capture ELISA for binding to CD4. Binding in the micromolar range was observed for some of the mimics, which stimulated further research towards more potent mimics of this binding site.

Chapter 5 presents an optimization study of the HIV gp120 mimics and demonstrates the general applicability of the approach that was described in the previous chapters. The method for the synthesis of libraries of discontinuous protein binding site mimics was applied on three different trivalent scaffold molecules, and the ring size of the cyclic peptides was varied. This resulted in a 10-fold improved binding to CD4, as was studied with ELISA.

The optimization study in chapter 5 had a limited scope, but presented many possibilities for further research on this topic. The parameters that influence epitope recognition of the mimics could be further investigated, and additional binding studies could be performed. Some initial research towards these goals has been performed already (*vide infra*), and additional challenges to extend the research described in this thesis still remain. The most appealing topics for further research will be discussed in the following paragraphs.

6.2 Outlook

6.2.1 – MTT assay

In addition to the ELISA experiments, a cell-based assay was performed to obtain information about the binding of the gp120 mimics in a more natural environment. This information could provide valuable knowledge for the development of more potent mimics.

The best binder from the competitive ELISA studies was further investigated in a 3-(4,5-dimethylthiazol-2-yl)-2,5-diphenyltetrazolium bromide (MTT) assay using $CD4^+$ T-cells.[2] This cell-killing assay measures the capacity of a virus, in the present study HIV-1, to induce lysis of target cells. Living cells convert MTT into a blue product (formazan). The amount of formazan can be quantified spectrophotometrically, and reflects the number of cells protected by the discontinuous epitope mimic against killing by the virus. The MTT assay was performed with two different viral strains; HIV-1 IIIB and HxB2. In addition to investigating the protection against cell killing by the virus, also the cytotoxicity of the discontinuous epitope mimics to the cells could be determined using this MTT assay. The cytoxicity was determined by incubating the cells in the presence of different concentrations of the discontinuous epitope mimic, in absence of the virus.

As a reference compound in these cell-based assays, Chicago Sky Blue (CSB) was used. This known inhibitor of the gp120-CD4 interaction was also used in the ELISA experiments and showed IC_{50} values in the same range as the discontinuous epitope mimics. Although CSB is known to inhibit the gp120-CD4 interaction, its mechanism of action is unknown.[3]

The pilot-experiment with CSB showed protection against killing by both viral strains at low micromolar concentrations as can be seen in Figure 1. Although the experiment was performed only once, these results encouraged us to perform the assay with the most potent CTV-scaffolded gp120 mimic. While CSB showed significant cytotoxicity at the highest concentration that was tested, the CTV-scaffolded mimic did not show any cytotoxicity (Figure 2). Unfortunately, no protection was observed in this first experiment either. Further research should be performed to explain these results, since many factors affect the outcome of these types of assays.

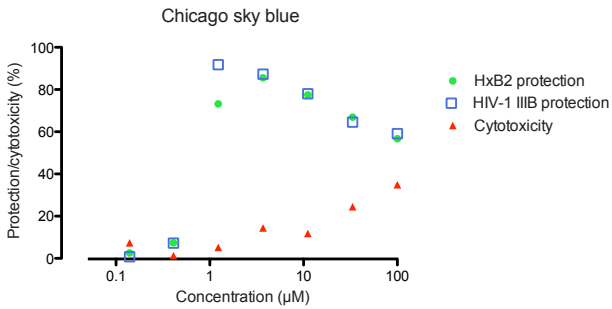

HIV-strain	IC_{50} (μM)
HxB2	0.82
HIV-1 IIIB A17	0.93

Figure 1 | Protection by CSB of MT2 cells against killing by HIV-1, and cytotoxicity of CSB to these cells.

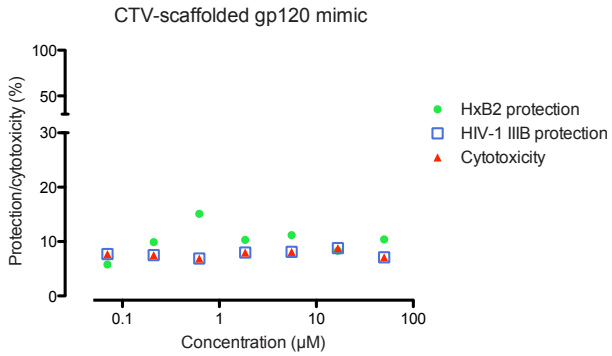

Figure 2 | Protection by the CTV-scaffolded gp120 mimic of MT2 cells against killing by HIV-1, and cytotoxicity of the mimic to these cells.

6.2.2 – Selectively addressable TAC-scaffold

After a screening of a collection of discontinuous epitope mimics with ELISA and the identification of active mimics, it would be attractive to be able to selectively re-synthesize the most potent mimic. For this purpose, the earlier discussed non-stop solid phase approach[4] could be employed, however this method is rather time-consuming. Since azide-functionalized cyclic peptides representing the epitope fragments of interest are already available, a method for re-synthesis of the most potent mimic using these building blocks would be preferred.

Recent developments in bio-orthogonal chemistry have resulted in the synthesis of a number of heterotrifunctional linkers.[5] One of these linkers makes use of orthogonally protected alkynes, allowing the stepwise introduction of azide-containing ligands to

the linker.[6] A similar approach might be translated to the TAC-scaffold, since the TAC-scaffold is equipped with three orthogonally protected amines.

6.2.3 – Immunization studies

Probably the most appealing future research on the gp120 discontinuous epitope mimics would involve the investigation their antigenic and immunological properties. Relatively small peptide-based compounds, like the gp120 mimics described here, are usually poor immunogens. A common way to increase the immune response of small peptides, is by conjugating them to a large carrier protein. Carrier proteins are chosen based on immunogenicity, solubility, and whether adequate conjugation with the carrier can be achieved. Probably the most commonly used carrier protein for peptide antigens is Keyhole Limpet Hemocyanin (KLH), which can be conjugated via maleimide chemistry. Since the TAC-scaffold has a fourth position available for functionalization and this position is located relatively far away from the cyclic peptides, this position would be ideal for conjugation to KLH (Figure 3).

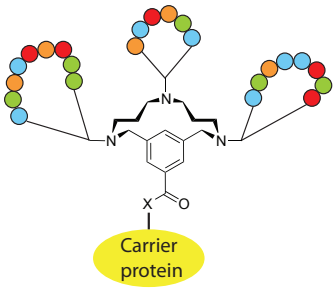

Figure 3 | TAC-scaffolded protein binding site mimics, conjugated to a carrier protein for immunization studies.

6.2.4 – Application of the synthetic approach to other targets

Another topic of future research based on the methodology described in this thesis, is the investigation of other targets in which discontinuous epitopes are involved. *Focused libraries* of cyclic peptides could be synthesized for mimicry of well-defined protein targets.

An example of a well-studied target with great value for vaccine development is the

stem region of hemagglutinin (HA), the major viral surface glycoprotein of the influenza virus. Despite the many differences in the biology of HIV infection and the influenza virus, parallels can be drawn between the two viruses and between the challenges of vaccine development against them. A major challenge for both an HIV-1 vaccine and a pandemic influenza vaccine is the extreme diversity and variability of the envelope glycoproteins, which are the major neutralizing determinants on the surface of the viruses.[7]

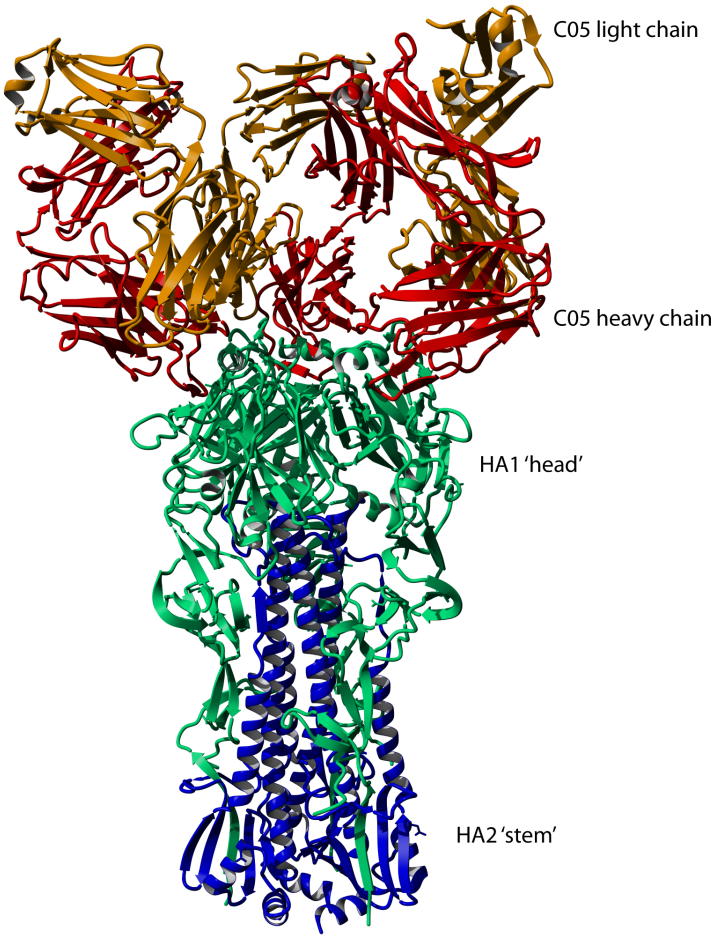

Figure 4 | Crystal structure of neutralizing antibody C05 in complex with trimeric haemagglutinin, revealing the location of the C05 epitope in the HA1 head region.

Recent studies have resulted in the isolation and characterization of neutralizing antibodies of influenza A.[8-13] Although many of these antibodies target a highly variable domain on HA1, the so-called 'head'-region of the haemagglutinin (HA) surface glycoprotein, some rare antibodies against HA1 were detected that achieve modest cross-reactivity (see Figure 4 for a crystal structure of a recently isolated cross-reactive antibody in complex with HA). This implies the involvement of more conserved binding sites, which could be valuable targets for mimicry by scaffolded cyclic peptides. The availability of detailed structural information on HA-antibody complexes, in combination with homology studies on HA, provides a good starting point for the development of mimics of the binding sites of interest.

References

(1) Heinis, C.; Rutherford, T.; Freund, S.; Winter, G. *Nature Chem. Biol.* **2009**, *5*, 502–507.

(2) Boucher, C. A.; Keulen, W.; van Bommel, T.; Nijhuis, M.; de Jong, D.; de Jong, M. D.; Schipper, P.; Back, N. K. *Antimicrob. Agents Chemother.* **1996**, *40*, 2404–2409.

(3) Clanton, D. J.; Moran, R. A.; McMahon, J. B.; Weislow, O. S.; Buckheit, R. W. J.; Hollingshead, M. G.; Ciminale, V.; Felber, B. K.; Pavlakis, G. N.; Bader, J. P. *J. AIDS* **1992**, *5*, 771.

(4) Chamorro, C.; Kruijtzer, J. A. W.; Farsaraki, M.; Balzarini, J.; Liskamp, R. M. J. *Chem. Commun.* **2009**, 821.

(5) Beal, D. M.; Jones, L. H. *Angew. Chem. Int. Ed.* **2012**, *51*, 6320–6326.

(6) Valverde, I. E.; Delmas, A. F.; Aucagne, V. *Tetrahedron* **2009**, *65*, 7597–7602.

(7) Karlsson Hedestam, G. B.; Fouchier, R. A. M.; Phogat, S.; Burton, D. R.; Sodroski, J.; Wyatt, R. T. *Nature Rev. Microbiol.* **2008**, *6*, 143–155.

(8) Steel, J.; Lowen, A. C.; Wang, T. T.; Yondola, M.; Gao, Q.; Haye, K.; García-Sastre, A.; Palese, P. *MBio* **2010**, *1*, 1–9.

(9) Ekiert, D. C.; Kashyap, A. K.; Steel, J.; Rubrum, A.; Bhabha, G.; Khayat, R.; Lee, J. H.; Dillon, M. A.; O'Neil, R. E.; Faynboym, A. M.; Horowitz, M.; Horowitz, L.; Ward, A. B.; Palese, P.; Webby, R.; Lerner, R. A.; Bhatt, R. R.; Wilson, I. A. *Nature* **2012**, *488*, 526–532.

(10) Throsby, M.; van den Brink, E.; Jongeneelen, M.; Poon, L. L. M.; Alard, P.; Cornelissen, L.; Bakker, A.; Cox, F.; van Deventer, E.; Guan, Y.; Cinatl, J.; Meulen, ter, J.; Lasters, I.; Carsetti, R.; Peiris, M.; de Kruif, J.; Goudsmit, J. *PLoS ONE* **2008**, *3*, e3942.

(11) Ekiert, D. C.; Bhabha, G.; Elsliger, M.-A.; Friesen, R. H. E.; Jongeneelen, M.; Throsby, M.; Goudsmit, J.; Wilson, I. A. *Science* **2009**, *324*, 246–251.

(12) Sui, J.; Hwang, W. C.; Perez, S.; Wei, G.; Aird, D.; Chen, L.-M.; Santelli, E.; Stec, B.; Cadwell, G.; Ali, M.; Wan, H.; Murakami, A.; Yammanuru, A.; Han, T.; Cox, N. J.; Bankston, L. A.; Donis, R. O.; Liddington, R. C.; Marasco, W. A. *Nature Struct. Mol. Biol.* **2009**, *16*, 265–273.

(13) Corti, D.; Voss, J.; Gamblin, S. J.; Codoni, G.; Macagno, A.; Jarrossay, D.; Vachieri, S. G.; Pinna, D.; Minola, A.; Vanzetta, F.; Silacci, C.; Fernandez-Rodriguez, B. M.; Agatic, G.; Bianchi, S.; Giacchetto-Sasselli, I.; Calder, L.; Sallusto, F.; Collins, P.; Haire, L. F.; Temperton, N.; Langedijk, J. P. M.; Skehel, J. J.; Lanzavecchia, A. *Science* **2011**, *333*, 850–856.

A

Appendices

Nederlandse samenvatting voor niet-ingewijden

Eiwitten vormen een grote klasse van biologische moleculen en vervullen allerlei belangrijke functies in organismen. Eiwitten zijn een bestanddeel van alle cellen en weefsels, en ze kunnen functioneren als bouwstoffen, enzymen, hormonen, antistoffen, transportmiddelen of als brandstof.

Eiwitten zijn niet alleen belangrijk voor de regulatie van processen binnen één organisme, maar ook voor interacties met invloeden van buitenaf. Eiwitten in het menselijk lichaam kunnen bijvoorbeeld ook interacties aangaan met eiwitten van virussen en bacteriën, en deze interacties spelen een belangrijke rol in allerlei ziekteprocessen. Door de interacties van eiwitten te bestuderen en te imiteren kunnen we ziekteprocessen beter begrijpen, en soms zelfs sturen. Dit kan leiden tot de ontwikkeling van nieuwe medicijnen.

Voor de ontwikkeling van nieuwe medicijnen is het belangrijk dat we goed weten hoe interacties tussen eiwitten plaatsvinden, en daarvoor moeten we weten hoe eiwitten eruit zien. Eiwitten zijn opgebouwd uit lange ketens van aminozuren die met *peptidebindingen* met elkaar zijn verbonden; het zijn eigenlijk een soort lange kralenkettingen waarbij de aminozuren de kralen zijn (zie Figuur 1). De functie van een eiwit wordt bepaald door meerdere factoren. De eerste belangrijke factor is het soort aminozuren (kralen) waaruit het eiwit (de ketting) is opgebouwd, en de volgorde van deze aminozuren in de lange keten. Er bestaan 20 verschillende aminozuren in de natuur, met allemaal net iets andere eigenschappen (vgl: kralen met 20 verschillende kleuren en groottes). Het soort aminozuren en hun volgorde in het eiwit wordt ook wel de *primaire structuur* genoemd. Niet alleen het soort en de volgorde van de aminozuren is bepalend voor de functie van het eiwit. Eiwitten zijn niet zomaar lange rechte slierten van aminozuren, maar de lange keten is opgevouwen in een hele specifieke driedimensionale structuur, ook wel de *tertiaire structuur* genoemd. Deze driedimensionale structuur is heel karakteristiek voor het eiwit, en bepaalt welke interacties het eiwit aan kan gaan met andere eiwitten of kleine moleculen. Bij dit soort interacties luistert het vaak heel nauw: het moet allemaal heel goed passen. Verkeerd gevouwen eiwitten zijn vaak de oorzaak van het ontstaan van ziektes. Bekende ziektes die veroorzaak worden door verkeerd gevouwen eiwitten zijn bijvoorbeeld de ziekte van Alzheimer, de ziekte van Parkinson of diabetes 2.

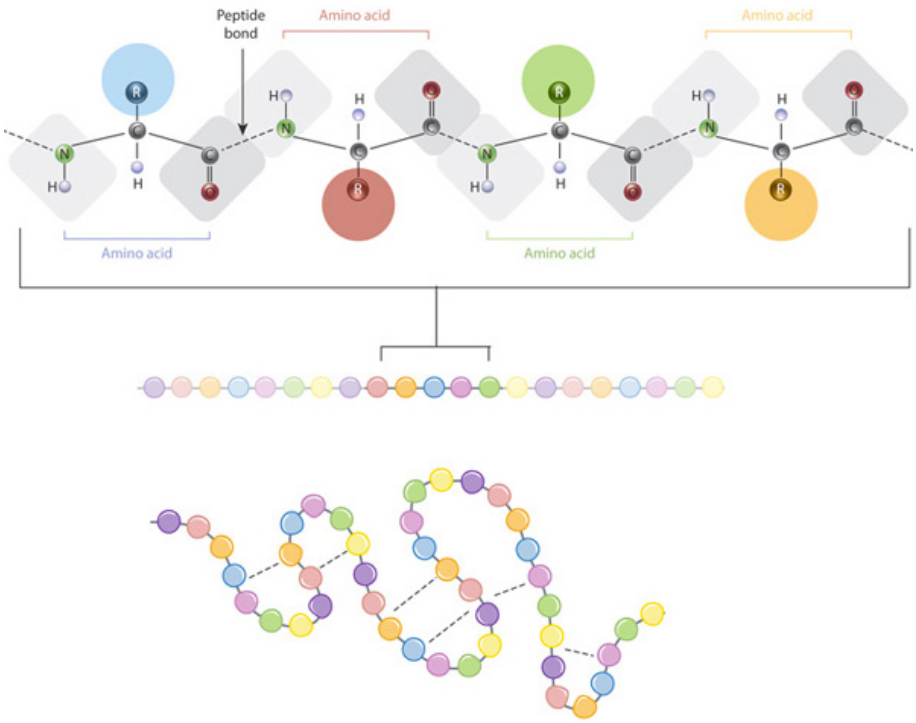

Figuur 1 | De structuur van eiwitten met van boven naar beneden de chemische weergave met peptide bindingen, de schematisch weergegeven primaire structuur (volgorde van aminozuren) en tertiaire structuur van het gevouwen eiwit.

Het bestuderen en imiteren van eiwitten is een complexe taak, waarvoor vaak wetenschappers met verschillende achtergronden samenwerken. Ten eerste willen wetenschappers weten welke eiwitten een rol spelen bij bepaalde ziekteprocessen. Dit soort informatie verzamelen chemici vaak in samenwerking met biologen en farmaceuten. Als men eenmaal een idee heeft welke eiwitten bij een bepaalde ziekte een cruciale rol spelen, hebben we een manier nodig om hun gedrag en driedimensionale structuur te kunnen bestuderen. Ook hierbij zijn vaak wetenschappers met verschillende achtergronden betrokken, van biologen tot natuurkundigen. Wanneer men een idee heeft gekregen van het gedrag en de structuur van het eiwit, wordt hier vaak een model van gemaakt. Dit kan een computermodel zijn, maar het allermooiste is het, als het eiwit op moleculair niveau nagemaakt kan worden. Dit soort imitatie-eiwitten, ook wel

eiwit mimetica, kunnen een heel gedetailleerd beeld geven van ziekteprocessen of zelfs dienen als medicijn ter behandeling of preventie van een ziekte.
Dit namaken van eiwitten is het werk van chemici, en dit proces is beschreven in dit proefschrift. In dit proefschrift is gekozen voor een specifiek eiwit, namelijk het eiwit gp120 van het HIV-virus. Het eiwit gp120 speelt een belangrijke rol bij het binnendringen van HIV in het menselijk lichaam. De eerste stap bij een HIV-infectie betreft een interactie van gp120 van HIV met het CD4 eiwit op menselijke cellen. In de strijd die wetenschappers voeren tegen HIV is deze gp120-CD4 interactie een belangrijk doelwit. Moleculen die deze interactie aanpakken kunnen bijdragen aan een medicijn, of misschien zelfs aan een vaccin tegen HIV.

Dit proefschift

Dit proefschrift beschrijft de ontwikkeling van een methode voor het namaken van eiwitten. Hierbij worden geen complete eiwitten nagemaakt, maar alleen die stukjes eiwit die belangrijk zijn voor interacties met andere eiwitten. Zoals al eerder besproken in deze samenvatting, is de driedimensionale structuur van een eiwit essentieel voor zijn functioneren. Ook wanneer er kleine stukjes van een eiwit nagemaakt worden, moet deze driedimensionale structuur nog steeds correct zijn. In het imitatieproces moet je dus goed weten welke stukjes belangrijk zijn voor de interactie, hoe de driedimensionale structuur van de stukjes eruit ziet en hoe deze stukjes ten opzichte van elkaar liggen. Bij veel interacties tussen eiwitten, en ook bij ons specifieke voorbeeld gp120, zijn vooral stukjes aan het oppervlak van het gevouwen eiwit betrokken. Als we even terugdenken aan het voorbeeld van de gevouwen kralenketting, dan bevinden deze stukjes zich vaak in een soort lusje aan de buitenkant van de gevouwen ketting. Het zijn kleine (bijna) cirkels van kralen. Korte stukjes eiwit worden ook wel *peptiden* genoemd, en cirkelvormige stukjes eiwit zijn dan *cyclische peptiden*.
Omdat het namaken van eiwitten een onderwerp is waar wetenschappers al enkele decennia lang aan werken, begint dit proefschrift in **hoofdstuk 1** met een overzicht van het werk dat al verricht is op dit gebied. Na een brede introductie wordt er specifiek gefocust op de rol en synthese van cyclische peptiden. Er word aandacht besteed aan verschillende manieren om deze moleculen te maken, en aan methodes om cyclische

peptiden te gebruiken voor het namaken van eiwitten. Hiervoor moeten meerdere cyclische peptiden aan elkaar gekoppeld worden tot één groot molecuul. Dit gebeurt vaak met behulp van een soort kapstok-molecuul (*moleculaire scaffold*), waaraan de verschillende cyclische peptiden opgehangen kunnen worden. Tot nu toe is het echter nog heel moeilijk om dat proces efficiënt uit te voeren, en kan men nog maar maximaal twee cyclische peptiden aan de kapstok hangen.

In **hoofdstuk 2** worden verschillende methoden beschreven om cyclische peptiden te synthetiseren. Er wordt gestreefd naar het ontwikkelen van een methode die werkt voor allerlei soorten aminozuursamenstellingen, en die dus heel algemeen toepasbaar is. Ook moeten de cyclische peptiden over een soort haakje beschikken, waarmee ze uiteindelijke aan de kapstok kunnen worden gehangen. Er zijn allerlei verschillende manieren uitgeprobeerd, en uiteindelijk is er een geschikte manier gevonden die werkt voor de belangrijke stukjes van het HIV gp120 eiwit. Er zijn drie belangrijke stukjes geselecteerd, en voor deze drie stukjes zijn drie cyclische peptiden met een ophang-haakje gemaakt. Een struikelblok in dit proces was niet alleen de efficiënte synthese, maar ook de zuivering van de moleculen en het vinden van een goed werkend haakje.

Hoofdstuk 3 beschrijft het proces van het aan de kapstok hangen van de cyclische peptiden uit hoofdstuk 2. Hoe groot moet die kapstok zijn? Passen de cyclische peptiden er wel aan? Of nemen die lus-achtige moleculen teveel plaats in en is de kapstok vol na het ophangen van 1 cyclisch peptide? Er zijn verschillende manieren om moleculen aan de kapstok te hangen. Moeten ze één voor één worden opgehangen of alle drie tegelijk? Dit wordt allemaal uitgetest en beschreven in hoofdstuk 3. Na verschillende pogingen en heel veel grondige analyse van het proces, komen we tot de conclusie dat een bepaald type haakje heel geschikt is, en dat er dan inderdaad drie cyclische peptiden aan de kapstok passen en opgehangen kunnen worden. Hoofdstuk 3 is een hoofdstuk dat vooral gaat over methode-ontwikkeling, en hierbij is het specifieke gp120 eiwit waar we ons verdere onderzoek op willen richten heel even naar de achtergrond geplaatst.

In **hoofdstuk 4** wordt gp120 weer erg belangrijk, want nu de methodes zijn ontwikkeld (hoofdstuk 2 en 3), willen we gp120 zo goed mogelijk namaken. De drie cyclische peptiden die in hoofdstuk 2 zijn gemaakt worden aan een kapstok gehangen via de methode die in hoofdstuk 3 is beschreven. Omdat de driedimensionale structuur van eiwitten cruciaal is, is het bij het ophangen van de cyclische peptiden ook heel belangrijk welk cyclisch peptide aan welk haakje hangt. Hier zijn meerdere mogelijkheden voor,

en we weten nog niet precies wat de beste is. Daarom besluiten we in ons onderzoek om een verzameling van alle mogelijke ophangcombinaties te maken. Als we alle combinaties hebben gemaakt, proberen we te verifiëren welke combinatie het beste past. Dit wordt gedaan in een biologisch experiment, waarin we ons namaak eiwit (het gp120-mimeticum) proberen te laten binden aan CD4 (de receptor waar gp120 bij HIV-infectie ook aan bindt). Het blijkt dat ons gp120-mimeticum behoorlijk op het natuurlijke eiwit lijkt, want we zien inderdaad binding aan CD4.
In **hoofdstuk 5** proberen we ons gp120-mimeticum nog verder te verbeteren, zodat het nog meer op het natuurlijke eiwit lijkt. Dit kan op meerdere manieren. De eerste manier die we proberen, is door verschillende kapstokmoleculen (*moleculaire scaffolds)* te gebruiken voor het ophangen van de drie cyclische peptiden. Dit is ook meteen een mooie test voor onze algemene methode voor het namaken van eiwitten: als de methode werkt voor verschillende kapstokmoleculen, dan kan de methode misschien ook wel gebruikt worden voor het namaken van andere eiwitten die een rol spelen in andere ziekteprocessen. Het blijkt dat de methode heel goed werkt en algemeen toepasbaar is, en bovendien geeft één van de nieuwe kapstokmoleculen heel goede resultaten in een biologisch testsysteem met CD4. We hebben dus een nog beter gp120-mimeticum gemaakt.

Zoals altijd het geval is met onderzoek, was het ook in dit promotie onderzoek: de tijd is op, maar het onderzoek is nog lang niet af. Sterker nog, het begint net leuk te worden. Daarom staan in **hoofdstuk 6** een aantal mogelijkheden beschreven voor een vervolgonderzoek. De gp120-mimetica zouden kunnen worden onderzocht in meer uitgebreide biologisch assays. Uiteindelijk willen we niet alleen weten of de eiwitmimetica actief zijn in plastic buisjes in het lab, maar ook of ze in menselijke cellen interacties kunnen hebben met hun partner-eiwitten. Nog verder vooruit kijkend, zouden we kunnen proberen om antistoffen op te wekken tegen de gp120-mimetica. Dit zou een belangrijke stap zijn in de ontwikkeling van een vaccin, in dit geval een HIV-vaccin. Daarnaast zou de methode die beschreven is in dit proefschrift kunnen worden toegepast op andere eiwitten die betrokken zijn bij andere ziektes. Hierbij kan bijvoorbeeld gedacht worden aan het griepvirus influenza, dat de laatste jaren ook vaak in het nieuws is vanwege epidemieën en agressieve varianten.

Curriculum Vitae

Gwenn Mulder werd op 3 september 1985 geboren te Mook en Middelaar. In de zomer van 2003 behaalde ze haar VWO-diploma met als richtingen Natuur & Gezondheid en Natuur & Techniek aan het Twents Carmelcollege te Oldenzaal. In september van datzelfde jaar startte zij met haar studie Scheikunde aan de Universiteit Utrecht. Na het behalen van haar bachelor-diploma (cum laude) vervolgde zij in september 2006 haar studie met de prestige master Drug Innovation, eveneens aan de Universiteit Utrecht. Haar eerste onderzoeksstage werd uitgevoerd onder begeleiding van Dr. ir. Dirk Rijkers en Ir. Cheng-Bin Yim in de vakgroep Medicinal Chemistry and Chemical Biology aan de universiteit Utrecht. Na het afronden van deze stage ontving zij een beurs van de Saal van Zwanenbergstichting om een tweede onderzoeksstage uit te voeren aan het CSIC (Consejo Superior de Investigaciones Científicas) te Madrid. Hier onderzocht zij een methode om prodrugs te synthetiseren, onder begeleiding van Prof. dr. María-José Camarasa en Dr. Sonsoles Velázquez. Na het behalen van haar masterdiploma (cum laude) in november 2008 startte zij in januari 2009 met haar promotieonderzoek onder begeleiding van Prof. dr. Rob Liskamp en Dr. ir. John Kruijtzer in de vakgroep Medicinal Chemistry and Chemical Biology aan de Universiteit Utrecht. De resultaten van het promotieonderzoek staan beschreven in dit proefschrift. Daarnaast werden deze resultaten gepresenteerd op verschillende symposia en (inter)nationale congressen.

Sinds april 2013 is Gwenn werkzaam als scientist bij ISA Pharmaceuticals in Leiden, waar zij onderzoek doet naar de werking van Synthetic Long Peptides (SLPs) tegen verschillende soorten kanker en virale infecties.

List of publications

Diez-Torrubia,A.; Cabrera, S.; de Castro, S.; García-Aparicio, C.; Mulder, G.E.; de Meester, I.; María-José Camarasa, M-J.; Balzarini, J.; Velázquez, S; Novel water-soluble prodrugs of acyclovir cleavable by the Dipeptidylpeptidase IV(DPP IV/CD26) enzyme. *Submitted*

Mulder, G.E.; Quarles van Ufford, H.C.; van Ameijde, J.; Brouwer, A.J.; Kruijtzer, J.A.W.; Liskamp, R.M.J.; Scaffold optimization in discontinuous epitope containing protein mimics of gp120 using smart libraries. *Org. Biomol. Chem.*, **2013**, 2676-2684.

Mulder, G.E.; Kruijtzer, J.A.W.; Liskamp, R.M.J.; A combinatorial approach toward smart libraries of discontinuous epitopes of HIV gp120 on a TAC synthetic scaffold. *Chem. Commun.*, **2012**, 48, 10007–10009.

Yim, C.Y.; Dijkgraaf, I, Merkx, R; Eekt, A; Mulder, G.E.; Rijkers, D.T.S.; Boerman, O.C.; Liskamp, R.M.J. Synthesis of DOTA-Conjugated Multimeric [Tyr3]Octreotide Peptides via a Combination of Cu(I)-Catalyzed "Click" Cycloaddition and Thio Acid/Sulfonyl Azide "Sulfo-Click" Amidation and Their in Vivo Evaluation. *J. Med. Chem.*, **2010**, 53, 3944-3953.

Elgersma, R.C.; Mulder, G.E.; Posthuma, G.; Rijkers, D.T.S.; Liskamp, R.M.J. Mirror image supramolecular helical tapes formed by the (inverso)-depsipeptide derivatives of the amyloidogenic peptide amylin(20-29). *Tetrahedron Lett.*, **2008**, 49, 987-991.

Elgersma, R.C.; Mulder, G.E.; Kruijtzer, J.A.W.; Posthuma, G.; Rijkers, D.T.S.; Liskamp, R.M.J. Transformation of the amyloidogenic peptide amylin (20-29) into its corresponding peptoid and retropeptoid: access to both an amyloid inhibitor and template for self-assembled supramolecular tapes. *Bioorg. Med. Chem. Lett.*, **2007**, 17(7), 1837-1842.

Conferences

Oral: Mulder, G.E.; Quarles van Ufford, H.C.; van Ameijde, J.; Brouwer, A.J.; Kruijtzer, J.A.W.; Liskamp, R.M.J.; Libraries of discontinuous epitope mimics of HIV gp120. Design & Synthesis, Structure & Reactivity, Oct. 2012, Lunteren, The Netherlands

Oral: Mulder, G.E.; Kruijtzer, J.A.W.; Liskamp, R.M.J.; Mimicry of the discontinuous epitope of HIV gp120, Bijvoet Symposium, April 2012, Soesterberg, The Netherlands

Oral and poster: Mulder, G.E.; Kruijtzer, J.A.W.; Liskamp, R.M.J.; Discontinuous epitope mimics of HIV gp120; Synthesis and biological activity, Chemistry As INnovating Science meeting, Nov. 2011, Maarssen, The Netherlands

Oral: Mulder, G.E.; Kruijtzer, J.A.W.; Liskamp, R.M.J.; Synthesis and evaluation of discontinuous epitope mimics of HIV gp120, Figon Dutch Medicine Days, Oct 2011, Lunteren, the Netherlands. Awarded with the 3rd prize.

Oral and poster: Mulder, G.E.; Kruijtzer, J.A.W.; Liskamp, R.M.J.;Discontinuous epitope mimics of HIV gp120; Synthesis and biological activity. 22nd American peptide symposium, June 2011, San Diego, USA

Oral: Mulder, G.E.; Kruijtzer, J.A.W.; Liskamp, R.M.J.; Mimicry of the discontinuous epitope of HIV gp120, June 2011, PhD competition, Department Day Pharmaceutical Sciences Utrecht. Awarded with the 1st prize.

Oral and poster: Mulder, G.E.; Kruijtzer, J.A.W.; Liskamp, R.M.J.; Mimicry of the discontinuous epitope of HIV gp120, International Max Planck Research School and Utrecht University joint Symposium, May 2011, Utrecht, The Netherlands

Poster: Mulder, G.E.; Kruijtzer, J.A.W.; Liskamp, R.M.J.; Synthesis of TAC-scaffolded peptide loops towards protein mimics containing discontinuous epitopes. Design & Synthesis, Structure & Reactivity, Oct. 2009, Lunteren, The Netherlands

Dankwoord

Lieve allemaal, het zit erop! Mijn aio-tijd is voorbij gevlogen! Ik herinner me mijn eerste dag op het lab nog goed. “Afblijven John K” was het eerste dat me opviel, met dikke zwarte stift geschreven op zo ongeveer alles dat ik tegenkwam. Juist ja. Toch voelde ik me vanaf het begin erg thuis bij MedChem en daar ben ik jullie allemaal erg dankbaar voor. Promoveren is niet gewoon een baan, maar een echt ontwikkelingstraject dat af en toe alle kanten op kan slingeren. Dan is het fijn om mensen om je heen te hebben die het onderzoek, of jou zelf, een beetje bij kunnen sturen. Ik hoop dat ik de afgelopen jaren al heb laten blijken hoezeer ik jullie hulp en aandacht altijd heb gewaardeerd, door zelf ook naar jullie te luisteren, mee te denken, even tussendoor tijd te maken om een sample te meten of gewoon door voor een lekker hapje eten bij de borrel te zorgen. Naast deze indirecte blijk van waardering wil ik ook graag een aantal mensen persoonlijk bedanken voor hun hulp de afgelopen jaren.

Allereerst wil ik mijn promotor **Rob Liskamp** bedanken. Jouw enthousiasme is ongeëvenaard, en dat werkt aanstekelijk en motiverend voor (PhD-) studenten. Dank voor het vertrouwen dat je al in mijn had toen je me tijdens mijn masterstage benaderde voor een PhD-positie in jouw lab. Dank ook voor de vrijheid die ik heb gekregen om me te ontwikkelen, zowel binnen het lab als daarbuiten op cursussen, congressen en symposia. Ook wil ik je bedanken voor de gang van zaken in het jaar van je sabbatical en in de periode van je start in Glasgow. Het was wel even schrikken om te horen te krijgen dat je promotor het laatste jaar van je promotie weg is en daarna een nieuw lab aan de andere kant van het kanaal gaat opstarten, maar het is allemaal goed gekomen. Lang leve Skype en email! Ik hoop dat je in Glasgow net zo’n mooie groep gaat opbouwen als je in Utrecht hebt gedaan. Het ga je goed!
Ook onmisbaar voor het onderzoek bij MedChem in het algemeen, en heel specifiek in mijn begeleidingsteam, is **John Kruijtzer**. Na 4 jaar schrik ik niet meer van stapels artikelen als muurdecoratie/vloerbedekking/armsteun of muismat, en weet ik dat je inderdaad dat ene artikel feilloos kunt vinden in je ‘archief’. In het begin was ik een beetje bang voor je met al je eigen speciale methodes, trucs, reagentia en gereedschap,

maar na een tijdje merkte ik dat je gewoon heel precies en kritisch bent. Het moet goed gebeuren, je wilt de beste spullen hebben voor je onderzoek, en dat kan ik alleen maar waarderen. Je kennis van (peptiden)chemie is bewonderenswaardig, ik vind het bijzonder hoe nauw jij de zaken in het lab blijft volgen en ik ben dankbaar dat ik zoveel van je heb mogen leren.
Dan iemand die eigenlijk niet direct iets met mijn onderzoek te maken had, maar wel als persoon altijd heel belangrijk voor me is geweest. **Dirk Rijkers**, negen jaar geleden heb jij mij als eerstejaars kennis laten maken met de wondere wereld van aminozuren en peptiden, en door jouw menselijke en didactische vaardigheden heeft dit onderzoek mij gegrepen en ben ik teruggekomen bij MedChem. De afgelopen jaren had jij vaak niet veel woorden nodig om te merken waar het probleem zat, en ben je er ondanks dat je dat op papier niet hoefde te doen toch altijd voor mij geweest. Heel veel dank daarvoor!
Soms is het ook fijn als iemand met een frisse blik naar je onderzoek kan kijken wanneer je het zelf even allemaal niet meer ziet, en je al je resultaten 'gewoon' bent gaan vinden. **Jack den Hartog**, hartelijk dank voor je input en hulp in de periode september-oktober 2011, en dank voor alle interesse die je daarna in mijn onderzoek hebt getoond.

Het functioneren van een lab valt of staat met de mensen die er werken, en wat dat betreft mag ik me gelukkig prijzen met de mensen die ik de afgelopen jaren om me heen had. Er is door de jaren heen heel wat veranderd in de samenstelling van de groep, maar ik zal bij het begin beginnen. **Hans J**, ik heb je gemist nadat je wegging bij MedChem. Manusje-van-alles, en essentieel voor het goed werkend houden van de mass spec en de HPLC's. Die onderhouden zichzelf niet! Dank dat je mij nog even in de avonduren wat (LC)MS skills hebt bijgebracht, daar heb ik erg veel aan gehad. **Bauke**, jouw passie voor je vak heeft mij vooral in mijn eerste jaar goed op weg geholpen. Altijd bescheiden, maar wat weet jij veel en wat kun je goed uitleggen. Dank dat je nog steeds altijd voor me klaar staat voor advies, of gewoon als luisterend oor. Ex-collega's en maatjes op de buur-lab's, **Ronald** ('wat zegt ze?'), jij hebt mij enthousiast gemaakt voor het doen van peptiden-gerelateerd onderzoek. **Cheng**, DOTA- en click-meester, jij hebt mij tijdens mijn master-stage geleerd wat doorzetten is. **Tony**, vooral in het begin van mijn PhD altijd in de buurt voor wat lab-hulp en ook recentelijk weer zeer behulpzaam bij de start van mijn nieuwe baan.

Collega's van het discontinue-epitoop project, dank voor de vele nuttige discussies op het lab en tijdens meetings. **Cristina**, hartelijk dank voor het delen van jouw ervaringen binnen dit project en het overdragen van je kennis. **Helmus**, koning van Putten én van de thiolen, hopelijk krijg je binnenkort nog wat mooie data terug en begint jouw boekje ook snel vorm te krijgen. **Paul**, ik vond het leuk dat jij het team compleet kwam maken. Helaas was dat pas op het moment dat ik de eindstreep al naderde. Fijn om kritisch elkaars stukken te lezen en te discussiëren over nieuwe projectlijnen. Ik hoop dat één van deze ideeën nog binnen jouw aio-tijd in de praktijk gebracht kan worden!

Studenten **Margo**, **Irina** en **Steven**, jullie hebben allemaal ervaren dat cyclische peptiden niet de makkelijkste verbindingen zijn om mee te werken. Hoewel er weinig van jullie werk terug te vinden is in dit boekje wil ik jullie wel bedanken voor het harde werken, en hoop ik dat jullie iets geleerd hebben tijdens jullie stages.

Veel dank ook aan de collega's en stafleden waar ik niet altijd direct veel mee te maken heb gehad, maar die toch zeker allemaal op hun eigen manier essentieel zijn voor het functioneren van de groep. **Ed**, **Rob Ruijtenbeek**, **Hans**, **Marcel**, **Nico**. Excuses als ik jullie niet allemaal bij naam noem, maar het feit dat je dit boekje nu in handen hebt betekent dat ook jij hier bedankt wordt.

Roland, je was niet direct betrokken bij mijn project, maar ik kon toch altijd bij je binnenlopen, dank daarvoor. **Arwin**, dank voor de hulp met glaswerk, apparatuur en praatjes wanneer dat nodig was. **Nathaniel**, I admire the way you always try to get the best out of people, including yourself. **Javier**, dank voor hulp met de ion-trap en voor het meten van een aantal lastige samples. **Mirjam Damen** en **Arjan Barendrecht**, dank voor het meten van een aantal high resolution MS samples.

Paula en **Natatia**, dank voor al het werk achter de schermen, en vooral in de laatste maand hebben jullie volgens mij ongemerkt nog een eindsprintje voor me ingezet. Dank daarvoor!

Núria, I liked having a desk closer to yours in the DDW building. Thanks for good conversations and sharing your view on many things in life! **Ray** en **Monique**, andere labs, andere projecten, maar toch leuk om af en toe van gedachten te wisselen. Ik ben blij dat jullie zo'n mooie stap hebben kunnen zetten naar het NKI. **Francesca**, I'm glad that you got such nice results after a difficult start of your project. Good luck finishing your own thesis. **Jinqiang**, my silent neighbour. I've missed you the last couple of months! I hope you're enjoying your new job in Montreal! **Ou**, good luck in this final year of

your project. **Rik**, dank voor de rondjes op de racefiets, een paar lekkere diners en je hulp bij de stabiliteitsassays. **Steffen**, dank voor het luisteren als ik weer eens tegen de lucht aan het praten was. Dank voor het delen van je encyclopedische kennis, zinnige en onzinnige wijsheden en voor de chocola als ik die nodig had. **Jeroen**, vooral in de fase van het opstarten van de ELISA's ben je erg behulpzaam geweest, dank daarvoor. **Linda**, jij hebt mij wegwijs gemaakt in de wereld van pipetten en 96-wells platen. Heel veel dank voor al je hulp met ELISA's. Zonder jou had de OBC-paper veel langer op zich laten wachten! **Kees**, **Bart**, **Burt**, **Edwin**, dank voor jullie kritische vragen bij mijn schiet-me-maar-af presentatie. Bart, dank voor je interesse in het verder verloop van mijn project, Edwin dank voor je interesse in zowel mijn project als zoektocht naar een nieuwe baan.

Monique Nijhuis en **Dorien de Jong**, dank voor jullie inzet, het meedenken en het uitvoeren van de MTT assay. Misschien kunnen mijn opvolgers nog eens een beroep doen op jullie kennis en faciliteiten.

En dan de laatst overgebleven Medchemmers, sommigen net nieuw en sommigen van jullie zijn inmiddels zelfs ook al begonnen aan een nieuwe baan. **Matthijs**, je hebt gekozen voor een bewonderenswaardig carrierepad, veel succes. **Alen**, thanks for some good conversations and delicious muffins. Good luck with your project! Lieve leipies, of beren, het was heel gezellig met jullie! Dank voor het verrijken van mijn woordenschat, de vele gezellige borrels, het weekendje Putten. Mannen en Hilde, het was een mooie tijd met een heel goed laatste jaar. Hoewel velen van ons afrondstress hadden, hebben we er met elkaar een mooie periode van gemaakt. **Jack**, HPLC-meister, dank voor de geitenfilmpjes, het ga je goed in Deutschland. **Peter**, dank voor de gezellige bbq's, ik hoop dat je nooit meer Italiaanse studenten krijgt (rotavaaaap?). **Loek**, ('wat zeg jij?') opperleipie, schrijf je boekje nog een keertje af. **Paul**, al eerder genoemd, ik wou dat ik zo goed dingen langs me heen kon laten gaan als jij dat kan. **Hilde**, ik heb je denk ik pas in het laatste jaar wat beter leren kennen. Dank voor het delen van frustraties en vreugde, onzin en wijsheid.

Lieve **Timo**, ook jou heb ik in het laatste jaar pas goed leren kennen, en wat ben ik daar blij om. Dank voor veel meer dan hier in een paar regels te vatten is.

Terwijl ik dit dankwoord schrijf zit ik al niet meer tussen mijn oude Medchem-maatjes, maar raas ik door weilanden ergens tussen Leiden en Utrecht. Hoewel ik nog maar net

begonnen ben met mijn nieuwe baan, wil ik ook **mijn collega's bij ISA** bedanken voor jullie interesse en de ruimte die jullie mij hebben gegeven voor het afronden van mijn promotie, heel fijn!
Meer zakelijk, maar toch ook heel belangrijk aan het eind van dit promotietraject: mijn sponsoren. **Marlé Nijhuis**, dank voor je genereuze sponsoring voor het drukken van mijn proefschrift. **UIPS** en **Shimadzu**, dank voor jullie bijdrage.

Natuurlijk en gelukkig heb ik de afgelopen jaren niet alleen maar in het lab gestaan en was er genoeg tijd over voor andere dingen die ik heel graag doe: sporten, koken en eten, en het liefst in goed gezelschap. En dat had ik. Lieve **Anna**, roomie, reismaatje en vriendin, wat fijn om leuke en minder leuke momenten met jou te kunnen delen. Aan de eettafel, bij een kop koffie, al hardlopend of zelfs op de racefiets. Lieve **Joyce**, al bijna 10 jaar kennen we elkaar, en ondanks dat we geen roomies meer zijn en niet meer in dezelfde stad wonen ben je nog erg belangrijk voor me. Lieve **Lot**, ik hoop dat als je straks niet meer in het OV woont maar gewoon in Utrecht, we weer als vanouds ijsjes kunnen eten bij Roberto. **Fietsmeiden** en **tennismaatjes**, fijn dat ik af en toe mijn werk kon vergeten en lekker in de buitenlucht kon sporten met jullie.
Annouck, wat onzettend leuk dat we elkaar nogsteeds met enige regelmaat zien. Na het Carmel zijn we hele verschillende richtingen ingeslagen, woonden we niet meer bij elkaar in de buurt, maar voelt het toch altijd weer vertrouwd als we elkaar opzoeken. Ik vind het heel bijzonder dat er ook een stukje van jouw werk terug te vinden is in dit boekje, en wel in het onderdeel dat waarschijnlijk de meeste aandacht zal krijgen: de cover! Dank voor alle tijd en aandacht die je daaraan hebt besteed, en dank ook voor de stoomcursus InDesign die je mij hebt gegeven en voor je hulp met de layout van het binnenwerk.
Lievelieve **Robbie**, slimme trouwe sportieve paranimf. Vanaf het eerste jaar scheikunde in 2003 toen jij nog niet wist hoe je spaghetti moest koken ben je mijn maatje. Studiemaatje, sportmaatje, bankhangmaatje en fijne gesprekspartner voor zinnige en minder zinnige gesprekken. In leuke en moeilijkere tijden. Wat ben jij een bijzondere vriend, en wat leuk dat jij mijn paranimf wilt zijn.
Yannic, gekke lieve broer en paranimf. We verschillen op veel punten zo veel, maar ergens is toch wel te merken dat we dezelfde opvoeding hebben gehad. Hoe verschillend onze werelden soms ook zijn, ik vind het altijd weer leuk om je te zien, met je bij te

praten, samen iets lekkers te koken en om/met je te lachen. Je roept altijd grappend dat ik het uithangbord van de familie ben, maar ik ben minstens zo trots op jou als jij op mij. Je had een kleine omweg nodig, maar je hebt je plek gevonden en je komt er wel!
Alwin en **de boys**, volgens mij moesten jullie net zo wennen aan mij als ik aan jullie, maar inmiddels voelt het vertrouwd in Heeswijk/Amsterdam en ben ik blij dat ik jullie heb leren kennen.
Lieve **ouders**, dank voor alles wat jullie me hebben meegegeven. Jullie hebben ervoor gezorgd dat ik zorgeloos kon studeren, hebben altijd interesse getoond in mijn studie en werk en hebben niet alleen de rol van ouder op je genomen, maar zonder je op te dringen ook vaak die van coach. Ik denk dat het vrij zeldzaam is om zulke slimme en betrokken ouders te hebben, en ik ben jullie daar erg dankbaar voor. **Pap**, hoewel je dit hele traject niet meer hebt mee kunnen maken ben je toch nog steeds erg belangrijk voor me. Op belangrijke momenten vraag ik me nog altijd af wat jij zou zeggen, en ik weet hoe trots je zou zijn geweest als je dit nog had kunnen lezen. **Mam**, ik heb het nog nooit geprobeerd, maar zelfs als ik je midden in de nacht zou bellen en zou vragen om langs te komen zou je zonder twijfel in de auto springen. Je bent er altijd, overal, en doet altijd je best voor Yannic en mij. En dat terwijl je soms misschien ook wel even genoeg hebt aan jezelf, want je hebt de laatste jaren heel wat voor de kiezen gekregen. Ik ben heel trots op de manier waarop je nu in het leven staat, je nieuwe baan hebt veroverd en altijd voor iedereen klaar staat.

Lieve allemaal, zonder jullie waren de afgelopen jaren een stuk saaier of moeilijker geweest. Het is klaar, het is feest, vier het met mij mee!

Gwenn